#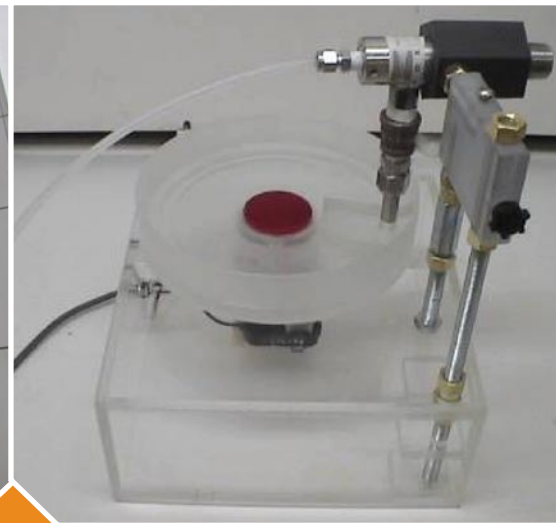 Theoretical and Experimental Analysis of Important Parameters for Determining the Impact of a Biological Attack on a Building

FINAL REPORT

Office of Research and Development
National Homeland Security Research Center

FINAL REPORT ON

Theoretical and Experimental Analysis of Important Parameters for Determining the Impact of a Biological Attack on a Building

Contract No. GS-10F-0275K
Task Order 1105

Prepared for
Joseph Wood and Les Sparks, Project Officers

U.S. ENVIRONMENTAL PROTECTION AGENCY
Research Triangle Park, NC

April 2008

Prepared by
Brian E. Hawkins, Ph.D. and Kent C. Hofacre

BATTELLE COLUMBUS OPERATIONS

505 King Avenue
Columbus, Ohio   43201-2693

Office of Research and Development
National Homeland Security Research Center, Decontamination and Consequence Management Division

Disclaimer

This report is a work prepared for the United States government by Battelle. In no event shall either the United States government or Battelle have any responsibility or liability for any consequences of any use, misuse, inability to use, or reliance on the information contained herein, nor does either warrant or otherwise represent in any way the accuracy, adequacy, efficacy, or applicability of the contents hereof.

Table of Contents

List of Figures

List of Tables

Glossary

ACH	Air change rate expressed as airflow in units of volume per hour divided by the zone volume in identical volume units (ASHRAE, 1991).
Filtration or Filtration Efficiency	The nominal efficiency with which a filter removes particles from an air stream.
Infiltration	Uncontrolled inward leakage of outdoor air into a building through cracks and interstices in any building element. Normally caused by pressure effects or differences in air density (ASHRAE, 1991). Also known as building air infiltration.
Leakage	Uncontrolled and unplanned flow between two zones of a building. Normally caused by slight pressure differences between the zones. Also know as interzonal leakage or room leakage.
Makeup Air	Air brought into a building from outside to replace that exhausted. Air intentionally brought into a building that was not previously circulated through the building (ASHRAE, 1991). Also known as outdoor air.
Recirculation	Air taken from a zone and returned to the zone after being passed through conditioning elements (ASHRAE, 1991). Also known as recirculated air.
Zone 1	Zone of release
Zone 2	Zone of interest
Zone 3	The lumped zone, which represents the bulk of the building, or the rest of the building.

Executive Summary

Although it is intuitive that building and heating, ventilation, and air conditioning (HVAC) system parameters play a major role in determining how an agent disperses after an indoor biological attack, how and to what extent those parameters affect the transport of contaminants is not well understood. A better understanding of how building and HVAC parameters affect the transport of an agent will improve the ability to mitigate the effects of a biological attack and aid in determining where resources in building protection are best directed. Therefore, the objective of this project was to theoretically and experimentally evaluate the effects that modifications to HVAC and building design and operation would have on the spread of biological agents (in aerosol form) within a building.

To this end, a three-zone model representation of a building was developed to determine which HVAC and building parameters are most important, and how accurately they need to be known, in determining the impact of an indoor bio-agent attack. The three-zone model consists of a zone of release and zone of interest, which are adjacent and of equal size, as well as a "lumped" zone, which represents the remainder of the building. All three zones are serviced by a single HVAC system with common recirculation.

The potential impact of an attack was quantified in terms of two performance metrics: the cumulative exposure to the agent after 30 minutes and the time to reach a critical exposure level (referred to as Ct) for that agent. A sensitivity analysis method was also developed for determining the required level of accuracy for each building and HVAC operating parameter, i.e., to determine how well each parameter must be known to accurately estimate the two performance metrics. The analysis method allows for investigation of the relative impact of each parameter, i.e., the change in the two performance metrics as a result of a change in a parameter.

Field tests were then performed to gather data for the validation of both the three-zone modeling concept and the sensitivity analysis method for determining parameter impact. To cover the broad range of parameters and conditions needed for testing, most of the tests were performed without duplicates. The field tests consisted of a series of tracer experiments under varying HVAC conditions in a test building. Visolite®, a fluorescent-tagged, calcium carbonate aerosol, was chosen as the tracer material. The aerosol was released using a custom-built eductor. The venue for these tests was a three-story building, located in Anniston, Alabama, that contained three separate air handling units (AHUs), each possessing its own supply and return ductwork and each servicing a different region of the building. After a few initial building alterations, the test venue was able to represent both a large and a small notional building, depending on which zones were chosen as the zone of release and zone of interest.

An initial analysis using model simulations revealed that makeup air and infiltration rates had little impact during an internal release scenario and system parameters were of greater importance than single-zone parameters (i.e., the recirculation rate of the entire building was more important than the

recirculation rate of the zone of interest). The initial analysis work also identified building size, interzonal leakage rate, recirculation rate, and filter efficiency as the key parameters affecting the selected performance metrics. The simulation results showed that as the building size increased, the filtration efficiency went from being a potentially dominant factor to a lesser factor compared to the interzonal leakage rate. The system recirculation was found to be of secondary importance but had a strong effect on the importance of the filtration efficiency for smaller buildings (i.e., for building volumes less than five times the zone of interest).

On the whole, the excellent agreement observed between experimental and model-predicted data validated the use of the three-zone model to approximate contaminant spread in a building. Excellent agreement between the lumped third zone in the model and multiple rooms throughout the test building validated the use of a three-zone model to predict contaminant levels in real buildings with more than three zones. Modeling, as supported by the experimental data, provides a useful tool for estimating and assessing which parameters significantly affect the spread of contaminant in a building. Buildings of varying size and HVAC performance can be assessed. It was demonstrated that changes in HVAC filter efficiency, air exchange, and building "size" could be varied with a predictable impact on contaminant spread.

Ancillary experiments suggest that the use of an in-room air cleaner can greatly reduce the exposure of the room's occupants. The magnitude of this reduction will vary greatly depending on the volume of the room, as well as the throughput and efficiency of the in-room air cleaner.

From this project it is clear that there is no one universal answer regarding which building or HVAC parameter is most important or how accurately it needs to be known. It depends on the release location, HVAC characteristics, building characteristics, and proximity of the zone of interest to the release location. This implies that the usefulness of mitigation strategies to protect buildings (or more precisely its occupants) must be considered on a case-by-case basis. The sensitivity analysis method discussed herein provides some indication of the general trends and identifies the most important parameters impacting contaminant spread for various combinations of HVAC parameters and building volumes relative to the zone of interest. The modeling approach developed here could be used to assess various scenarios and buildings of specific interest, without the need for extensive knowledge of HVAC and building parameters. Using the modeling tool developed for initial analysis may be useful in determining the merits of modifying the building to enhance the protection of occupants or to mitigate the spread of contaminants.

Recommendations for future study focus on two aspects of the well-mixed model: usability and applicability. The usability of the model could be improved by developing a user-friendly graphical user interface (GUI), which would allow casual users (e.g., building operators) to rapidly perform simple impact analyses for a building of interest given limited building

information (e.g., HVAC settings, building and room volumes). The development of a GUI would increase the utility and impact of this effort by making the model available to more people. Also recommended is an enhancement to expand the applicability of the tool by developing and verifying an analogous model for a building with a more complex HVAC ductwork scheme. The present model is applicable only to a building with one common return ductwork system. Developing an analogous model that effectively represents buildings with multiple return ductwork systems (i.e., multiple air handling units) and performing an experimental verification, similar to this work, would aid in making a model more applicable to large buildings with more complex air handling schemes.

In general, the spread of a contaminant following the release of a biological agent within a building is affected by the building characteristics (e.g., building volume, air infiltration rates, or room-to-room leakage) and parameters of the HVAC system. However, a quantitative understanding of the relative impacts that each of the building and HVAC parameters has on contaminant dispersion is needed. A better understanding of these parameters' impacts will improve the ability to protect buildings from a biological attack. Therefore, a project was undertaken in which theoretical and experimental analyses were conducted to determine the impact that HVAC and building modifications have on the spread of particulate agents within a building. The results of the theoretical analyses would guide the design of experiments, and the experiments would help to validate the model.

A building test bed in Anniston, Alabama, was selected for the experimental program, as it allowed for access and control of most of the parameters of interest. The size of the building was also shown to influence which controllable building or HVAC parameter was important regarding the control of contaminant spread. Although the size of the building is not a controllable parameter in actual applications, the test bed facility did allow manipulation of room sizes so that "large" and "small" building configurations could be assessed.

2.0
Objective

The objective of this project was to evaluate the impact that modifications to HVAC and building design and operation have on the spread of biological (aerosolized) agents within a building. In the course of conducting this project—specifically the theoretical analysis of important parameters for determining the impact of an attack on buildings —it became apparent that another objective would also be to experimentally demonstrate the application of the three-zone, well-mixed model.

The approach and development of a three-zone, well-mixed model is described. The experimental methods used during this study are detailed. A series of experiments at a test bed were used to experimentally confirm the usefulness of a three-zone, well-mixed volume model in simulating a "real" building. The results are then used to analyze what parameter changes had the largest impact on potential building performance, and conclusions that can be made from this work are stated.

4.1 General Approach

The modeling approach taken was to develop an algorithm to estimate contaminant transport in a notional building as a function of time. The model allowed building parameters (e.g., HVAC airflow, filter efficiency) to be investigated. The model was used to generate time-dependent contaminant concentration profiles in zones of interest, which were then used as performance metrics for estimating exposures. Model parameters were then varied over a range of conditions so that the changes in performance metrics could be assessed. These changes in performance metrics were then used to determine the most important parameters and how well they need to be known. (In a separate but related project, a more mechanistic model of contaminant transport based on aerosol dynamics is being developed. That model considers contaminant concentrations in zones of a notional building and how HVAC flow, air exchange rates, infiltration rates, and other parameters impact those concentrations. That model has been leveraged for consistency with this simplified approach as briefly discussed below. The simplified model approach, input parameters of interest, performance metrics, and data interpretation/analysis process are discussed in Sections 4.2 through 4.5 with a few illustrative examples.)

The model approach used for this analysis of building and HVAC parameters and their effect on hazard exposure is purposely general to allow consideration for a range of building types and sizes. The analysis is based on relative changes in exposure in a zone of interest with changes in building or HVAC parameters. The absolute determination of whether a change in HVAC or building parameter is important (whether a resulting exposure was reduced below a lethal concentration, for example) is not determined by this analysis. Absolute determination of those effects is dependent on scenario attack parameters such as agent release, building occupant exposure durations, and agent type. So, for example, in some scenarios it may have significantly different impacts on occupants if a 90% efficient filter is used and in other scenarios it may not make a difference. That is not to say that the model presented here is not valid for estimating resulting aerosol and other contaminant concentrations as a function of time and zone for specific release and building operating scenarios, just that the approach presented here for determining the effects of various parameters is not an absolute approach. The fact that the model developed here is generalized and based on relative change in exposure does not diminish its usefulness. The model allows for quick assessment and sensitivity analysis, with little specific building information. Thus, it is very applicable for building engineers and planners.

The HVAC Aerosol Dynamics Model, HVACADM, developed under a separate project, was leveraged here for investigating the effects of different contaminant behavior mechanisms and considerations on the degree of protection a building may provide occupants against a chemical or biological (CB) attack on the building. (Although the primary focus of the modeling and experimental program is for agents in particulate form, the approach could also be adapted for chemical agents as well.) To leverage the HVACADM model to address the objectives of this task, a simplified model that focuses on mass balances around three zones was developed. This simplified model allows the parameters affecting contaminant transport to be assessed without the use of mechanistic models.

The goal of the project is two-fold: (1) determine which parameters are most important for predicting the impact of a CB attack on a building and (2) determine the degree of accuracy to which these parameters needs to be known for practical purposes (i.e., at what point the level of exposure becomes insensitive to a change in the parameters controlling the contaminant spread and exposure).

The nomenclature used to define building and HVAC parameters in this report follows as closely as possible that used by the American Society of Heating, Refrigerating, and Air-Conditions Engineers (ASHRAE). In this fashion, consistent use of terms is intended to aid with an understanding of the model approach and results. Definitions of the key terms are provided in the Glossary section of this report.

4.2 Simplified Model Development

The simplified model is based on the well-mixed zone methodology, which implies instantaneous, perfect mixing within a zone and thus a uniform concentration throughout the zone volume. A mass balance was applied to each well-mixed zone to derive the governing equations for the model (see Equation 1 and Figure 1).

$$[Accumulation]=[Input]\text{-}[Output]+[Generation] \quad (1)$$

The accumulation term accounts for changes in the concentration of agent within the zone volume, the input term accounts for agent that is added to the zone via the input streams (makeup air, recirculation, infiltration, and interzonal leakage entering the zone), the generation term accounts for a release within the zone, and the output term accounts for agent removed from the zone via the output streams (exhaust, recirculation, and interzonal leakage leaving the zone). In this model, a zone could be an individual room or a group of rooms served by a common HVAC system.

The mass balance can be expressed in terms of particle concentration by dividing both sides of the equation by the zone volume; explicitly writing out the terms for a balance around Zone 1 yields Equation 2.
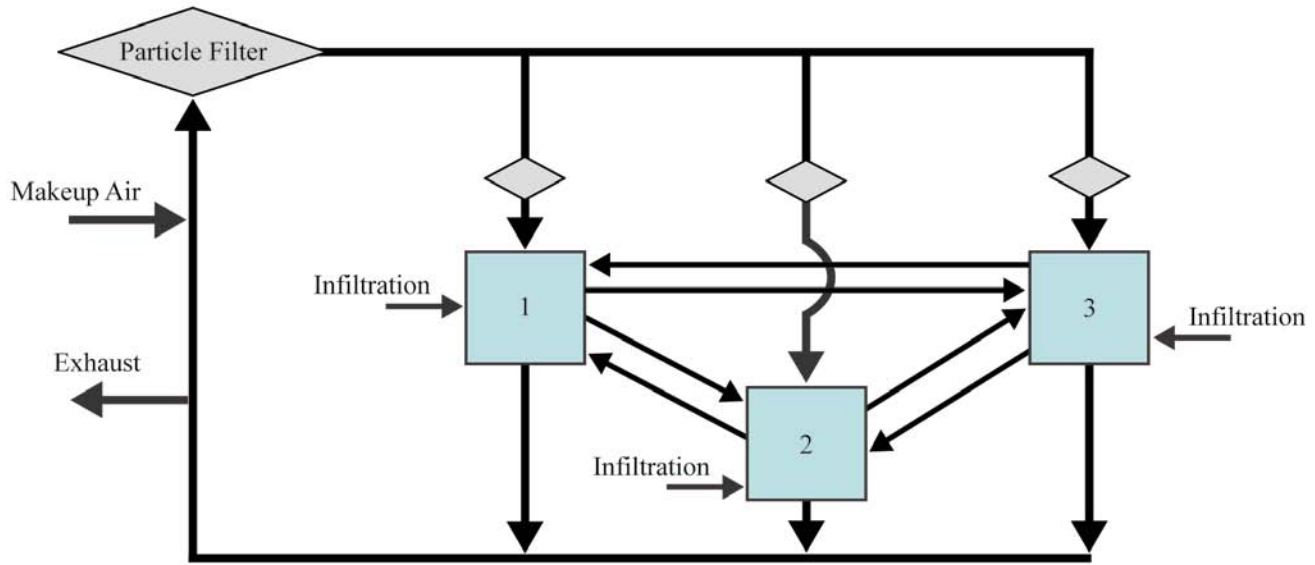
Figure 1. Well-Mixed Zone Model Diagram

$$\left[\frac{dC_1(t)}{dt}\right] = \left[(1-\eta_{filter})(1-\eta_1)\frac{Q_{i,1}+Q_{R,1}}{V_1}C_{vent}(t) + \frac{Q_{inf,1}}{V_1}C_{inf}(t) + \frac{Q_{21}}{V_1}C_2(t) + \frac{Q_{31}}{V_1}C_3(t)\right]$$

$$- \left[\frac{Q_{R,1}}{V_1}C_1(t) + \frac{Q_{i,1}}{V_1}C_1(t) + \frac{Q_{12}}{V_1}C_1(t) + \frac{Q_{13}}{V_1}C_1(t)\right] + \left[\frac{G_1}{V_1}\right] \qquad (2)$$

Where

$C_1(t)$ is the concentration of contaminant in both the well-mixed Zone 1 volume and the streams exiting Zone 1 (an unknown function of time),

t is the time,

η_{filter} is the fractional efficiency of the particulate filter used in the HVAC system for general makeup air and recirculation,

η_1 is the fractional efficiency of an additional particulate filter used for the makeup air and recirculation of Zone 1,

$Q_{i,1}$ is the makeup airflow rate of fresh air into Zone 1,

V_1 is the volume of Zone 1,

$C_{vent}(t)$ is the concentration of the contaminant in the makeup air stream prior to filtration,

$Q_{inf,1}$ is the infiltration flow rate into Zone 1,

$C_{inf}(t)$ is the concentration of the contaminant in the infiltration stream,

Q_{21} is the interzonal leakage from Zone 2 to Zone 1,

$C_2(t)$ is the concentration of the contaminant in both the well-mixed Zone 2 and the streams exiting Zone 2 (an unknown function of time),

Q_{31} is the interzonal leakage from Zone 3 to Zone 1,

$C_3(t)$ is the concentration of the contaminant in both the well-mixed Zone 3 and the streams exiting Zone 3 (an unknown function of time),

$Q_{R,1}$ is the recirculation flow rate for Zone 1,

Q_{12} is the interzonal leakage from Zone 1 to Zone 2,

Q_{13} is the interzonal leakage from Zone 1 to Zone 3, and

G_1 is the generation rate of agent per unit time in Zone 1.

Next, Euler's Method, a numerical solution approach, is applied by converting the derivative to a simple difference ($dt \to \Delta t$, $dC_1 \to \Delta C_1 = C_{1,t+\Delta t} - C_{1,t}$), and solving for $C_{1,t+\Delta t}$ yields Equation 3.

$$C_{1,t+\Delta t} = C_{1,t} + \Delta t\left[(1-\eta_{filter})(1-\eta_1)\frac{Q_{i,1}+Q_{R,1}}{V_1}C_{vent}(t) + \frac{Q_{inf,1}}{V_1}C_{inf}(t) + \frac{Q_{21}}{V_1}C_{2,t} + \frac{Q_{31}}{V_1}C_{3,t}\right]$$

$$- \Delta t\, C_{1,t}\left[\frac{Q_{R,1}}{V_1} + \frac{Q_{i,1}}{V_1} + \frac{Q_{12}}{V_1} + \frac{Q_{13}}{V_1}\right] + \Delta t\left[\frac{G_1}{V_1}\right] \qquad (3)$$

Where

$C_{1,t+\Delta t}$ is the concentration in Zone 1 at the next time step ($t+\Delta t$),

$C_{1,t}$ is the concentration in Zone 1 at the current time step,

$C_{2,t}$ is the concentration in Zone 2 at the current time step,

$C_{3,t}$ is the concentration in Zone 3 at the current time step, and

Δt is the size of the time increment.

It is important to note that this is a simplified numeric solution and thus requires a small time increment (≤ 0.10 min). Similar equations are then written for the other zones.

The concentration of the contaminant in the HVAC stream prior to filtration (C_{vent}) can easily be calculated as a weighted average of its constituents (see Equation 4).

$$C_{vent} = \frac{(Q_{i,1}+Q_{R,1})C_{1,t} + (Q_{i,2}+Q_{R,2})C_{2,t} + (Q_{i,3}+Q_{R,3})C_{3,t}}{(Q_{i,1}+Q_{R,1}) + (Q_{i,2}+Q_{R,2}) + (Q_{i,3}+Q_{R,3})} \cdot \frac{(Q_{R,1}+Q_{R,2}+Q_{R,3})}{(Q_{R,1}+Q_{R,2}+Q_{R,3}) + (Q_{i,1}+Q_{i,2}+Q_{i,3})}$$

$$+ \frac{Q_{i,1}C_{i,t} + Q_{i,2}C_{i,t} + Q_{i,3}C_{i,t}}{(Q_{R,1}+Q_{R,2}+Q_{R,3}) + (Q_{i,1}+Q_{i,2}+Q_{i,3})} \qquad (4)$$

While this effort will not specifically consider the effects of local exhaust, the effects of local exhaust could be incorporated into the model through the adjustments of $C_{i,t}$, which denotes the concentration in the makeup air (i.e., the HVAC air intake). Using the model, it would be possible to study local exhaust effects by quantifying the results of varying the makeup air concentration as a function of the exhaust concentration.

Once Euler's Method has been used to obtain the concentration within each zone as a function of time, the cumulative exposure within each zone can be calculated by numerical integration; e.g., for Zone 1 (see Equation 5):

$$E_1 = \int C_1(t)\,dt \qquad (5)$$

Where E_1 denotes the cumulative exposure in Zone 1.

The mass balance approach described above allows for time- and location-dependent concentrations to be predicted for each zone of the building. Those time-dependent concentration estimates are then used in Section 7.0, when the model results are compared to the measured aerosol concentration for the various release scenarios, building configurations, and HVAC operating conditions.

Experimental Methods

5.1 Test Design

Introductory note: A Quality Assurance Project Plan (QAPP) was developed for the experimental program discussed in this chapter and was approved by the EPA project lead. The QAPP was not approved by the EPA QA officer; however, this final report does address the officer's key QA concerns.

The test design for this experimental work was guided by the effort in developing the simple three-zone, well-mixed model described in Section 4.0. This effort identified the filtration efficiency, leakage, system recirculation, and building size relative to the room of release as the key parameters in assessing the impact of an indoor CB attack. Other parameters (e.g., the infiltration and makeup air) were found to have a lesser impact on the resulting concentrations and exposures in comparison to the aforementioned parameters of filtration efficiency, leakage, and system recirculation. This initial modeling analysis was used as a basis to design the experimental field study. Filtration efficiencies ranging from no filtration (i.e., the natural loss of aerosol in ductwork and other AHU components) to a high-efficiency filter (i.e., a 95% dioctyl phthalate [DOP] rated filter) were selected to cover a range of possible filtration efficiencies. Natural losses of aerosol were treated as a filtration efficiency to represent the lower possible range of filtration efficiencies. Recirculation

rates of 3, 5, and 7 air changes per hour (ACH) were initially planned to cover the range of likely system recirculation rates; however, due to limitations of the HVAC system, it was not possible to achieve recirculation rates above 6 ACH. Therefore, it was decided to encompass only the low (3 ACH) and moderate (5 ACH) recirculation conditions. Two leakage conditions were chosen as goals for the study: low leakage ($\leq$0.4 ACH) and high leakage ($\geq$0.6 ACH). These selections were made due to the desire for a natural leakage path as would occur in any common building (as opposed to a forced leakage with a small fan) and the resulting lack of control over the leakage rates. The high and low leakage values were chosen to approximate "loose" and "tight" building construction, respectively.

A tiered test matrix was initially designed to provide a planned approach of study for numerous possible test outcomes and contingencies. This matrix provided adequate coverage of the range of parameters of interest to demonstrate that the model findings were accurate with respect to estimating the effects of building/HVAC parameters and contaminant concentration. Rapid analysis and reduction of results were then used to decide which tests in the tiered matrix would be performed. The final test matrices are shown in Tables 1 and 2 for moderate and low recirculation.

Table 1. Moderate Recirculation Test Matrices

Recirculation	Building Size	Leakage	Filtration
"Moderate" (5 ACH)	"Large"	"Low" (0.175 ACH)	"Low" (10%)
			"Moderate-Low" (25%)
			"Moderate-Low" (25%)
			"Moderate" (50%)
			"High" (90%)
		"High" (1.025 ACH)	"Low" (10%)
			"Moderate" (50%)
			"High" (90%)
	"Small"	"Low" (0.125 ACH)	"Low" (10%)
			"Moderate" (50%)
			"High" (90%)
		"High" (1.175 ACH)	"Low" (10%)
			"Moderate" (50%)
			"High" (90%)

"Large" notional building / "Low" leakage denotes a closed door position
"Large" notional building / "High" leakage denotes a door ajar position
"Small" notional building / "Low" leakage denotes a door open 20 cm
"Small" notional building / "High" leakage denotes a door fully open

Table 2. Low Recirculation Test Matrices

Recirculation	Building Size	Leakage	Filtration
"Low" (3 ACH)	"Large"	"Very Low" (0.050 ACH)	"Moderate" (50%)
		"Low" (0.200 ACH)	"Low" (10%)
			"Moderate" (50%)
			"High" (90%)
		"High" (0.950 ACH)	"Moderate" (50%)
	"Small"	"Moderate" (0.725 ACH)	"Low" (10%)
			"Moderate" (50%)
			"High" (90%)

"Large" notional building / "Very Low" leakage denotes a closed door position
"Large" notional building / "Low" leakage denotes a door partially ajar
"Large" notional building / "High" leakage denotes a door open about 1 cm
"Small" notional building / "Moderate" leakage denotes a door open 70 cm

5.2 Test Building Description

The venue for these tests was a three-story building, located in Anniston, Alabama. The building's HVAC system consisted of three separate air handling units (AHUs), each servicing a specific region of the building (see Figure 2). The 1st floor of the building did not possess an active HVAC system (shaded in white in Figure 2). Air handler 1 (AHU1) serviced approximately 2/3 of the 3rd floor of the building (shaded in blue in Figure 2). Air handler 2 (AHU2) serviced approximately 2/3 of the 2nd floor of the building (shaded in red in Figure 2). Air handler 3 (AHU3) serviced a multi-floor region of the building consisting of approximately 1/3 of the 2nd and 3rd floors (shaded in green in Figure 2). Each of the AHUs possessed its own supply and return ductwork. Since the simple well-mixed model considers only a simple HVAC system with a common supply and return ductwork, a subsection of the test building, defined as the HVAC region serviced by AHU3, was selected for subsequent study. The HVAC region serviced by AHU3 was of particular interest for this study because it spanned multiple floors and would require the least number of building modifications to provide a suitable test venue.

Each supply vent and return duct was equipped with a simple, manually operated damper that controlled the fractioning of supply and return flows using "path of least resistance" principles. While this simple construction prevented the creation of significant pressure differences between zones, it is believed to be representative of typical HVAC design. The fraction of total airflow recirculated (and thus the fraction of fresh air) was adjusted via variable flow controllers and a central computer control system. In addition, the total airflow delivered by the air handling unit was also controlled via the computer control system.

Some initial building alterations were required prior to testing to allow for the desired test conditions. These alterations involved the extension of existing walls to create independent zones, the addition of new walls to create independent zones, and the creation of a number of return inlets within the newly created zones. The alterations made to the building were performed by professional contractors and are described in detail below, as well as illustrated in Figures 3 and 4.

The test bed contains three independent air handling units that service three independent HVAC regions. Throughout this document the terms "test volume" and "building" will be used interchangeably to refer to the HVAC region that constitutes the easternmost portion of the top two floors of the building (i.e., the portion shaded in green in Figure 2). The building construction is a standard commercial design in which a limited number of walls extend beyond the drop ceiling to the slab. For the purposes of modeling the building, it is important to note that only walls that extend to the slab define a zone. Prior to alterations, the HVAC region contained only four independent zones of approximately the same size (i.e., two on each floor). As discussed previously, this effort required both large and small notional building scenarios. To achieve this, walls were either added or extended to define new zones. Again, it is important to note that "large" and "small" refer to the size of the building relative to the zone of interest. For example, a 3,000 m³ building composed of 100 rooms that are each 30 m³ in volume is equivalent to a 50,000 m³ building composed of 100 rooms that are each 500 m³ in volume. The building size relative to the zone of interest for both of these examples would be 100, making each of them a "large" notional building.

On the upper floor (3rd floor), a portion of an existing wall was extended to the slab and a new slab-to-slab wall was constructed to split Room B209 into two independent zones. The newly created zones were approximately equal in volume with each representing approximately one-tenth (1/10) of the test volume. These alterations created the zone of interest and zone of release for the "small" notional building and are illustrated in Figure 3. In addition, a door was incorporated into the new wall to provide a variable leak path between the zone of release and zone of interest.

On the lower floor (2nd floor), the existing walls that defined a series of small rooms were extended to the slab to create four independent zones. Each of the newly created zones was approximately one-seventy-fifth (1/75) of the test volume. Two of the zones, B113 and B114, were used as the zone of interest and the zone of release, respectively, for the "large" notional building. These alterations are illustrated in Figure 4. Doors were also added to the walls between each of the newly created zones to provide a variable leak path between the zones.
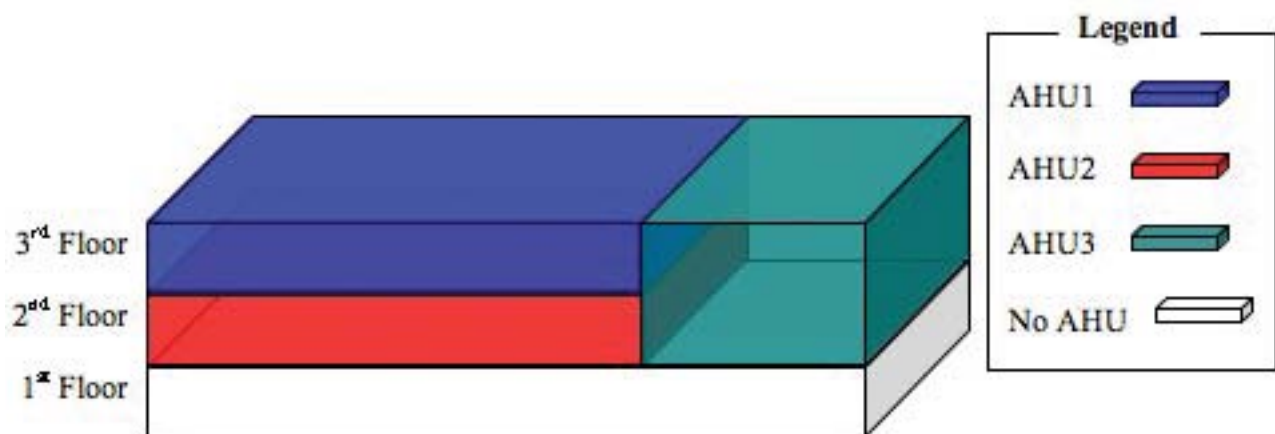
Figure 2. Test Building HVAC Region Diagram

While each of these newly created zones already possessed a makeup air inlet (i.e., a fresh air supply vent), most lacked a return inlet (i.e., a recirculated air intake). For this reason, return inlets were added to each of the newly created zones (see Figures 3 and 4). Each return inlet was equipped with a damper to adjust the recirculated airflow taken from each zone. These building alterations produced an experimental test volume suitable for the planned experiments. The test volume is considered to represent exceptionally tight construction. All doors possessed high quality seals and sweeps. All walls were well caulked and sealed. For this reason, the leakage observed under various door positions during this study should not necessarily be taken as standard leakage rates for other buildings.
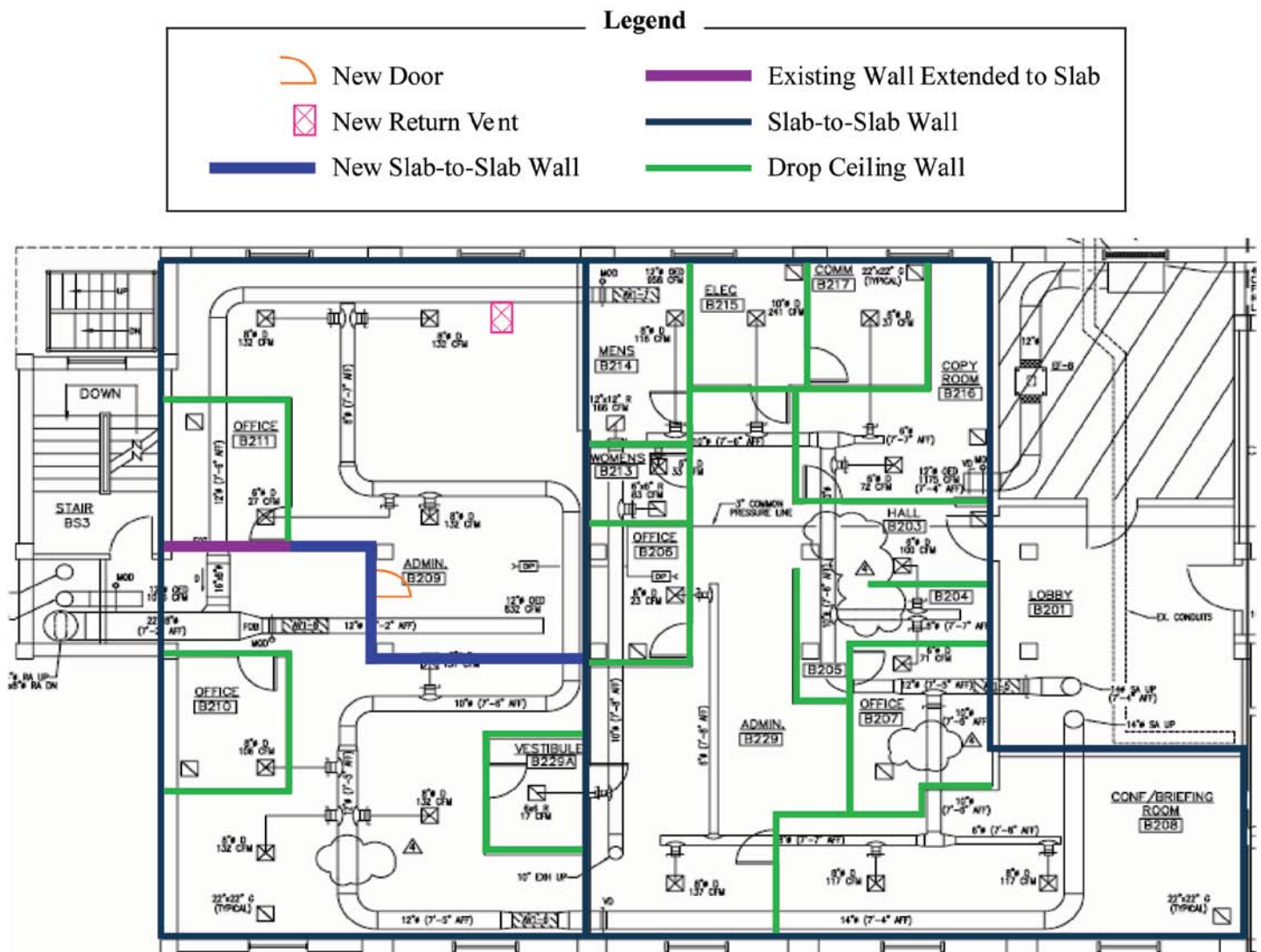
Figure 3. Alterations to the Upper Floor (3rd Floor) of the Test Volume
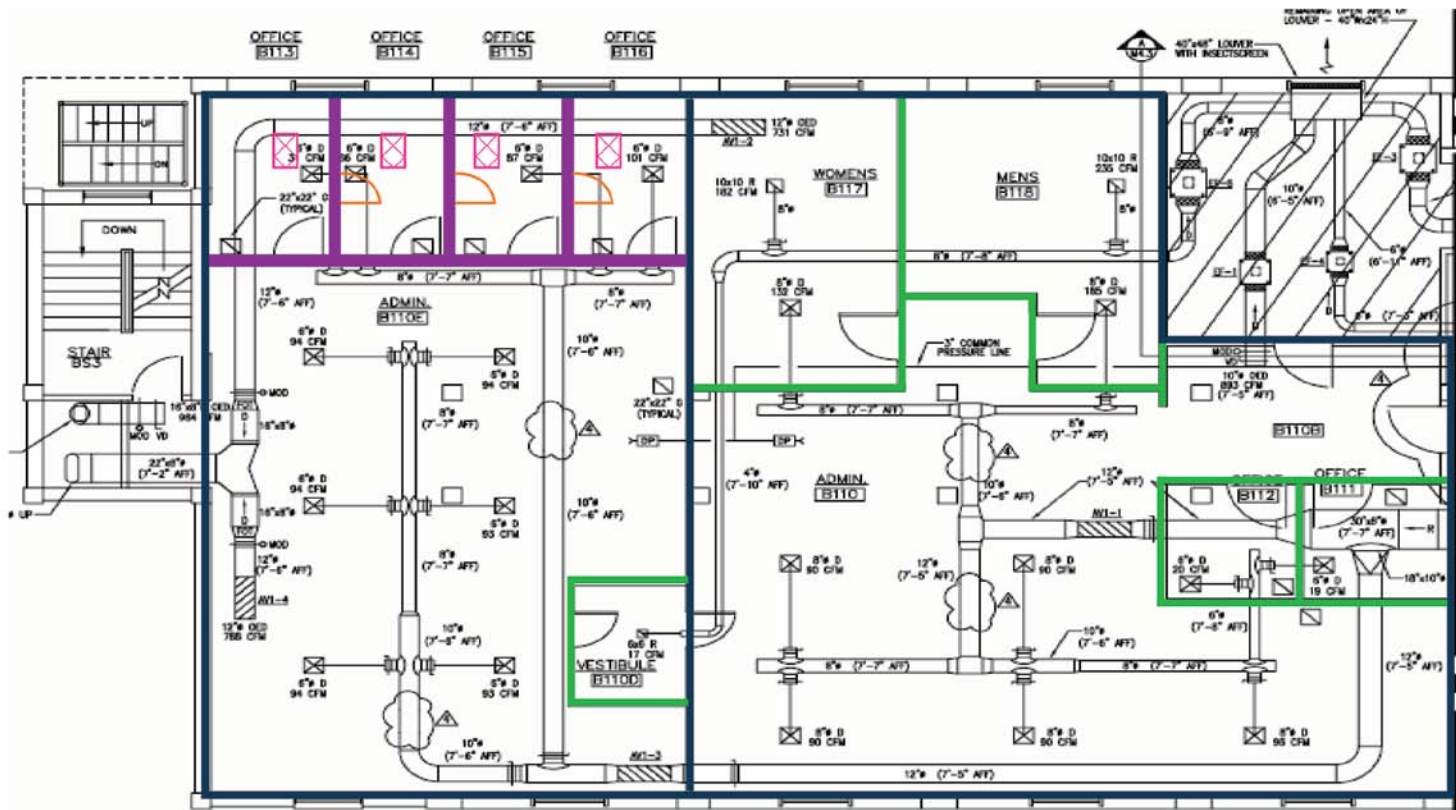
Figure 4. Alterations to the Lower Floor (2nd Floor) of the Test Volume

5.3 Release Methods

Visolite®, a fluorescent-tagged, calcium carbonate (chalk) dust, was used as the innocuous aerosol tracer. A particulate aerosol was chosen as the tracer for this effort because of the advantages of existing filtration systems and real-time measurement systems, such as optical particle counters. It is important to note that while a particulate aerosol was used for this experimental effort, the model and analysis presented here is valid for any contaminant that does not appreciably deposit or adsorb on surfaces during the timeframe of interest.

The amount of Visolite® to be released was estimated based on the results of previous indoor air quality field studies performed by Battelle. These previous results, combined with past experience, suggested that a release of 1 to 20 grams of Visolite® would be sufficient to produce the desired test aerosol. The main elements of the release mechanism are an air supply, an eductor, a grooved turntable, and a rotary motor (see Figure 5). Air flowing through the eductor creates a suction that pulls the Visolite® powder from the grooved turntable. Provided the powder is evenly distributed within the groove of the turntable, the speed at which the motor rotates the turntable defines the release rate of the aerosol.

In previous work this eductor type mechanism has proven its effectiveness in dispersing similar quantities of a powder aerosol. The particle size distribution of Visolite® aerosolized via this eductor mechanism is shown in Figure 6. Since it is possible that the solid aerosol dissemination will produce nuisance dust levels that are temporarily above suggested safety limits, the release will be triggered by an electronic timer to avoid any potential exposure of test personnel.
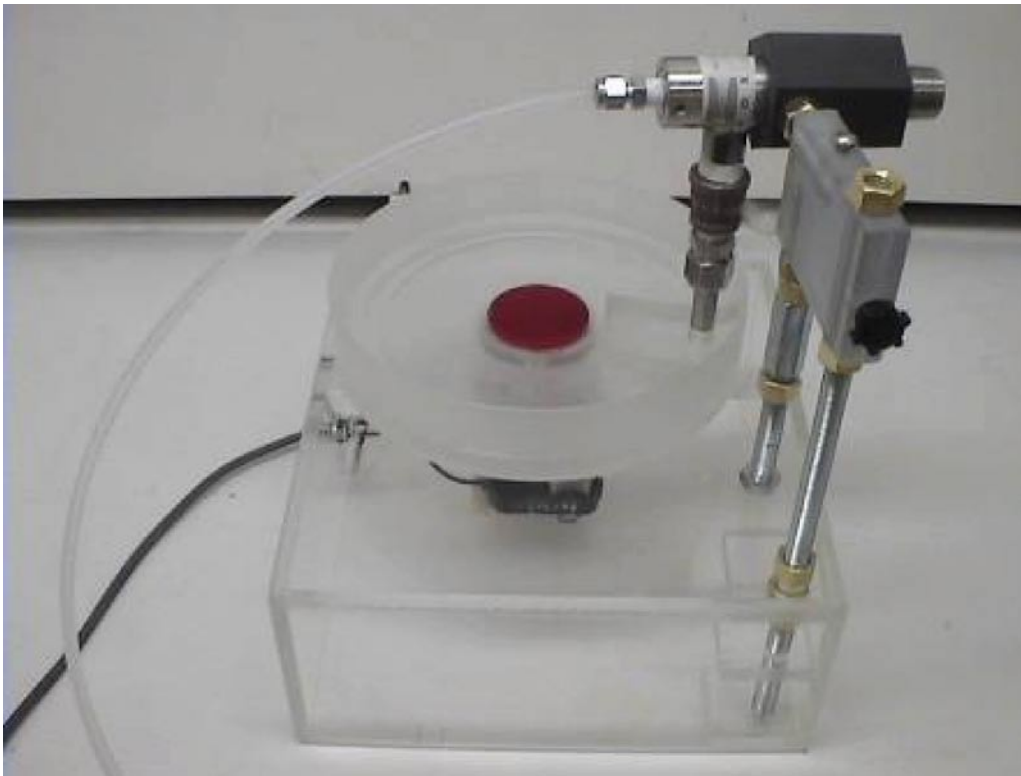
Figure 5. Photograph of the Particulate Eductor Release Mechanism
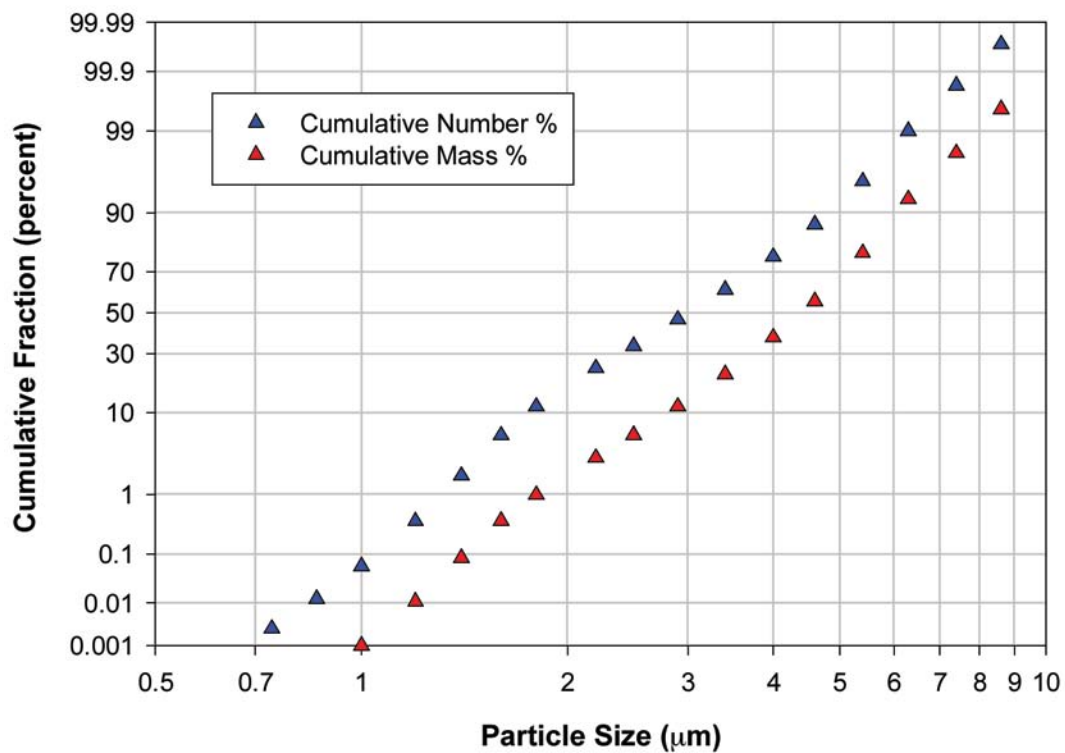
Figure 6. Particle Size Distribution of Visolite® Aerosolized with an Eductor Release Mechanism Operating at a Gas Flow Rate of 100 lpm as Measured by an Aerosizer®

5.4 Sampling Methods

During the testing period, five handheld particle counters (MetOne model HHPC-6, manufactured by Hach Ultra Analytics, see Figure 7) were used to monitor aerosol levels at selected locations within the area of interest. The MetOne particle counter uses optical particle counting techniques (i.e., measuring the scattered light as particles pass through a laser) to provide data on six particle size ranges from 0.3 to 20 µm (0.5 to 0.7 µm, 0.7 to 1.0 µm, 1.0 to 2.0 µm, 2.0 to 5.0 µm, 5.0 to 10.0 µm, and 10.0 to 20 µm). Since the Visolite® particles are being used only as a tracer or indicator, the particle size distributions were not of interest, only particle concentration. For this effort, particle concentrations from the MetOne channel ranging from 2.0 to 5.0 µm were used as the indicator of the Visolite® concentration. Figure 8 shows a typical example of MetOne data gathered in the zone of interest during testing. Typical background levels can be observed in the time period prior to release (i.e., time less than zero). The Data Quality Objectives (DQOs) and an electronic archive of the data gathered during this work can be found in Appendices C and D, respectively.

The MetOne particle counter is lightweight and automated, making it easy to deploy/recover, which facilitates rapid turnaround. Pretest procedures involve turning the instrument on and pressing the start button. MetOne particle counters were factory calibrated prior to use in this study. In addition, the outputs from the multiple MetOne units used in this study were compared against each other to ensure sizing consistency throughout the study. When not in use, MetOne particle counters were run continuously on HEPA-filtered air to flush and clean the devices.

The apparent discrepancy between the particle size distribution in comparison to Figure 6 is attributed to a difference in the operating principle of the particle sizer (optical versus time of flight) and a potential error in the sizing of a fluorescent particle using optical means. This does not significantly impact this work since the 2.0 to 5.0 µm channel is used as a tracer (i.e., the exact size range of particles measured by a given channel is not critical to this study as long as it is constant throughout experimentation).

Figure 7. Photograph of MetOne Handheld Optical Particle Counter
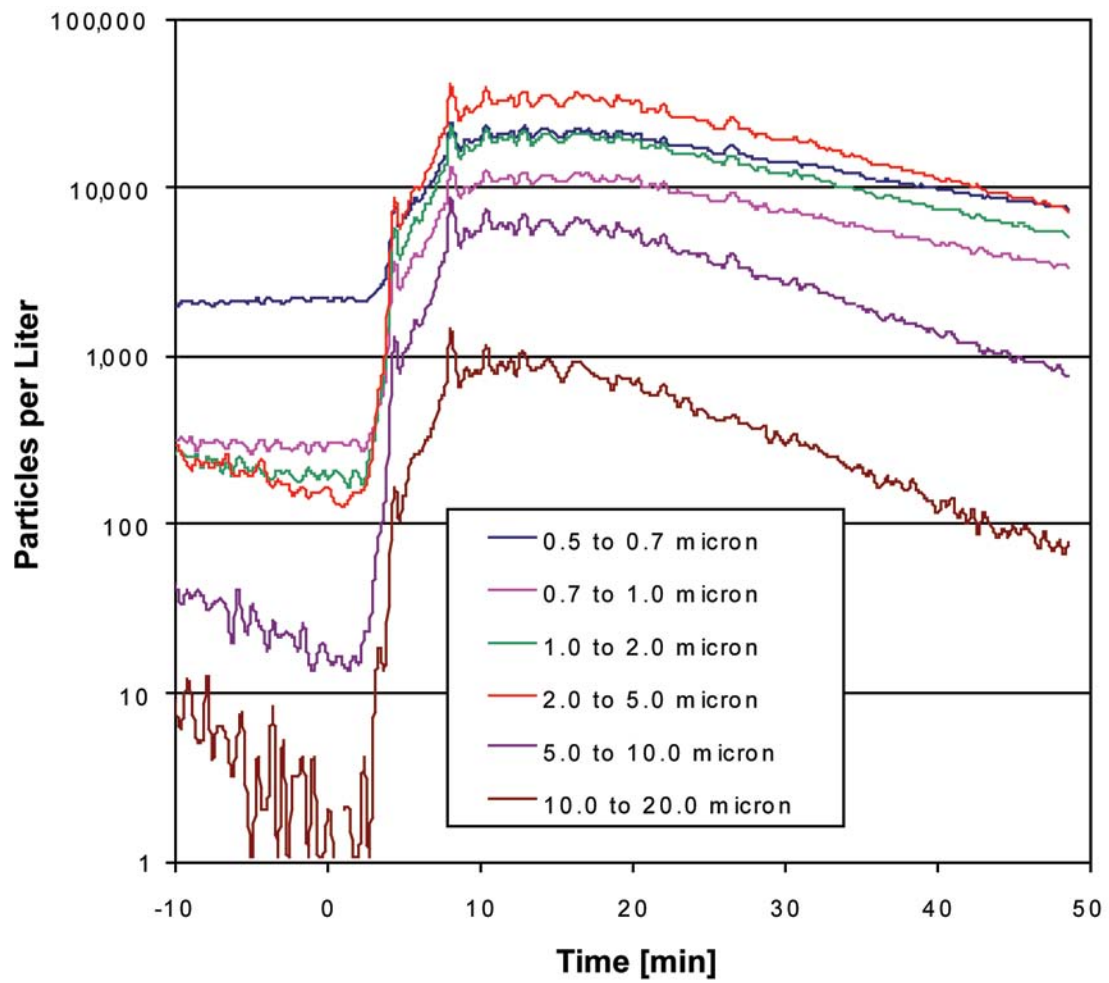
Figure 8. Typical Particulate Data Gathered by a MetOne During Testing

Prior to conducting the experimental study, a number of preliminary efforts were required to ensure relevant, usable data. These preliminary efforts consisted of initial building alterations, airflow measurements, and initial leakage tests.

Since the main goal of the experimental work was comparison with a model, the actual values of HVAC parameters were of critical importance. To this end, a brief series of HVAC parameter quantification tests was performed to experimentally determine, or in some cases verify, the actual values of key HVAC parameters. These tests can be divided into airflow measurements and leakage tests. Airflow measurements consisted of measuring the volumetric flow rate or face velocity at all ductwork throughout the test bed. Leakage tests were initially intended to provide a direct measure of the interzonal leakage under operational conditions. Unfortunately, due to leakage across a return damper, the intended method was no longer viable and a combinatorial approach was adopted.

6.1 Airflow Measurements

The first portion of the preliminary characterization tests consisted of measuring the airflow using various anemometers, adjusting the blower and Phoenix valve settings that control the HVAC flows, and subsequently remeasuring the airflows.

A balometer (ALNOR model number APM 150) and an anemometer (Davis model number LCA30 VT) were used to measure flow (see Figure 9 for photograph). These methods were sufficient for experimentally measuring the system recirculation and makeup air rates for each zone.

The low, moderate, and high recirculation rates initially planned for this study were intended to cover a range of recirculation rates from 3 to 7 ACH. However, due to limitations of the HVAC system, it was not possible to achieve recirculation rates greater than 6 ACH. Therefore, it was decided to reduce the scope of the study to encompass only the low and moderate recirculation conditions. In addition, the use of four mixing fans each in both the zone of interest and zone of release of the "small" notional building were added to enhance mixing. Tables 3 and 4 contain the results for moderate recirculation flow measurements made on the lower and upper floors, respectively, while Table 5 contains summary information in the form of air exchange rates for the moderate recirculation condition (nominally 5 ACH). Similarly, Tables 6 and 7 contain the results for low recirculation flow measurements made on the lower and upper floors, respectively, while Table 8 contains summary information in the form of air exchange rates for the low recirculation condition (nominally 3 ACH).
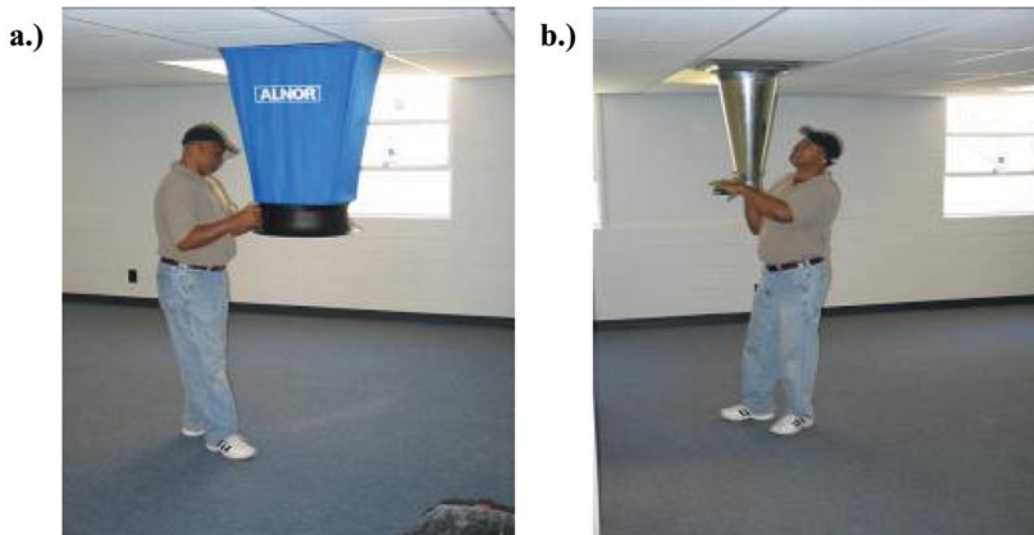
Figure 9. Photographs of Flow Measurement Using a.) a Balometer and b.) an Anemometer

Table 3. Lower Floor Airflow Measurements Under Moderate Recirculation

Zone ID	Room Number	Room Volume [ft³]	Vent ID	Type	Measured Flow [cfm]
L1	**B113**	561	S1	Supply	56
			R1	Return	54
L2	**B114**	561	S2	Supply	55
			R2	Return	58
L3	**B115**	561	S3	Supply	56
			R3	Return	57
L4	**B116**	557	S4	Supply	57
			R4	Return	56
L5	**B110E**	7,417	S5	Supply	140
			S6	Supply	144
			S7	Supply	128
			S8	Supply	120
			S9	Supply	142
			S10	Supply	132
			R5	Return	860
	B110D	381	N/A		
L6	**B110**	7,709	S11	Supply	151
			S12	Supply	170
			S13	Supply	145
			S14	Supply	148
			S15	Supply	153
	B111	484	S16	Supply	53
	B112	421	S17	Supply	56
	B110B	1,092	N/A		
	B117	1,790	S18	Supply	209
			R6	Return	1,280
	B118	1,826	S19	Supply	194

N/A is defined as not applicable.

Bold room numbers are those rooms that nominally represent the zone and are referred to as nominal room numbers in other tables.

Table 4. Upper Floor Airflow Measurements Under Moderate Recirculation

Zone ID	Room Number	Room Volume [ft³]	Vent ID	Type	Measured Flow [cfm]
U1	B209A	3,989	S20	Supply	114
			S21	Supply	110
			S22	Supply	101
			S24	Supply	110
			R7	Return	499
	B211	579	S23	Supply	66
U2	B209B	3,420	S25	Supply	171
			S26	Supply	187
			R8	Return	445
	B210	512	S27	Supply	106
	B229A	379	N/A		
U3	B229	3,125	S28	Supply	190
	B203	513	S29	Supply	137
	B204	380	N/A		
	B205	99	N/A		
	B206	477	S30	Supply	61
	B207	745	S31	Supply	67
	B208	3,175	S32	Supply	141
			S33	Supply	113
	B213	252	S34	Supply	90
	B214	621	S35	Supply	171
			R9	Return	1,240
	B215	490	S36	Supply	75
	B216	1,030	S37	Supply	110
	B217	508	S38	Supply	116

N/A is defined as not applicable.

Bold room numbers are those rooms that nominally represent the zone and are referred to as nominal room numbers in other tables.

Table 5. Moderate Recirculation Airflow Summary

Zone ID	Nominal Room Number	Zone Volume [ft³]	Measured Makeup Air [ACH]	Measured Recirculation [ACH]
L1	B113	561	1.0	5.0
L2	B114	561	1.0	4.9
L3	B115	561	1.0	5.0
L4	B116	557	1.0	5.1
L5	B110E	7,798	1.0	5.1
L6	B110	13,322	1.0	4.8
U1	B209A	4,568	1.1	5.5
U2	B209B	4,311	1.1	5.4
U3	B229	11,415	1.1	5.6

Table 6. Lower Floor Airflow Measurements Under Low Recirculation

Zone ID	Room Number	Room Volume [ft³]	Vent ID	Type	Measured Flow [cfm]
L1	**B113**	561	S1	Supply	37
			R1	Return	32
L2	**B114**	561	S2	Supply	38
			R2	Return	39
L3	**B115**	561	S3	Supply	38
			R3	Return	39
L4	**B116**	557	S4	Supply	36
			R4	Return	38
L5	**B110E**	7,417	S5	Supply	86
			S6	Supply	93
			S7	Supply	71
			S8	Supply	85
			S9	Supply	84
			S10	Supply	88
			R5	Return	510
	B110D	381		N/A	
L6	**B110**	7,709	S11	Supply	108
			S12	Supply	130
			S13	Supply	116
			S14	Supply	114
			S15	Supply	126
	B111	484	S16	Supply	38
	B112	421	S17	Supply	36
	B110B	1,092		N/A	
	B117	1,790	S18	Supply	170
			R6	Return	998
	B118	1,826	S19	Supply	160

N/A is defined as not applicable.

Bold room numbers are those rooms that nominally represent the zone and are referred to as nominal room numbers in other tables.

Table 7. Upper Floor Airflow Measurements Under Low Recirculation

Zone ID	Room Number	Room Volume [ft³]	Vent ID	Type	Measured Flow [cfm]
U1	**B209A**	3,989	S20	Supply	63
			S21	Supply	80
			S22	Supply	68
			S24	Supply	73
			R7	Return	341
	B211	579	S23	Supply	58
U2	**B209B**	3,420	S25	Supply	97
			S26	Supply	115
			R8	Return	270
	B210	512	S27	Supply	63
	B229A	379	N/A		
U3	**B229**	3,125	S28	Supply	133
	B203	513	S29	Supply	80
	B204	380	N/A		
	B205	99	N/A		
	B206	477	S30	Supply	30
	B207	745	S31	Supply	30
	B208	3,175	S32	Supply	95
			S33	Supply	69
	B213	252	S34	Supply	38
	B214	621	S35	Supply	125
			R9	Return	780
	B215	490	S36	Supply	38
	B216	1,030	S37	Supply	67
	B217	508	S38	Supply	80

N/A is defined as not applicable.

Bold room numbers are those rooms that nominally represent the zone and are referred to as nominal room numbers in other tables.

Table 8. Low Recirculation Airflow Summary

Zone ID	Nominal Room Number	Zone Volume [ft³]	Measured Makeup Air [ACH]	Measured Recirculation [ACH]
L1	B113	561	1.0	2.9
L2	B114	561	1.0	3.1
L3	B115	561	1.0	3.1
L4	B116	557	1.0	2.9
L5	B110E	7,798	1.0	2.9
L6	B110	13,322	1.1	3.4
U1	B209A	4,568	1.1	3.4
U2	B209B	4,311	1.0	2.9
U3	B229	11,415	1.0	3.1

6.2 Leakage Tests

The second portion of the preliminary characterization tests consisted of tests designed to determine the interzonal leakage under normal operating conditions. According to the results from the theoretical simulations, the quantification of the interzonal leakage rate represents a key measurement for this study. The interzonal leakage was to be measured by setting the HVAC system to run with 100% fresh air (i.e., no recirculation, with a greatly increased fresh air makeup air rate) and performing tracer gas tests with SF_6. Assuming there was no cross-contamination between the building exhaust and fresh air inlet, any SF_6 that entered the zone of interest must be due to interzonal leakage. By performing this leakage test at the various HVAC conditions planned for this study, an experimental measure of a key parameter could be determined. Other leakage measurement methods involve the overpressurization of the zone of interest and do not reflect normal building operation (ASTM, 2003).

The results of the initial leakage test indicated that significant recirculation was occurring (see Appendix A). Upon further investigation, it became apparent that significant leakage was occurring across the recirculation damper and that reducing that leakage to zero was not feasible given the materials and time constraints of the study. While it was possible to estimate the actual recirculation using the theoretical model, this represented an indirect method of estimating the interzonal leakage, which depended heavily on the model-predicted value of the recirculated airflow. For this reason, a combinatorial approach to determining the leakage was adopted.

Under a combinatorial approach, the leakage rates for a given building configuration (i.e., door position and recirculation rate) are estimated using the results of a single experiment. A leakage estimate was obtained by varying the leakage parameter within the model to find a value that resulted in good agreement between experimentally measured and model-predicted results for a single experiment (i.e., a minimum in the square of the error between model-predicted and experimentally measured values). The resulting estimated leakage rates are then used for all tests under that building configuration (i.e., door position and recirculated air rate). The resulting leakage estimate should be valid for any filtration efficiency since the filtration efficiency impacts the concentration in the zone, not the leakage rate (i.e., the flow rate across the leak path). In this fashion, a combinatorial approach effectively used a portion of the experimental data to directly estimate the interzonal leakage rate. The application of this combinatorial method is further clarified in the Results section of this report.

The test approach, which was adopted on-site, required a reorganization of the originally planned test matrices. Furthermore, since manual adjustments were needed for each recirculation condition, test matrices were organized by recirculation rate for efficiency reasons. Initially, all possible combinations of three filtration levels and two leakage levels were performed for two notional buildings for the moderate recirculation rate. This provided a solid basis for comparison of the experimental and model-predicted results, as well as the large body of data required for the combinatorial approach. Based on the interim results, it was agreed that a reduced test matrix was appropriate for the low recirculation condition given the excellent agreement of experimental and model results observed for the moderate recirculation condition (Sparks, 2005). For this reason, a limited matrix using three filtration levels and three leakage levels for the two notional buildings was executed for the low recirculation condition. Tables 9 and 10 contain the moderate and low recirculation test matrices, respectively.

The "large" notional building can be simplified in terms of three well-mixed zones and is shown in Figure 10. Room B113, which had a volume of 560 ft^3, was the zone of release (shaded blue in Figure 10). Room B114, which had a volume of 560 ft^3, was the zone of interest (shaded in cyan in Figure 10). Several rooms constituted the lumped zone, which represented the rest of the building in the model. The lumped zone had a volume of approximately 42,480 ft^3. Room B110, which had a volume of approximately 7,710 ft^3, was selected as representative of the lumped zone for the rest of the building (shaded in green in Figure 10). With the entire test volume constituting approximately 43,600 ft^3, the zone of interest and zone of release each represented approximately one-seventy-fifth (1/75) of the test volume.

The "small" notional building can be simplified in terms of three well-mixed zones and is shown in Figure 11. Room B209B , which had a volume of 4,310 ft^3, was the zone of release (shaded blue in Figure 11). Room B209A, which had a volume of 4,570 ft^3, was the zone of interest (shaded in cyan in Figure 11). Due to the size of both the zone of release and the zone of interest, four standard house fans were used in each of these zones to promote mixing. Room B110, which had a volume of approximately 7,710 ft^3, was selected as the room that would represent the lumped zone for the rest of the building (shaded in green in Figure 11). With the entire test volume constituting approximately 43,600 ft^3, the zone of interest and zone of release each represented approximately one-tenth (1/10) of the test volume.

In addition to the aforementioned zones, Room B115, which had an approximate volume of 560 ft3, was selected as an additional sampling location for the "large" notional building tests (shaded gold in Figure 10). By comparing the "large" notional building experimental test data from Rooms B115 and B110, the validity of using a lumped zone to approximate the majority of the test volume can be established. Experimental data gathered during this study indicate that the concentrations measured in Room B115 were indistinguishable from those in Room B110, thus showing the validity of the lumped zone approach (lumping multiple rooms into a single zone for modeling purposes). This agreement is shown graphically in Figure 12. After establishing the validity of this assumption, data from Room B110 and Room B115 were averaged to produce the lumped zone concentration curves for subsequent "large" notional building tests.

Table 9. Moderate Recirculation Test Matrix Results Key

Tracer	Recirculation	Building Size	Leakage	Filtration	Results Shown in Figure #
Particulate	"Moderate" (5 ACH)	"Large"	"Low" (0.175 ACH)	"Low" (10%)	15
Particulate				"Moderate-Low" (25%)	12
Particulate				"Moderate-Low" (25%)	13
Particulate				"Moderate" (50%)	14
Particulate				"High" (90%)	16
Particulate			"High" (1.025 ACH)	"Low" (10%)	18
Particulate				"Moderate" (50%)	17
Particulate				"High" (90%)	19
Particulate		"Small"	"Low" (0.125 ACH)	"Low" (10%)	25
Particulate				"Moderate" (50%)	20
Particulate				"High" (90%)	22
Particulate			"High" (1.175 ACH)	"Low" (10%)	24
Particulate				"Moderate" (50%)	21
Particulate				"High" (90%)	23

"Large" notional building / "Low" leakage denotes a closed door position
"Large" notional building / "High" leakage denotes a door ajar position
"Small" notional building / "Low" leakage denotes a door open 20 cm
"Small" notional building / "High" leakage denotes a door fully open

Table 10. Low Recirculation Test Matrix Results Key

Tracer	Recirculation	Building Size	Leakage	Filtration	Results Shown in Figure #
Particulate	"Low" (3 ACH)	"Large"	"Very Low" (0.050 ACH)	"Moderate" (50%)	27
Particulate			"Low" (0.200 ACH)	"Low" (10%)	30
Particulate				"Moderate" (50%)	28
Particulate				"High" (90%)	31
Particulate			"High" (0.950 ACH)	"Moderate" (50%)	29
Particulate		"Small"	"Moderate" (0.725 ACH)	"Low" (10%)	33
Particulate				"Moderate" (50%)	32
Particulate				"High" (90%)	34

"Large" notional building / "Very Low" leakage denotes a closed door position
"Large" notional building / "Low" leakage denotes a door partially ajar
"Large" notional building / "High" leakage denotes a door open about 1 cm
"Small" notional building / "Moderate" leakage denotes a door open 70 cm

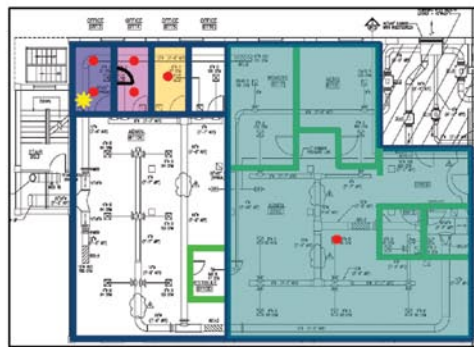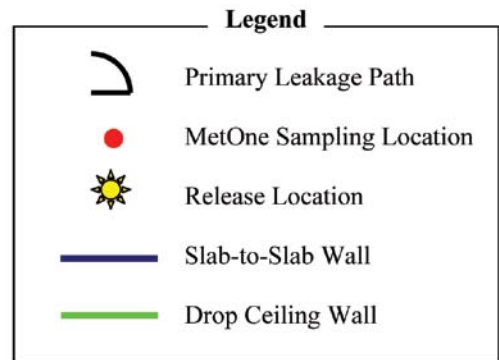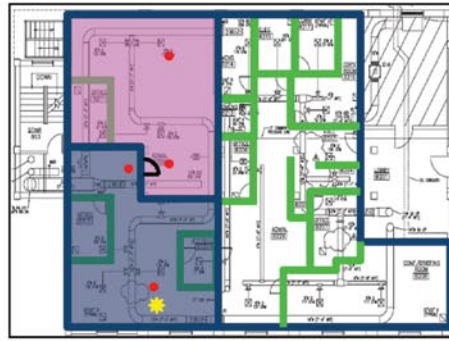**Figure 10.** Sampling Scheme for "Large" Notional Building

* B115 is the second room that comprises the lumped zone.
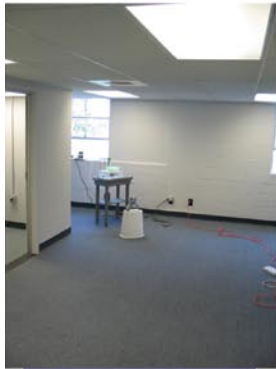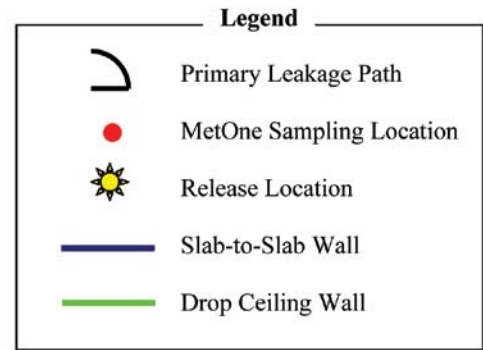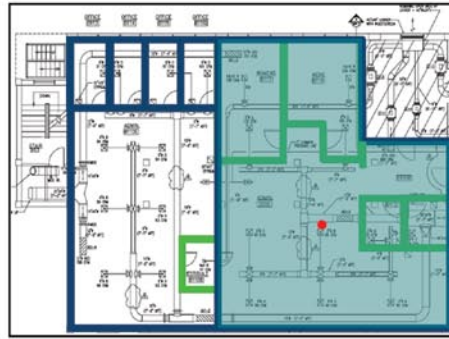
Figure 11. Sampling Scheme for "Small" Notional Building

The initial set of tests focused on the "large" notional building under moderate recirculation (5 ACH, see Tables 3 through 5 for further details). Figures 12 through 16 contain graphical comparisons of experimental and model-predicted data for four filtration levels at conditions of "low" leakage (i.e., the door between B113 and B114 closed). Both experimental and model-predicted data are presented as concentration in particles per liter (ppl) as a function of time with a release occurring at time zero. Experimental data presented are from the 2.0 to 5.0 µm channel of MetOne particle counters. Under the combinatorial approach, this set of experimental curves was used to estimate the "low" leakage rate, as well as the filtration efficiencies. Estimates were obtained by varying a parameter within the model to find a value that resulted in good agreement between experimentally measured and model-predicted results for a single experiment (i.e., a minimum in the square of the error between model-predicted and experimentally measured values). The resulting parameters were then used for subsequent tests under the appropriate conditions. Figure 12 illustrates the validity of the lumped zone assumption by comparing two of the constituent zones (B110 in green and B115 in gold). The good agreement exhibited in Figure 12 is indicative of all the "large" notional building results. As a result of this agreement, the lumped zone curves in other "large" notional building graphical comparisons will represent an average of these two zones. This validates the use of the lumped zone assumption and illustrates how a three-zone model can be used to provide useful information on real buildings with more than three zones. In addition, good agreement was observed between the two samplers placed in the zone of interest, supporting the well-mixed assumption in the small, 6′x10′ zone of interest (see Figure 13). As a result of this good agreement, data from the two samplers located in the zone of interest were numerically averaged to represent this zone. A comparison of Figures 12 and 13 also provides a limited demonstration of the repeatability of these results.

In general, all experimental data gathered over the course of this study exhibit imperfect mixing in the form of a mixing lag. The mixing lags observed seemed to correlate well with zone volume, meaning that smaller zones exhibited smaller mixing lags (see Figures 14 and 20). A mixing lag is a delay in the rise of a zone's experimental concentration in comparison to the perfect mixing exhibited by a theoretical model-predicted curve (see Figure 12). In addition to this, the experimentally observed release zone data collected during "large" notional building tests exhibit a plateau during the initial peak. This plateau was due to the saturation limit of the MetOne handheld particle counters used in this study. While a reduction in release mass could eliminate this sampling artifact, the release mass was nominally held constant to provide sufficient particulate levels in the lumped zone (i.e., the rest of the building) during high filtration tests.

The estimates of the effective filtration efficiency gleaned from this series of tests provide valuable insight. The results of this study indicate that even with no filter installed, the basic HVAC system used in the test bed is 10% efficient in removing particulate in the 2.0 to 5.0 µm range (see Figure 15). The data indicate that the MERV 7 and MERV 8 filters used during this

test performed below the rated efficiency of their respective MERV ratings (25% estimated during this study versus a specification of roughly 50 to 70% for the MERV 7, 50% estimated during this study versus a specification of 70% for the MERV 8). The MERV 7 results are consistent with those of a related project (referred to here as Task 2; Hecker, 2006), while no data from Task 2 were available for the MERV 8 filter. The 95% DOP filter used during testing performed slightly below the rated efficiencies (90% estimated during this study versus a specification of 95%+ for the 95% DOP). Task 2 data on the 95% DOP filter indicate a filtration efficiency greater than 99% over the applicable particle size range (Hecker, 2006). It is possible that the discrepancy between the results of this study and the rated efficiencies for the MERV 8 and 95% DOP filter are due to these estimates being made in an operating building rather than in a specially designed test fixture as used to obtain a MERV rating (i.e., leakage around the filters or leaks in ducting could be responsible for the reduced filtration efficiencies).

Figure 17 contains a graphical comparison of experimental and model-predicted data for the "high" leakage condition at moderate filtration (i.e., MERV 8 filter). Under the combinatorial approach these data were used to estimate the leakage rate associated with the "high" leakage condition (i.e., door between B113 and B114 ajar). Having successfully estimated both leakage rates (Figures 12 and 17) as well as effective filtration efficiencies (Figures 12 through 16), the remaining tests performed on the "large" notional building under moderate recirculation illustrate direct comparisons between experimental data and model predictions. Figures 18 and 19 graphically illustrate comparisons between experimental data and model predictions in which the value of all the HVAC parameters have previously been determined. Although the agreement between the experimental and model-predicted lumped zone (i.e., the rest of the building) suggests a slight error in the filtration efficiency estimates, on the whole, the agreement between experimental and model-predicted data for the "large" notional building under moderate recirculation is excellent.

Given the promising results of the initial test set, a second set of tests was undertaken focusing on the "small" notional building under moderate recirculation conditions (5 ACH, see Tables 3 through 5 for further HVAC flow details). Figures 21 and 22 contain graphical comparisons of the experimental and model-predicted data for two leakage conditions with a moderate filtration level (i.e., a MERV 8 filter). Under the combinatorial approach previously adopted, these two comparisons were used to estimate the leakage rates for the "small" notional building under moderate recirculation. Again, leakage estimates were obtained by varying the leakage parameter within the model to find a value that resulted in good agreement between experimentally measured and model-predicted results for a single experiment (i.e., a minimum in the square of the error between model-predicted and experimentally measured values). The resulting leakage parameter was then used for all tests performed under the given combination of door position and recirculated air rate.

Figure 12. Comparison of Experimental and Model-Predicted Data for "Large" Notional Building with Moderate Recirculation (5 ACH), Low Leakage (0.175 ACH), Moderate-Low Filtration (25% / MERV 7 Filter), Standard Makeup Air (1 ACH), and Standard Infiltration (0.5 ACH).
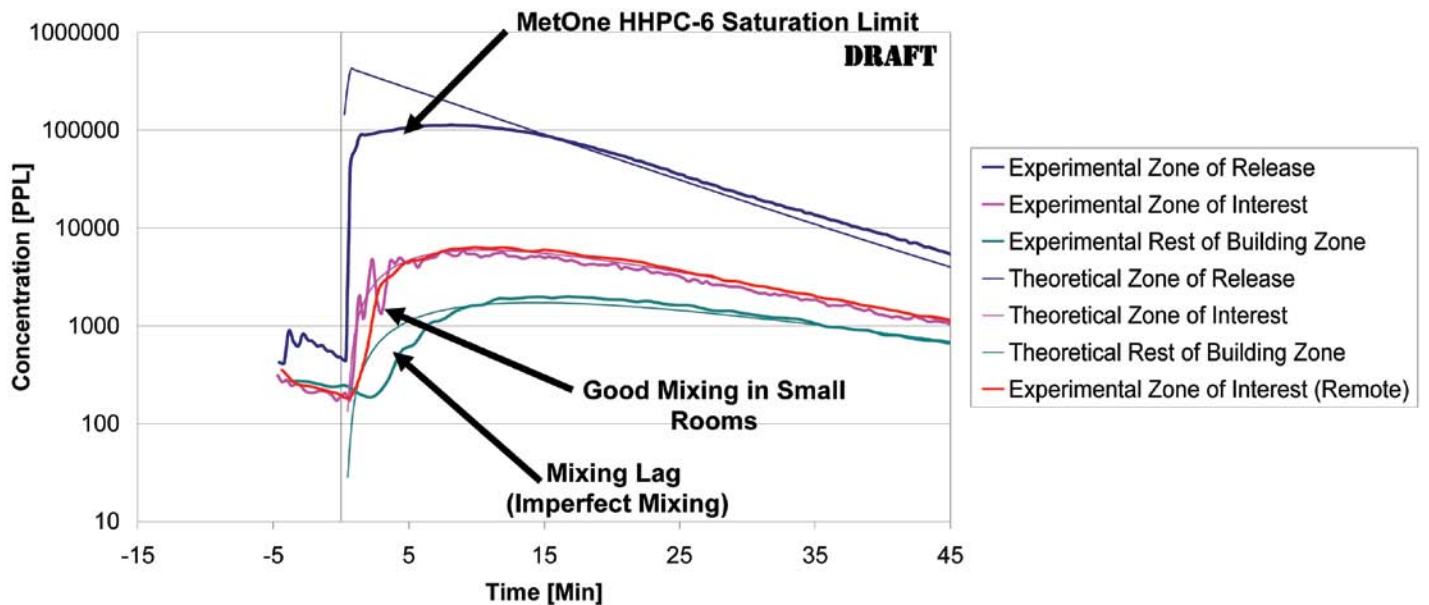
Figure 13. Demonstration of Repeatability by Comparison of Experimental and Model-Predicted Data for "Large" Notional Building with Moderate Recirculation (5 ACH), Low Leakage (0.175 ACH), Moderate-Low Filtration (25% / MERV 7 Filter), Standard Makeup Air (1 ACH), and Standard Infiltration (0.5 ACH).
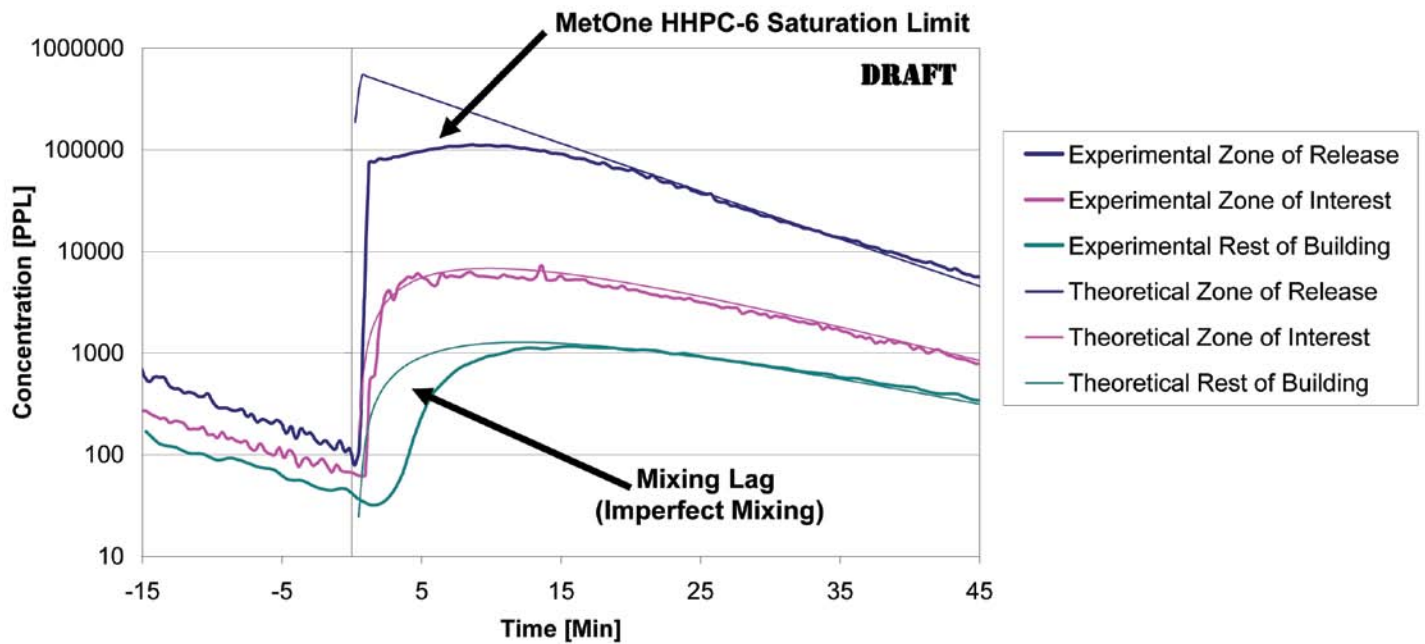
Figure 14. Comparison of Experimental and Model-Predicted Data for "Large" Notional Building with Moderate Recirculation (5 ACH), Low Leakage (0.175 ACH), Moderate Filtration (50% / MERV 8 Filter), Standard Makeup Air (1 ACH), and Standard Infiltration (0.5 ACH).
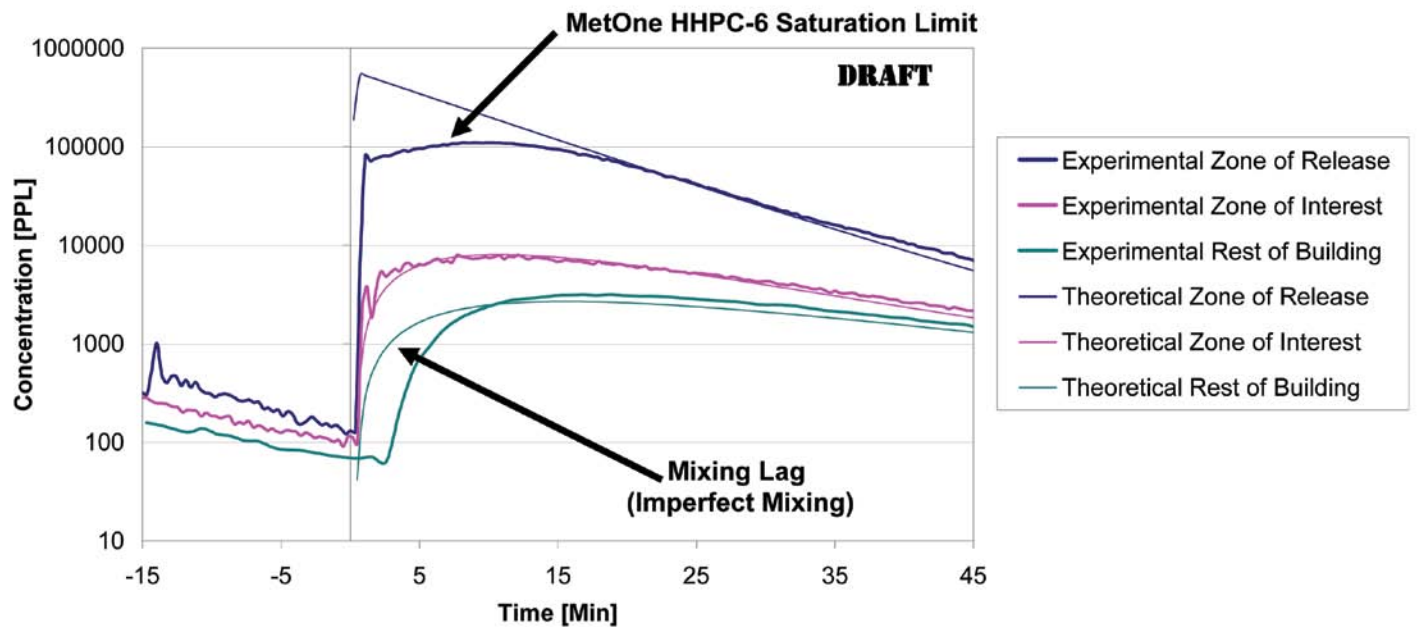
Figure 15. Comparison of Experimental and Model-Predicted Data for "Large" Notional Building with Moderate Recirculation (5 ACH), Low Leakage (0.175 ACH), Low Filtration (10% / No Filter), Standard Makeup Air (1 ACH), and Standard Infiltration (0.5 ACH).
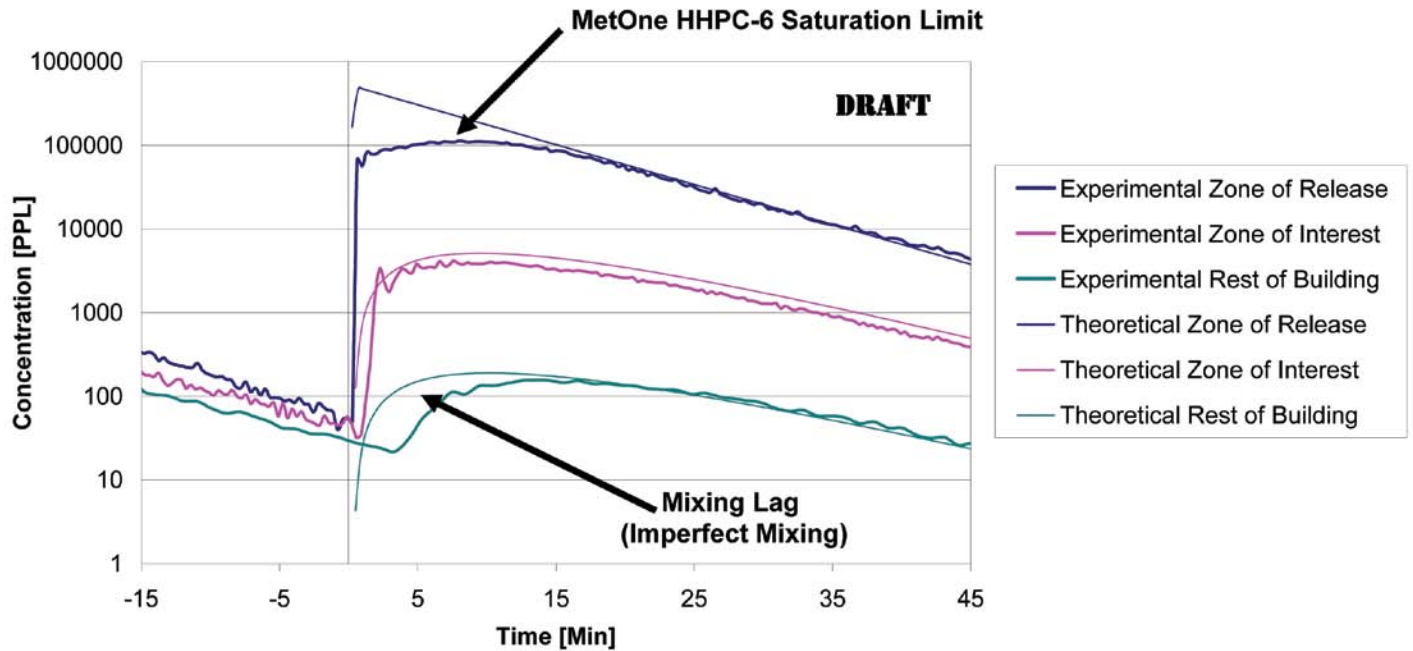
Figure 16. Comparison of Experimental and Model-Predicted Data for "Large" Notional Building with Moderate Recirculation (5 ACH), Low Leakage (0.175 ACH), High Filtration (90% / 95% DOP), Standard Makeup Air (1 ACH), and Standard Infiltration (0.5 ACH).
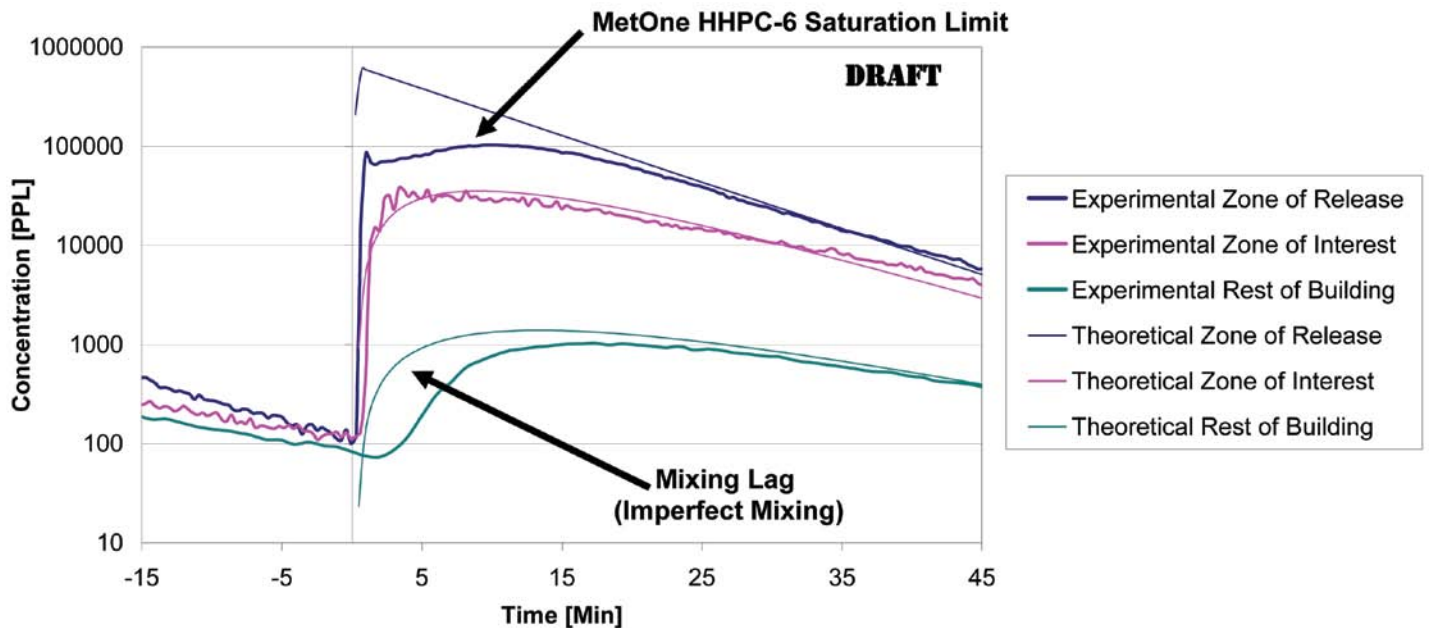
Figure 17. Comparison of Experimental and Model-Predicted Data for "Large" Notional Building with Moderate Recirculation (5 ACH), High Leakage (1.025 ACH), Moderate Filtration (50% / MERV 8), Standard Makeup Air (1 ACH), and Standard Infiltration (0.5 ACH).
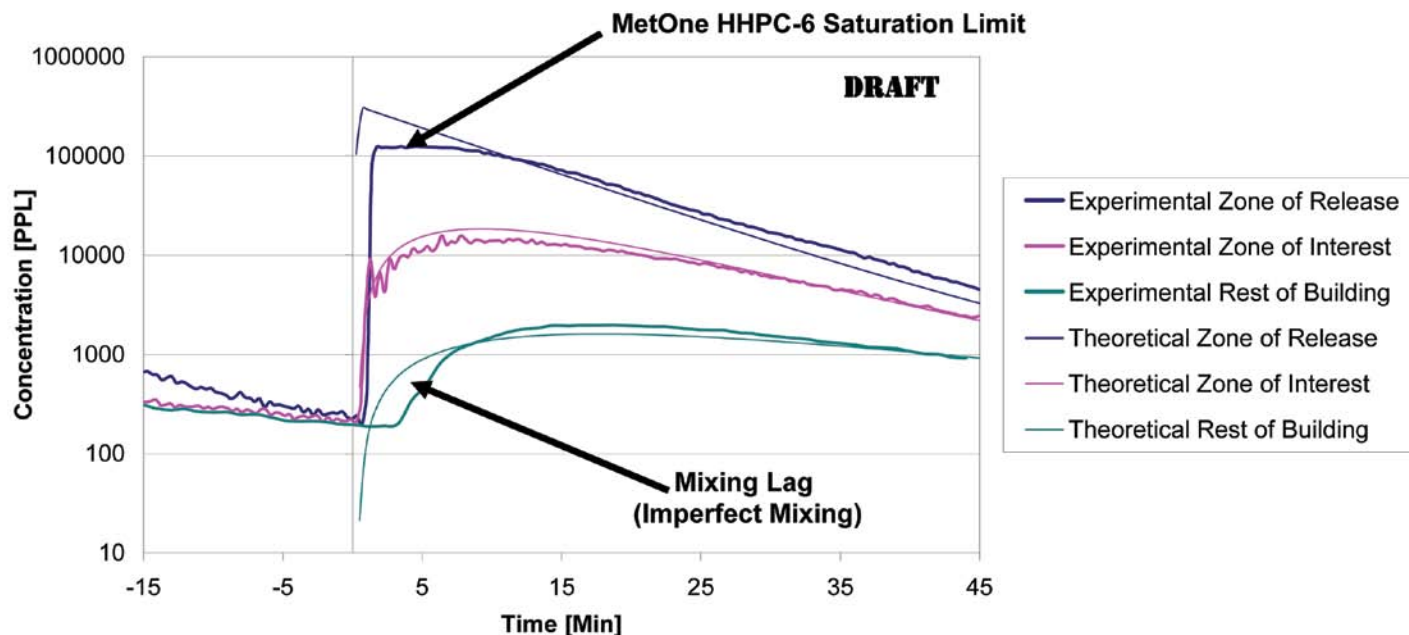
Figure 18. Comparison of Experimental and Model-Predicted Data for "Large" Notional Building with Moderate Recirculation (5 ACH), High Leakage (1.025 ACH), Low Filtration (10% / No filter), Standard Makeup Air (1 ACH), and Standard Infiltration (0.5 ACH).

Figure 19. Comparison of Experimental and Model-Predicted Data for "Large" Notional Building with Moderate Recirculation (5 ACH), High Leakage (1.025 ACH), High Filtration (90% / 95% DOP), Standard Makeup Air (1 ACH), and Standard Infiltration (0.5 ACH).

Figure 20. Comparison of Experimental and Model-Predicted Data for "Small" Notional Building with Moderate Recirculation (5 ACH), Low Leakage (0.125 ACH), Moderate Filtration (50% / MERV 8), Standard Makeup Air (1 ACH), and Standard Infiltration (0.5 ACH).

Throughout the tests for the "small" notional building, a mixing lag was observed within both the zone of release and the zone of interest. This mixing lag is evident when comparing samplers located at different areas of the two zones (for the zone of release, compare the dark blue and light blue lines in Figures 21 and 22; for the zone of interest, compare the cyan and red lines in Figures 21 and 22). Note that locations labeled "remote" were located farther from the source of particles (e.g., the release source in the zone of release or the primary leakage path in the zone of interest). From Figures 21 and 22, it is clear that, even with the assisted mixing of the house fans, there was a finite lag in the transport and mixing of Visolite® across the zones. However, it is also clear that, after that finite mixing lag, the volume appears to have been well mixed and subsequently agrees very well with model predictions.

Since the filtration efficiencies have already been estimated from the initial "large" notional building tests, the remaining four tests illustrated direct comparisons between experimental and model-predicted data. Figures 22 through 25 graphically illustrate the excellent agreement between experimental data and model predictions. The slight discrepancies observed can easily be attributed to an initial mixing lag and a combination of experimental error in measured and estimated parameters. This excellent agreement was a clear indication that the three-zone, well-mixed model is accurate in simulating the effects of changes in filtration efficiency and interzonal leakage rates for a notional building. Thus, after a cursory analysis of the data, a subsequent series of tests was focused on the effects of changing the recirculation.

Figure 21. Comparison of Experimental and Model-Predicted Data for "Small" Notional Building with Moderate Recirculation (5 ACH), High Leakage (1.175 ACH), Moderate Filtration (50% / MERV 8), Standard Makeup Air (1 ACH), and Standard Infiltration (0.5 ACH).

Figure 22. Comparison of Experimental and Model-Predicted Data for "Small" Notional Building with Moderate Recirculation (5 ACH), Low Leakage (0.125 ACH), High Filtration (90% / 95% DOP), Standard Makeup Air (1 ACH), and Standard Infiltration (0.5 ACH).

Figure 23. Comparison of Experimental and Model-Predicted Data for "Small" Notional Building with Moderate Recirculation (5 ACH), High Leakage (1.175 ACH), High Filtration (90% / 95% DOP), Standard Makeup Air (1 ACH), and Standard Infiltration (0.5 ACH).

Figure 24. Comparison of Experimental and Model-Predicted Data for "Small" Notional Building with Moderate Recirculation (5 ACH), High Leakage (1.175 ACH), Low Filtration (10% / No filter), Standard Makeup Air (1 ACH), and Standard Infiltration (0.5 ACH).
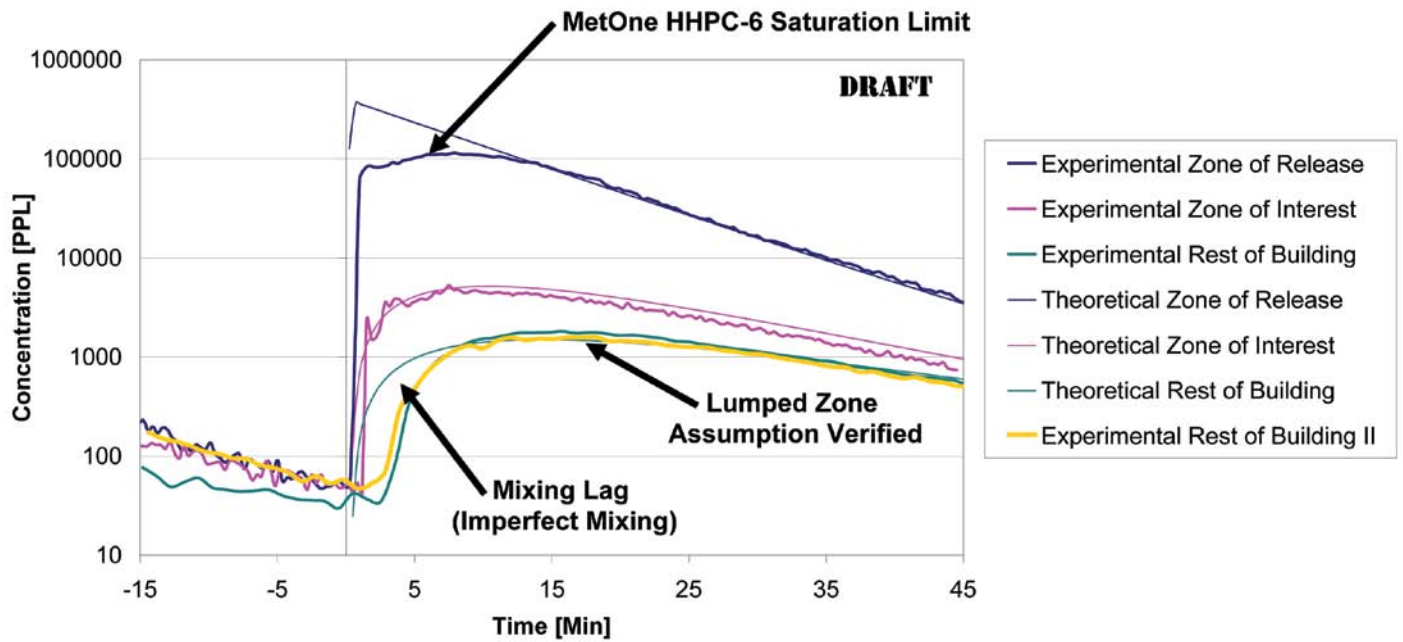
Figure 25. Comparison of Experimental and Model-Predicted Data for "Small" Notional Building with Moderate Recirculation (5 ACH), Low Leakage (0.125 ACH), Low Filtration (10% / No filter), Standard Makeup Air (1 ACH), and Standard Infiltration (0.5 ACH).

After establishing the validity of the model in terms of changing the filtration efficiency and interzonal leakage for both a "large" and "small" notional building in the first two test sets, the third set of tests focused on verifying the effects of changing the recirculation rate. This process was complicated by a lack of precise control over the interzonal leakage rate. That is, a change in the recirculation rate or the door position can and will result in a significantly altered leakage value. Figure 26 illustrates this through photographs of the various door positions that produce various interzonal leakage rates at moderate and low recirculation. It is of particular interest that after altering the air handling unit, Phoenix valves, and dampers to produce the low recirculation condition (see Tables 6 through 8 for details), the interzonal leakage rate changed from approximately 0.175 ACH to 0.05 ACH for an identical door position (i.e., a closed door). This variation indicates that the interzonal leakage rate can be extremely sensitive to the HVAC operating conditions. In addition, it is important to note the large variation in interzonal leakage that results from a slight change in the door position. This sensitivity of the interzonal leakage rate to changes in HVAC operating conditions and door position strongly support

the decision to use a combinatorial approach to estimate the leakage under normal operating conditions rather than use a more standard blower door test method that estimates the leakage under increased pressures and extrapolates to the standard operating pressure.

Thus, due to the lack of precise control over the interzonal leakage rate, an initial set of tests at low recirculation was necessary to estimate the door position that would produce a leakage level within an acceptable range. Figures 27 through 29 contain graphical comparisons of experimental and model-predicted data for three leakage levels (i.e., varying door positions) for the "large" notional building under low recirculation (3 ACH, see Tables 6 through 8 for further details) and moderate filtration (i.e., MERV 8 filter). Under the combinatorial approach, these experiments were used to estimate the "very low," "low," and "high" leakage rates under varying conditions (i.e., door position between B113 and B114). Experimental data and model predictions based on previously estimated HVAC parameters are graphically displayed in Figures 30 and 31.
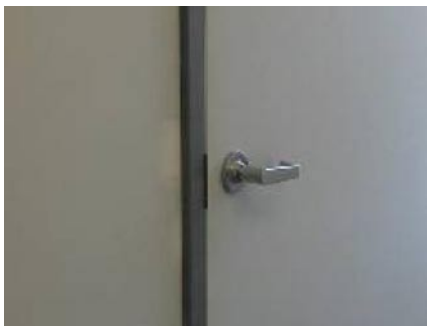
Recirculation	Leakage		Recirculation	Leakage		Recirculation	Leakage
Moderate (5 ACH)	0.175 ACH		Moderate (5 ACH)	1.025 ACH		Moderate (5 ACH)	Not Run
Low (3 ACH)	0.050 ACH		Low (3 ACH)	Not Run		Low (3 ACH)	0.200 ACH

Figure 26. Photographs of Various Door Positions for the "Large" Notional Building (i.e., the door between B113 and B114) and Recirculation Rates (i.e., low or moderate) with Corresponding Interzonal Leakage Rates
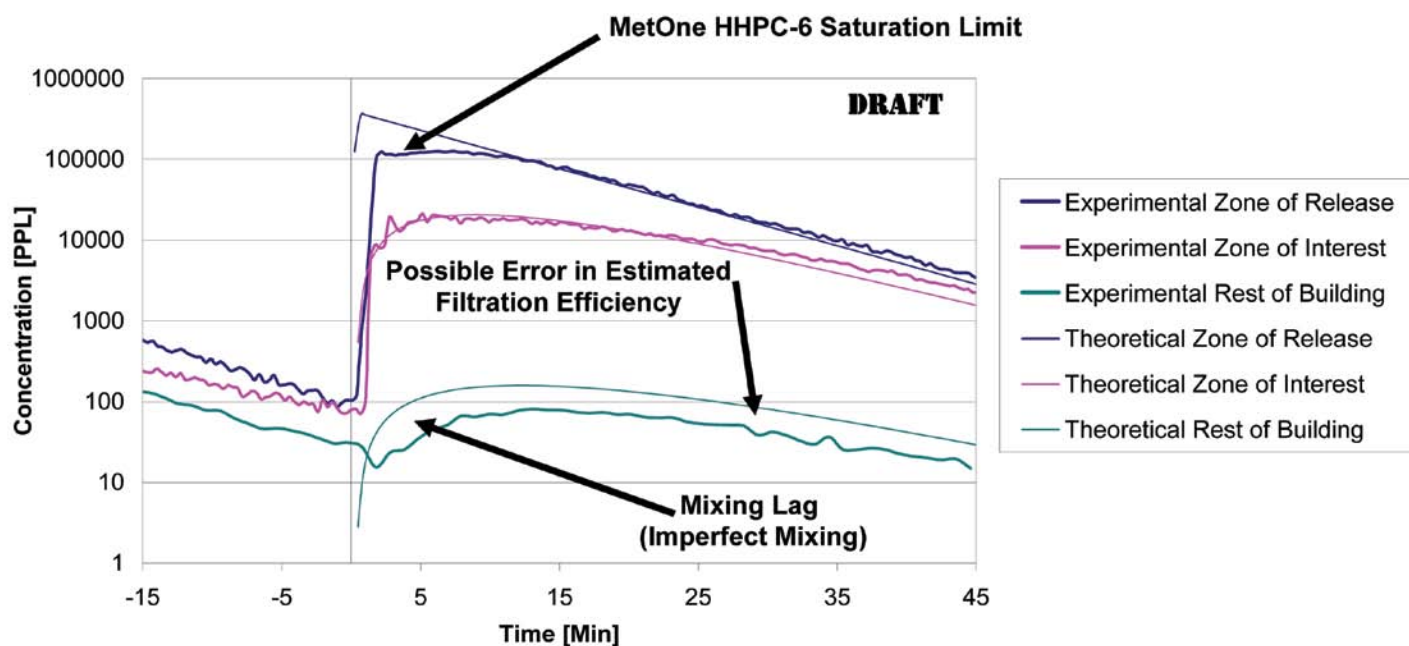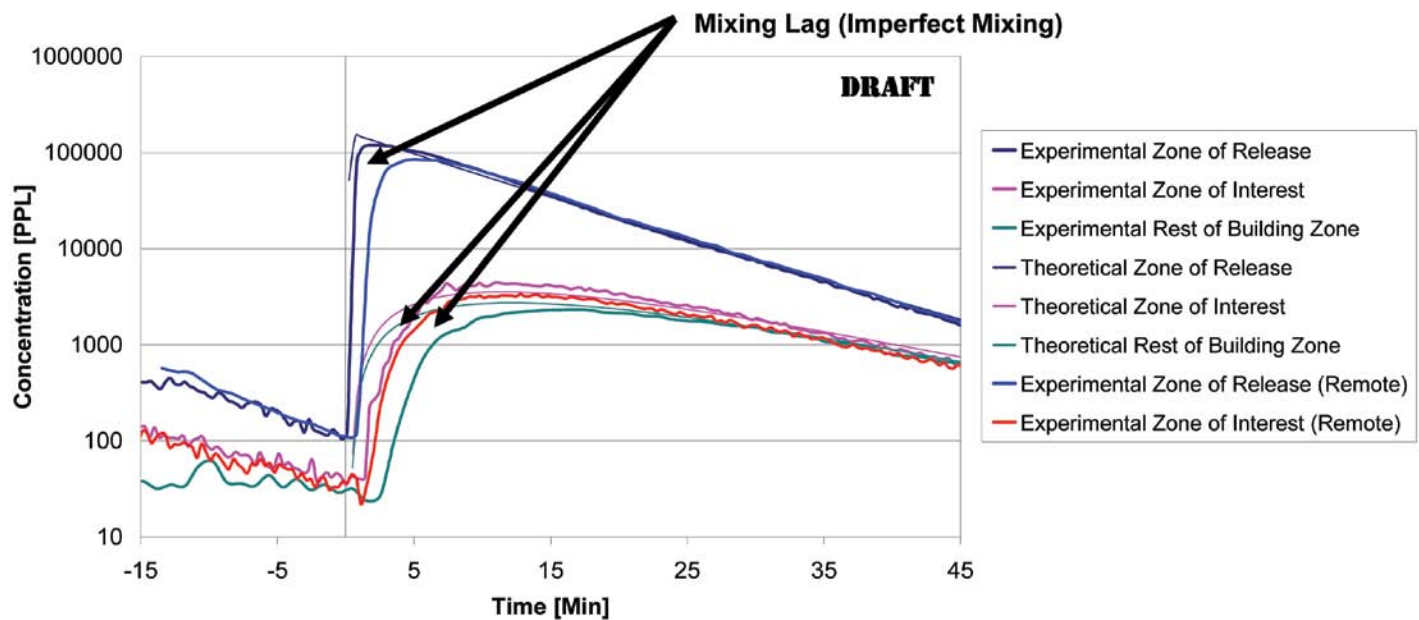

Figure 27. Comparison of Experimental and Model-Predicted Data for "Large" Notional Building with Low Recirculation (3 ACH), Very Low Leakage (0.05 ACH), Moderate Filtration (50% / MERV 8 filter), Standard Makeup Air (1 ACH), and Standard Infiltration (0.5 ACH).

Figure 28. Comparison of Experimental and Model-Predicted Data for "Large" Notional Building with Low Recirculation (3 ACH), Low Leakage (0.200 ACH), Moderate Filtration (50% / MERV 8 filter), Standard Makeup Air (1 ACH), and Standard Infiltration (0.5 ACH).

Figure 29. Comparison of Experimental and Model-Predicted Data for "Large" Notional Building with Low Recirculation (3 ACH), High Leakage (0.950 ACH), Moderate Filtration (50% / MERV 8 filter), Standard Makeup Air (1 ACH), and Standard Infiltration (0.5 ACH).
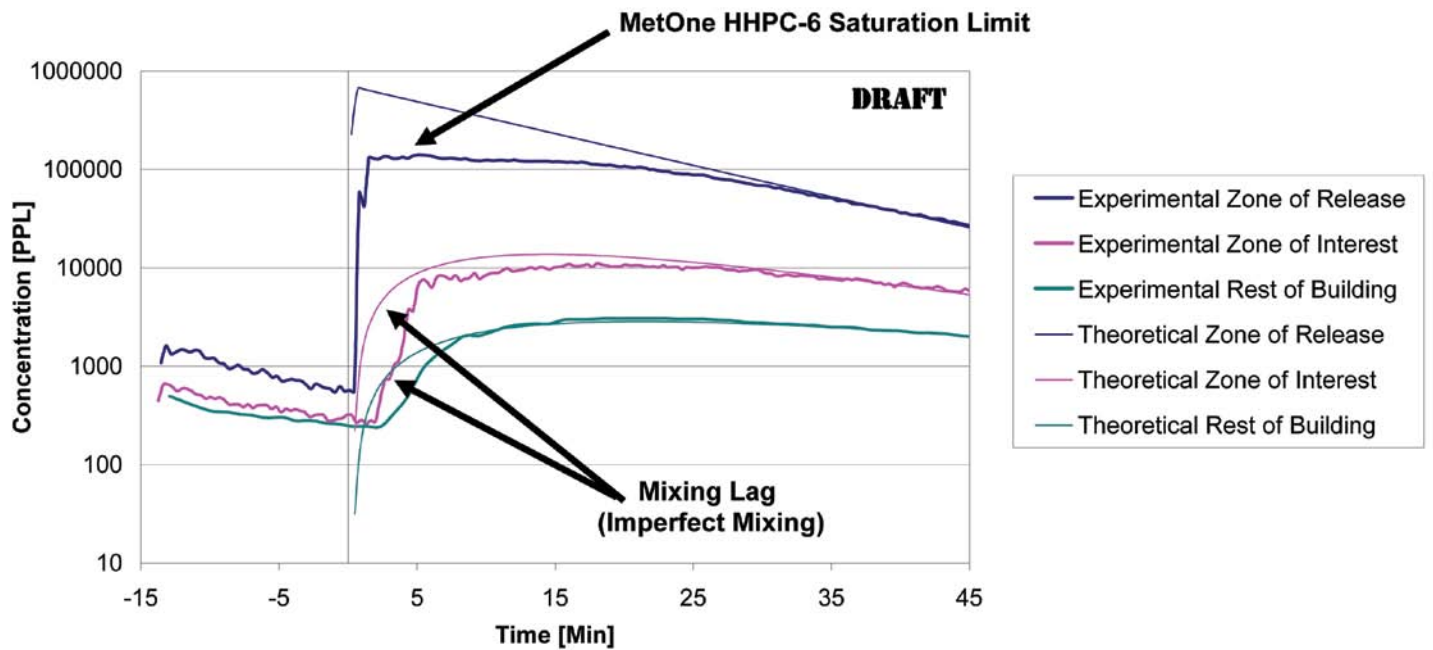
Figure 30. Comparison of Experimental and Model-Predicted Data for "Large" Notional Building with Low Recirculation (3 ACH), Low Leakage (0.200 ACH), Low Filtration (10% / No filter), Standard Makeup Air (1 ACH), and Standard Infiltration (0.5 ACH).
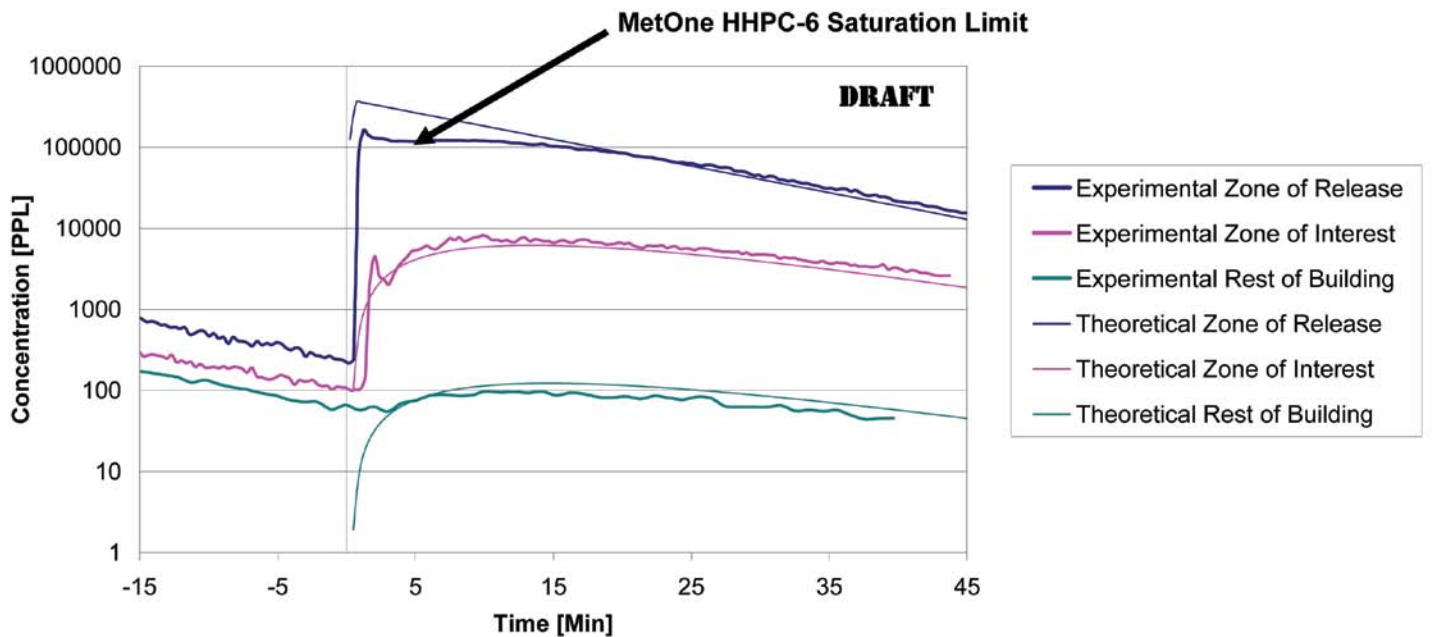
Figure 31. Comparison of Experimental and Model-Predicted Data for "Large" Notional Building with Low Recirculation (3 ACH), Low Leakage (0.200 ACH), High Filtration (90% / 95% DOP filter), Standard Makeup Air (1 ACH), and Standard Infiltration (0.5 ACH).

As with previous comparisons, the agreement between experiment and model for the "large" notional building under low recirculation was generally quite good.

Given the excellent agreement between model and experimental data, a reduced number of runs, consisting of three levels of filtration efficiency at one leakage condition, were executed for the "small" notional building under low recirculation. The leakage rate was estimated from the moderate filtration test (see Figure 32), leaving the remaining two tests as a direct comparison of model-predicted and experimentally measured data (see Figures 33 and 34). Again, the agreement observed between

experimental and model curves for a "small" notional building under "low" recirculation is rather favorable.

The excellent agreement observed between model-predicted and experimental data for changing recirculation rates indicates that the three-zone, well-mixed model is accurate in simulating the effects of changes in the recirculation rate for a notional building. The consistent nature and excellent quality of the model agreement with experimental data indicates that, in addition to accurately simulating the effects of changes in filtration efficiency and interzonal leakage rates, the model can accurately predict the effects of changing recirculation rates for a notional building.
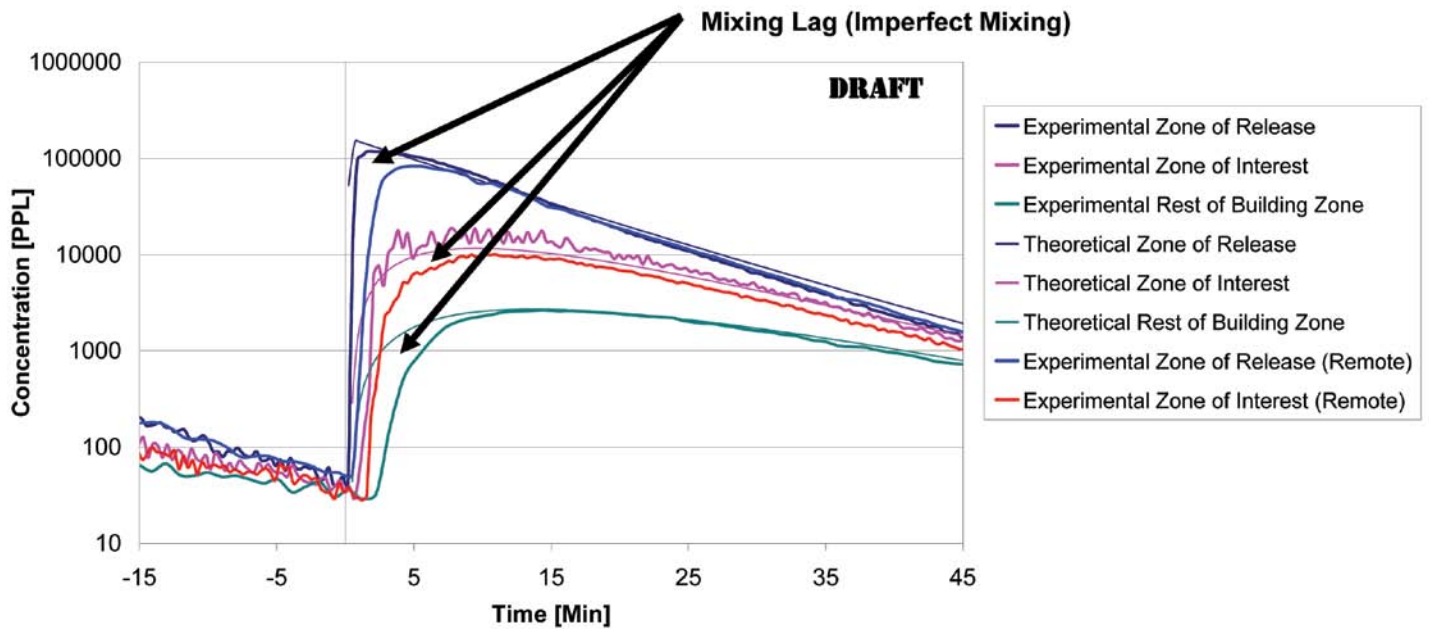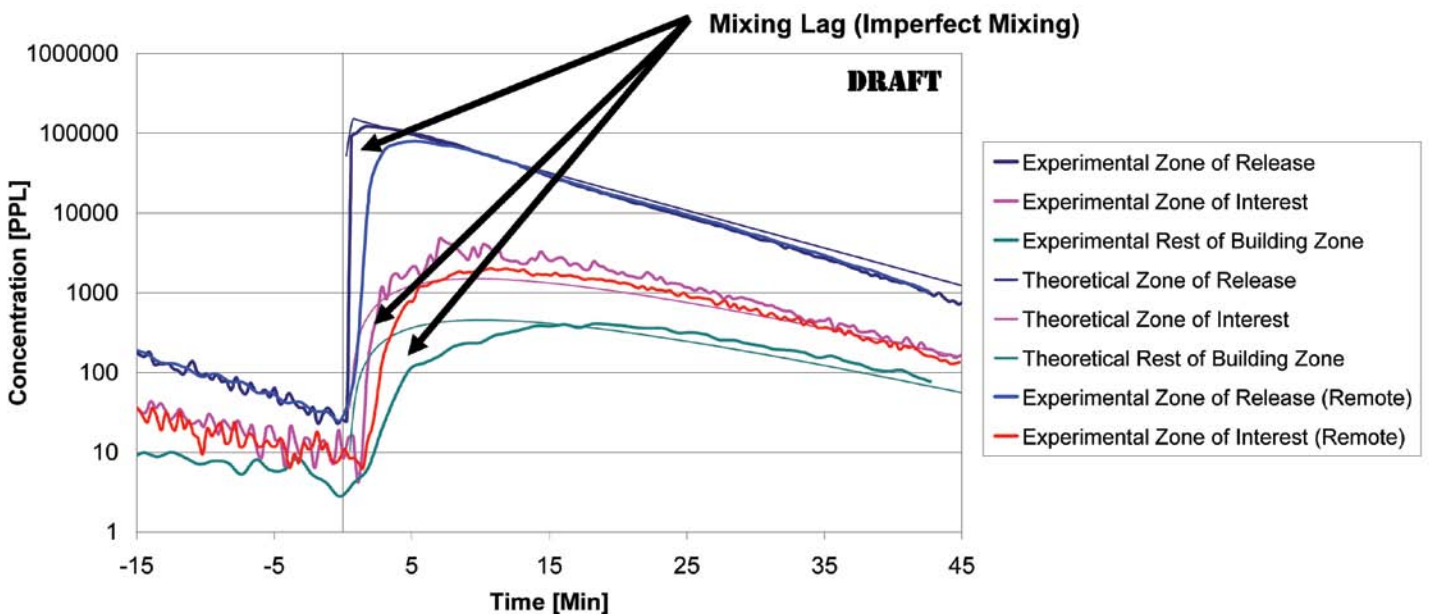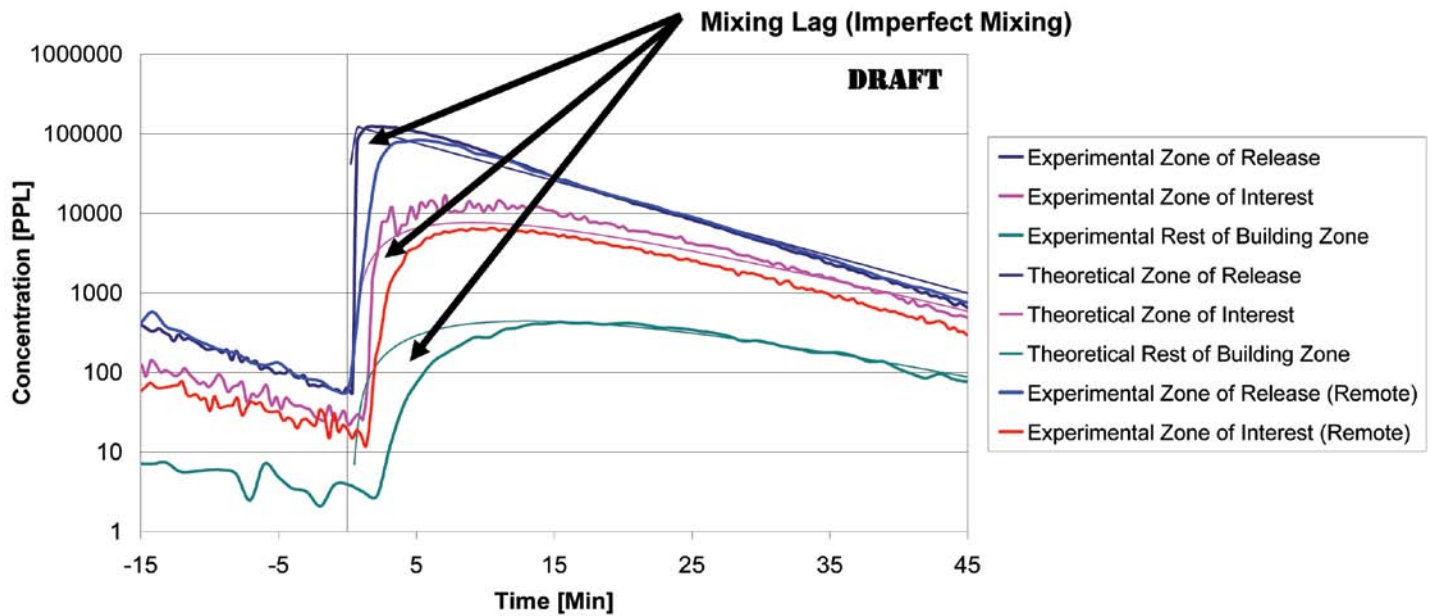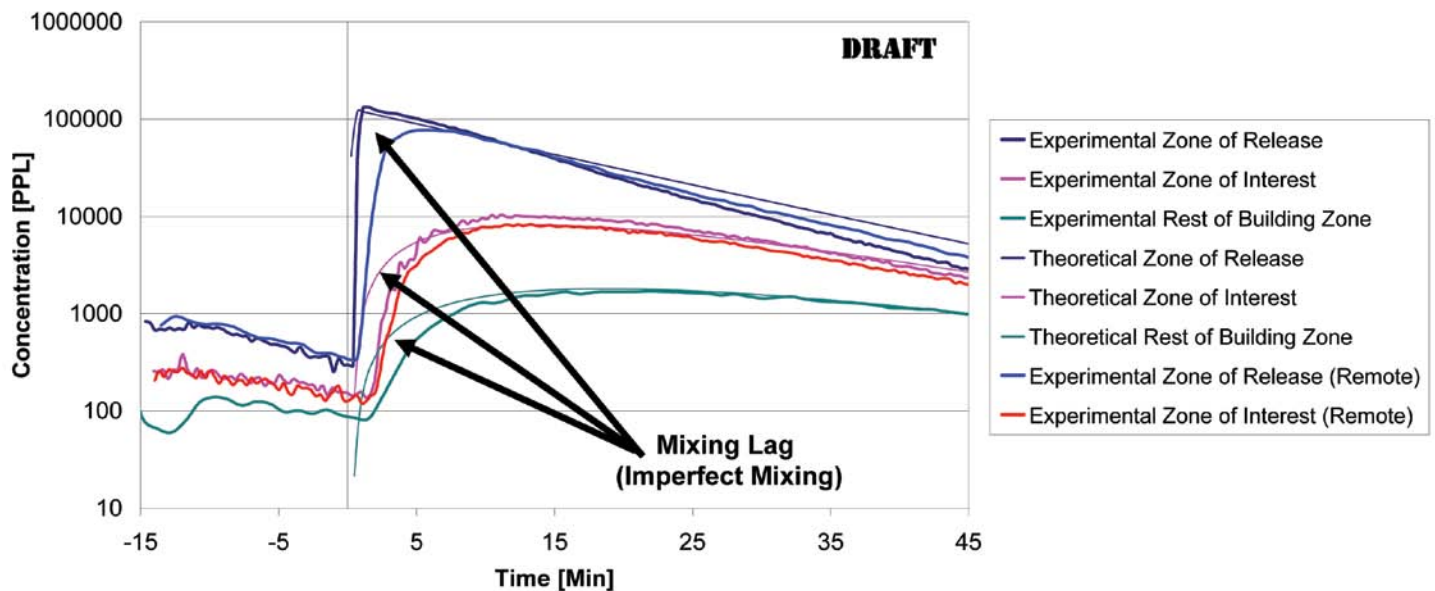

Figure 32. Comparison of Experimental and Model-Predicted Data for "Small" Notional Building with Low Recirculation (3 ACH), Moderate Leakage (0.725 ACH), Moderate Filtration (50% / MERV 8 filter), Standard Makeup Air (1 ACH), and Standard Infiltration (0.5 ACH).
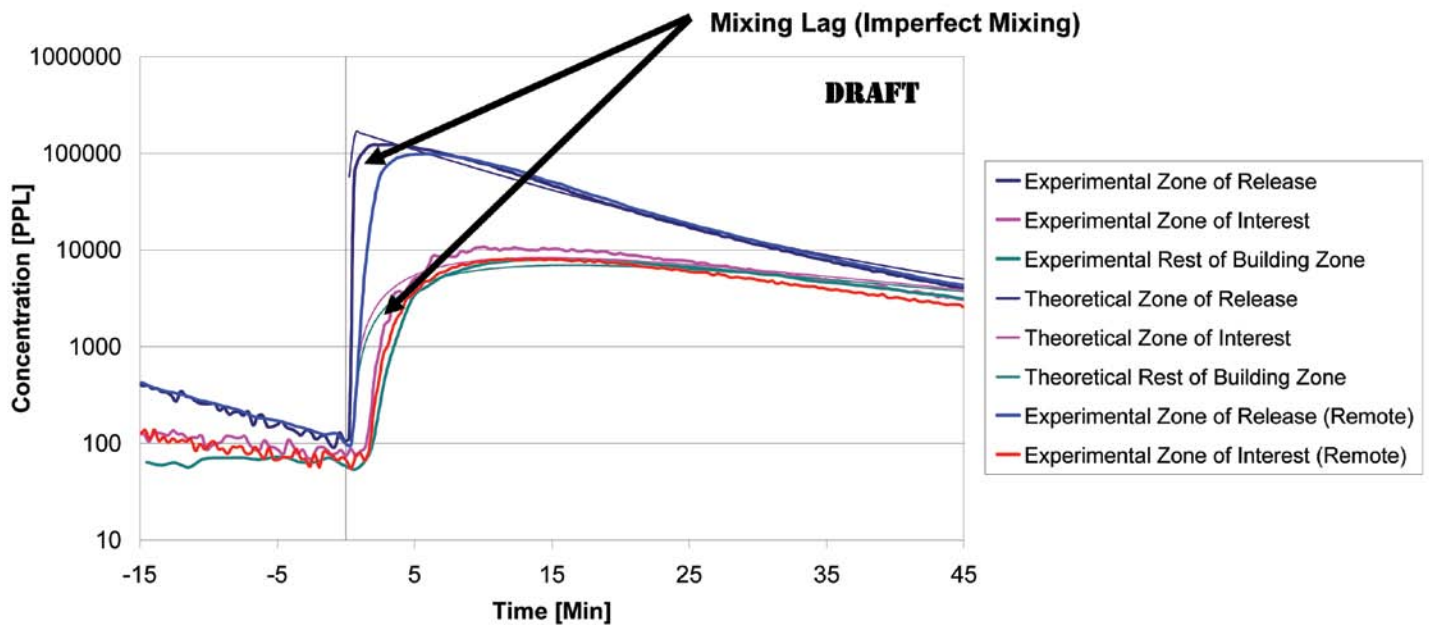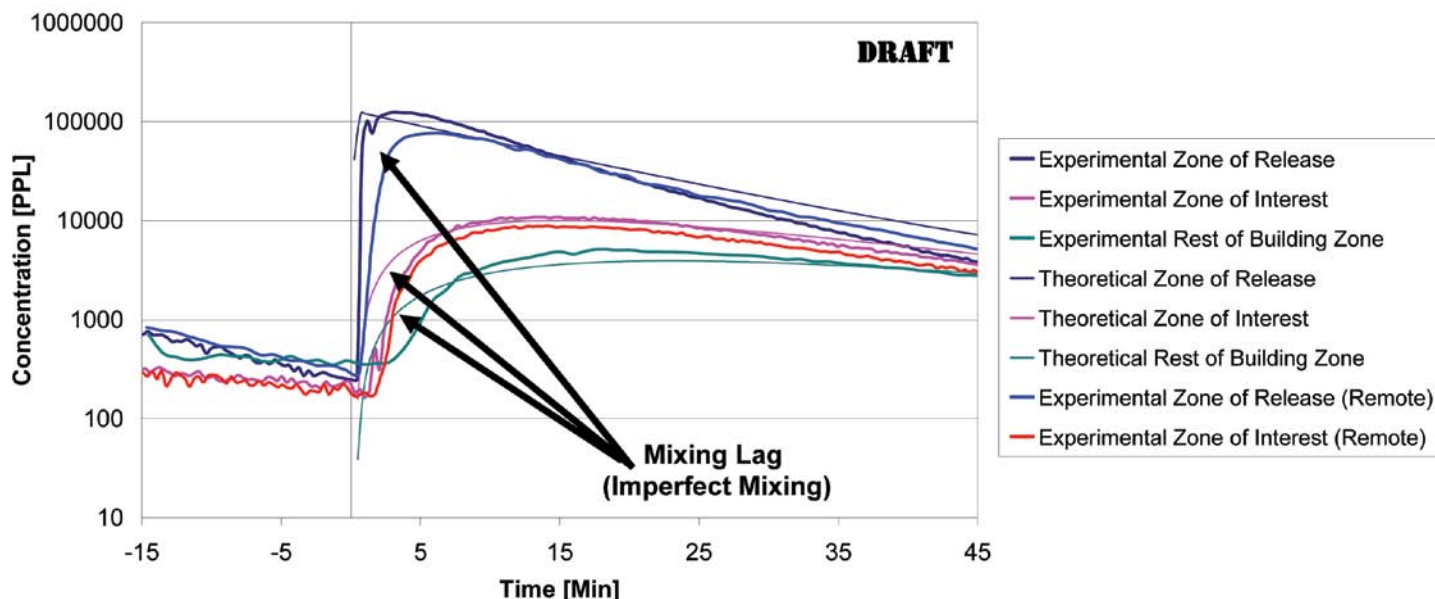
Figure 33. Comparison of Experimental and Model-Predicted Data for "Small" Notional Building with Low Recirculation (3 ACH), Moderate Leakage (0.725 ACH), Low Filtration (10% / No filter), Standard Makeup Air (1 ACH), and Standard Infiltration (0.5 ACH).
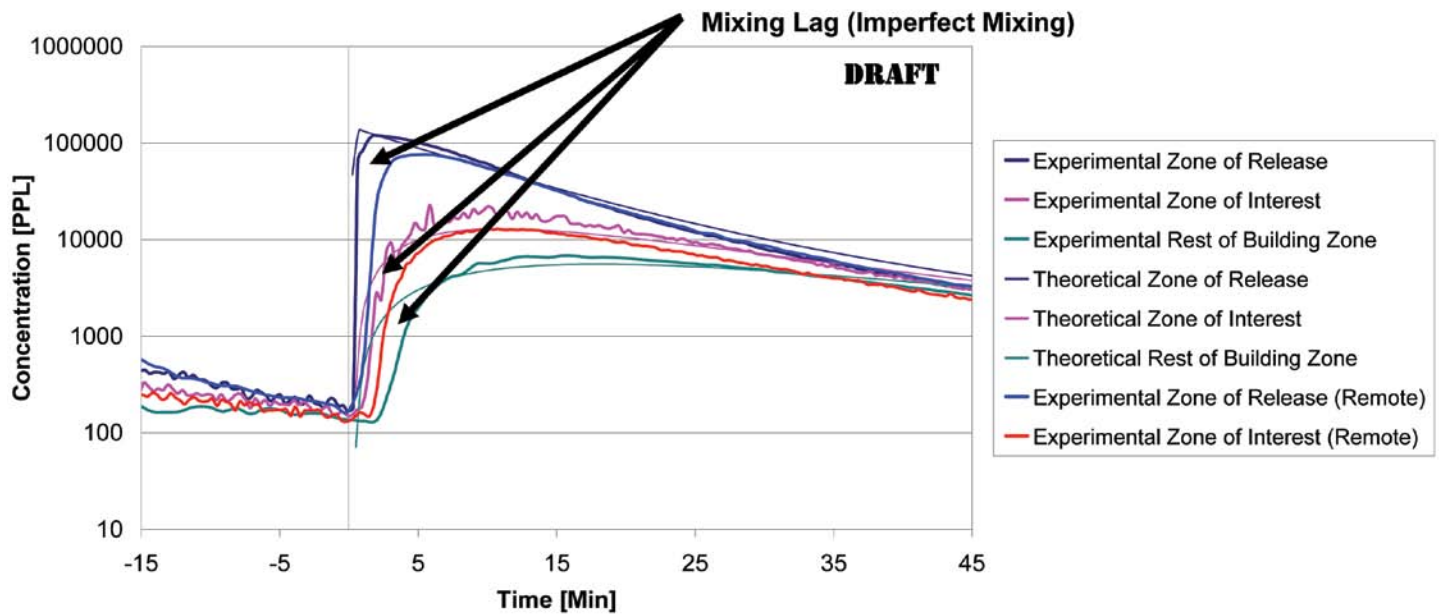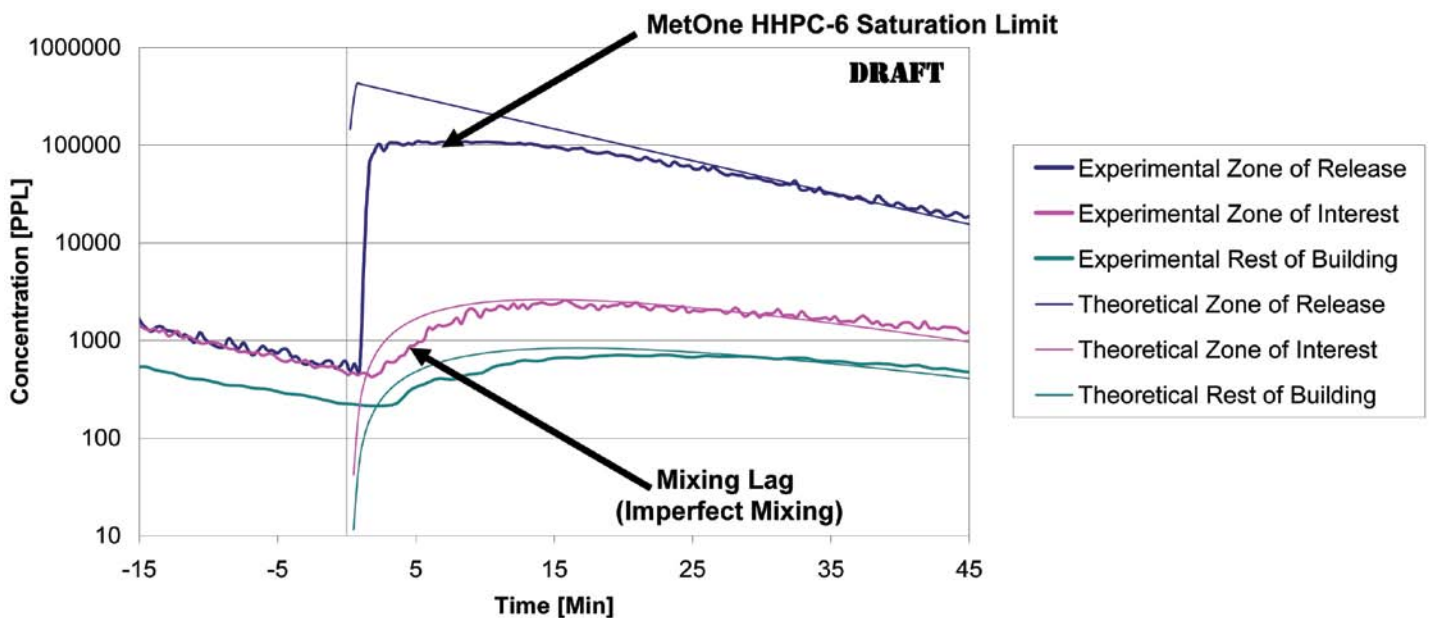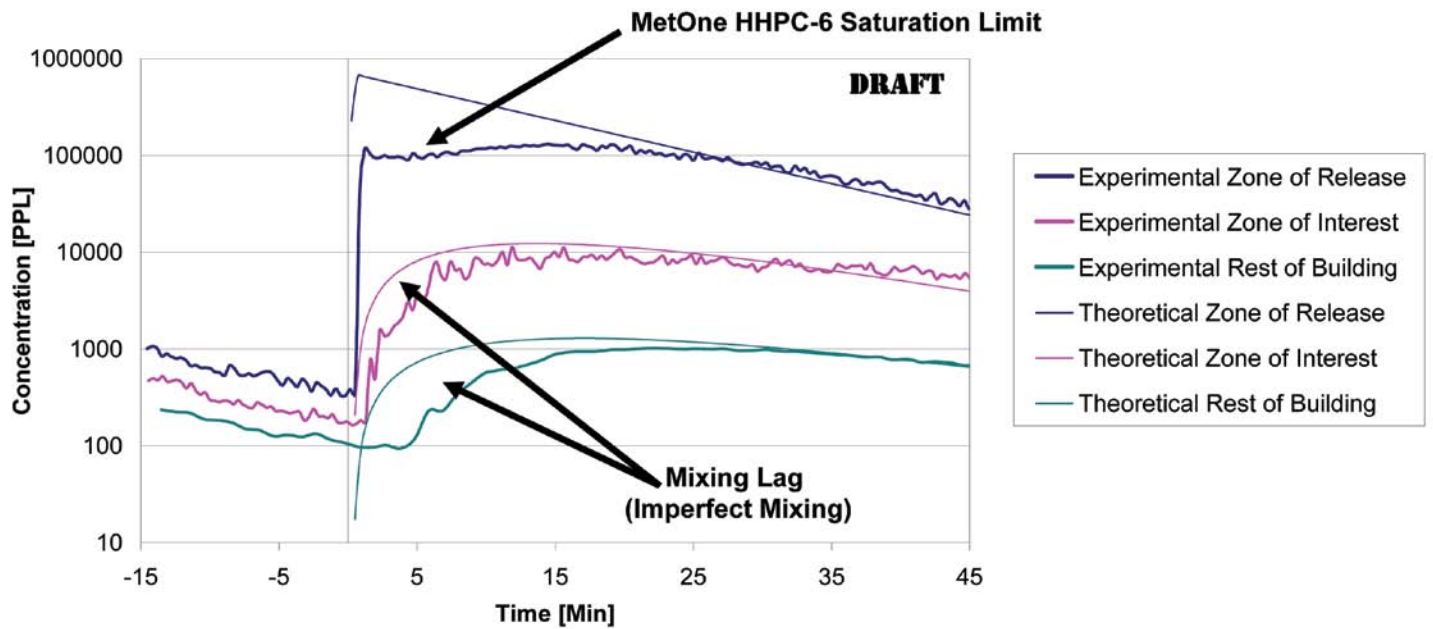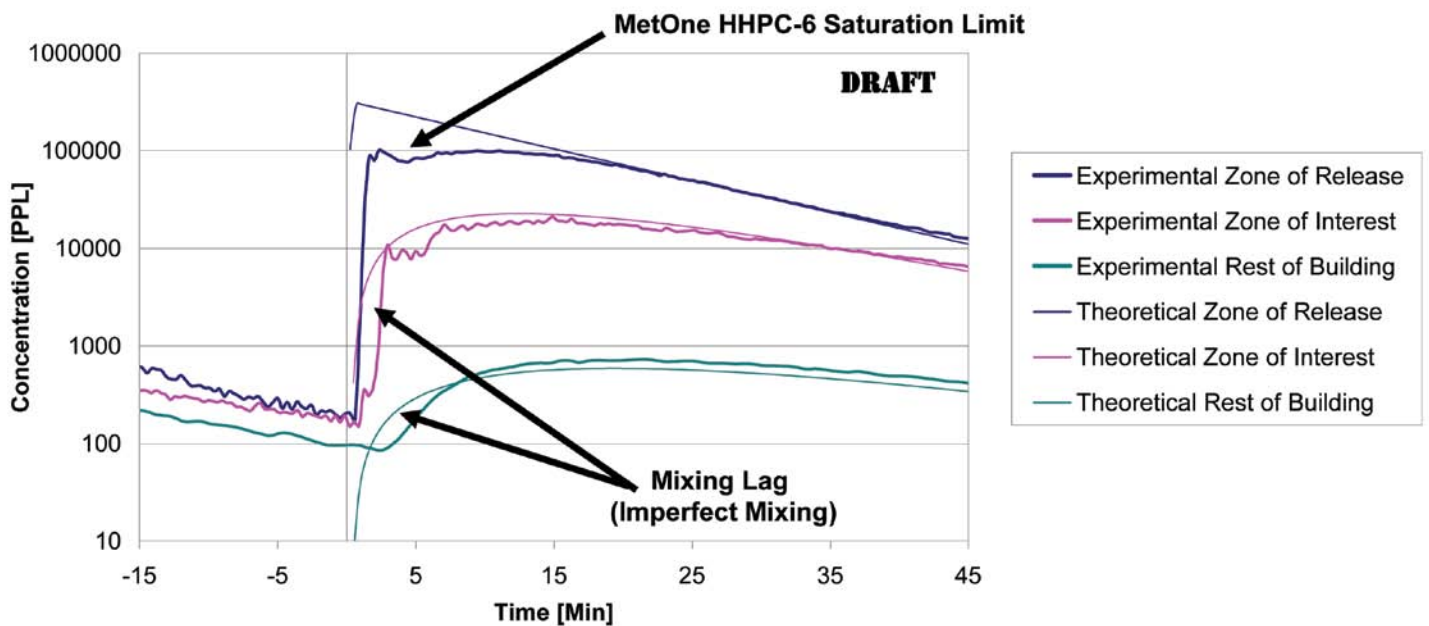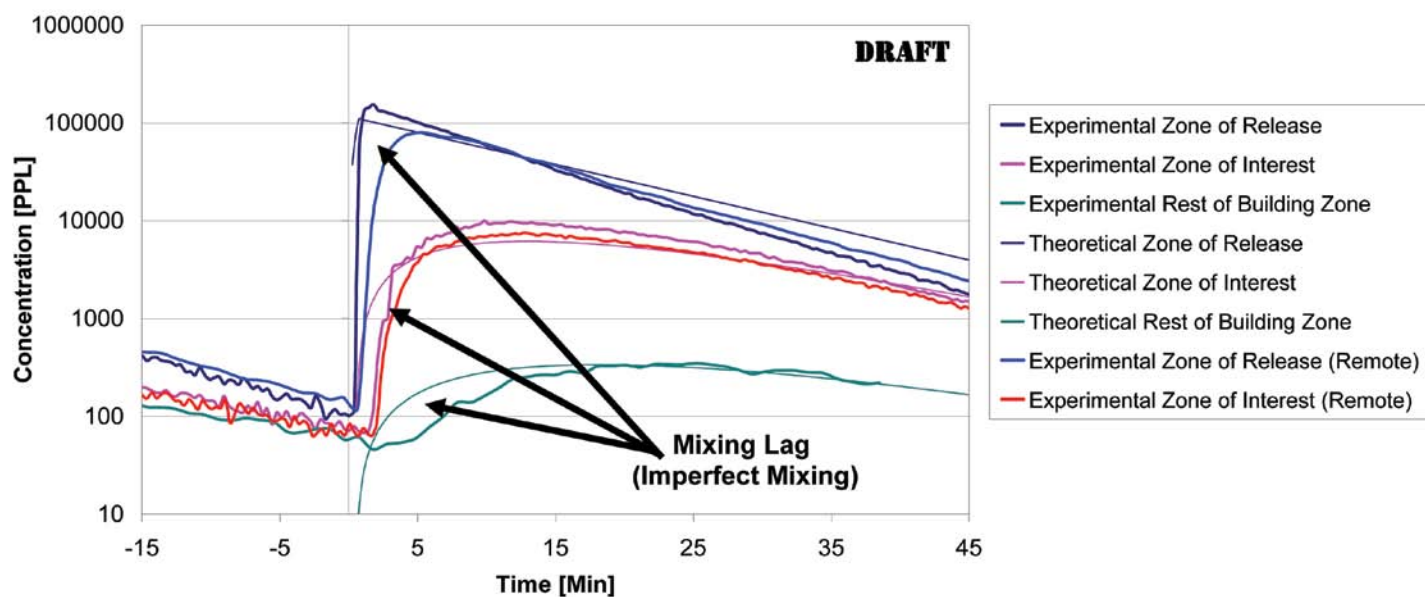

Figure 34. Comparison of Experimental and Model-Predicted Data for "Small" Notional Building with Low Recirculation (3 ACH), Moderate Leakage (0.725 ACH), High Filtration (90% / 95% DOP filter), Standard Makeup Air (1 ACH), and Standard Infiltration (0.5 ACH).

8.0
Discussion of Experimental Results

There was excellent agreement between experimentally observed and model-predicted data. For this comparison, the time to reach a critical exposure (Ct) of 50,000 particles per liter (ppl)* minutes, and the cumulative exposure at 30 minutes, were selected as the performance metrics to compare model estimates with measured data. These performance metrics were selected to allow comparison of the different operating conditions and hence the effect of varying building/HVAC operating variables of interest. Tables 11 and 12 contain the tabulated performance metrics for experimental and model-predicted data for moderate and low recirculation conditions, respectively. Given that the average percentage errors are 9% for the time to reach the Ct and 13% for the exposure at 30 minutes, it is clear that the excellent agreement, which has been displayed graphically in Figures 12 through 34, is also present in the calculated performance metrics. That is to say that the model-predicted performance metrics agree well with the experimentally determined performance metrics within the experimental variability.

Ideally, a stringent analysis of parameter impact would be conducted using the experimental data. This type of analysis would compare two experiments in which only a single parameter of interest varied and would quantify the change in performance metrics due to the change in the parameter of interest. A slight variation in the mass released and a lack of precise control over the leakage preclude this type of stringent analysis. Due to the formation of small deposits within the eductor nozzle, the mass released during each test varied by approximately +/- 0.6 grams from the mass loaded into the release mechanism. For this reason, comparisons between experimental results convolute the effects of changing both a release variable (i.e., the release mass) and key system variables (i.e., an HVAC parameter). In addition, it was not possible to "dial" in the leakage value when considering different notional buildings (i.e., different rooms) or differing recirculation flow rates. This lack of precise control over the leakage is due to the realistic nature of the leakage path and driving force used in this study. The natural leakage path of a door and the natural driving force of slight HVAC flow imbalances resulted in realistic results but did not provide precise control of the leakage itself. Because of the excellent agreement of model estimates with experimental results, the model allows for this type of stringent analysis to be made with confidence.

While the variable release mass and a lack of precise control over the leakage preclude a stringent analysis of parameter impact from the experimental results, some generalizations concerning parameter impact can be made from the experimental data gathered during this study. For "large" notional buildings, the significant changes in performance metrics between high and low leakage rates suggest that the leakage is the dominant parameter (see Table 11). In comparison, it appears that changes in the filtration efficiency and system recirculation rate have lesser impacts on the performance metrics for a "large" notional building scenario (see Tables 11 and 12). In contrast to the "large" notional building results, the results for a "small" notional building imply that the filtration efficiency is the dominant parameter while the leakage may play a secondary role (See Table 11). These generalities represent the trends observed in the experimental data. Given the excellent agreement between modeled and experimental data, the following section (Section 9.0) develops an approach to determining the relative impact of key parameters and to finding out how well a parameter must be known to assess an attack.

Table 11. Comparison of Experimental and Predicted Performance Metrics for the Zone of Interest for the "Moderate" Recirculation Condition

Recirculation	Building Size	Leakage	Filtration	Experimentally Measured		Model-Predicted	
				Time to Ct of 50,000 ppl*min [min]	Exposure @ 30 min [ppl*min]	Time to Ct of 50,000 ppl*min [min]	Exposure @ 30 min [ppl*min]
"Moderate" (5 ACH)	"Large"	"Low" (0.175 ACH)	"Low" (10%)	9.1	1.8×10^5	9.25	1.9×10^5
			"Moderate-Low" (25%)	14.5	1.0×10^5	12.75	1.1×10^5
			"Moderate-Low" (25%)	12.0	1.2×10^5	11.5	1.3×10^5
			"Moderate" (50%)	11.2	1.3×10^5	10.25	1.4×10^5
			"High" (90%)	15.6	8.1×10^4	12.75	1.1×10^5
		"High" (1.025 ACH)	"Low" (10%)	6.1	3.1×10^5	5.5	3.8×10^5
			"Moderate" (50%)	3.4	6.5×10^5	4.75	7.1×10^5
			"High" (90%)	4.8	4.0×10^5	5.00	4.1×10^5
	"Small"	"Low" (0.125 ACH)	"Low" (10%)	10.6	2.0×10^5	10.25	2.1×10^5
			"Moderate" (50%)	18.7	7.7×10^4	17.75	8.1×10^4
			"High" (90%)	N/R	3.1×10^4	N/R	4.7×10^4
		"High" (1.175 ACH)	"Low" (10%)	7.4	3.0×10^5	7.0	3.1×10^5
			"Moderate" (50%)	7.5	2.5×10^5	7.25	2.4×10^5
			"High" (90%)	8.6	1.7×10^5	9.25	1.5×10^5

N/R denotes that the specified cumulative Ct was not reached.

Table 12. Comparison of Experimental and Predicted Performance Metrics for the Zone of Interest for the "Low" Recirculation Condition

Recirculation	Building Size	Leakage	Filtration	Experimentally Measured		Model-Predicted	
				Time to Ct of 50,000 ppl*min [min]	Exposure @ 30 min [ppl*min]	Time to Ct of 50,000 ppl*min [min]	Exposure @ 30 min [ppl*min]
"Low" (3 ACH)	"Large"	"Very Low" (0.050 ACH)	"Low" (10%)	27.8	5.4×10^4	24.0	6.3×10^4
		"Low" (0.200 ACH)	"Moderate-Low" (25%)	4.7	4.3×10^5	5.3	5.5×10^5
			"Moderate" (50%)	8.8	2.1×10^5	8.0	2.9×10^5
			"High" (90%)	8.1	2.5×10^5	7.5	3.3×10^5
		"High" (0.950 ACH)	"Low" (10%)	10.2	1.75×10^5	12.0	1.5×10^5
	"Small"	"Low" (0.125 ACH)	"Low" (10%)	10.9	1.9×10^5	10.0	2.0×10^5
			"Moderate" (50%)	10.8	1.7×10^5	12.0	1.4×10^5
			"High" (90%)	10.4	2.2×10^5	9.3	2.4×10^5

While it is neither feasible nor realistic to conduct experiments under all possible conditions and configurations, the model represents a tool that can easily and reasonably be used to analyze a tremendous number of possible conditions and building configurations. This section focuses on developing an approach to determining which parameter has the largest impact and subsequently applying that approach to a number of combinations of system parameters and building configurations.

9.1 Impact Analysis Approach

In evaluating the impacts of changing various system variables, it is necessary to choose some type of performance metrics for quantifying the protection of the building occupants. Two performance metrics were considered in this study: (1) the level of exposure in the zone of interest (Zone 2) over the first 30 minutes ($E_{30,2}$), and (2) the time to reach an effective dosage Ct of interest (t_{Ct}). These metrics represent the severity and speed of the exposure, respectively, and provide an accurate description of the impact of HVAC parameters on exposure in the zone of interest. The exposure metric ($E_{30,2}$) alone can yield valuable information

about the performance of the system to reduce total exposure. The examination of only the time to reach an effective Ct (t_{Ct}) gives an indication useful for response time analysis. While the specific details of the chosen performance metrics (e.g., 30 minutes as the timeframe for the exposure metric) relate to acute hazards, which likely occur in the unsteady state immediately following a release, alternative details could be chosen to apply this approach to longer timeframes. In this respect, this impact analysis approach is very flexible and could be applied to numerous different scenarios through the choice of appropriate performance metrics.

The combination of these exposure metrics summarizes valuable information about the performance of the system, while conclusions based on only one metric may ignore critical performance details. For example, while time-based metrics are important for evacuation and protection strategies, they do not directly correlate to the total exposure for a given scenario. In a similar fashion, exposure-based metrics do not provide any indication of how quickly a critical exposure value is realized within a zone.
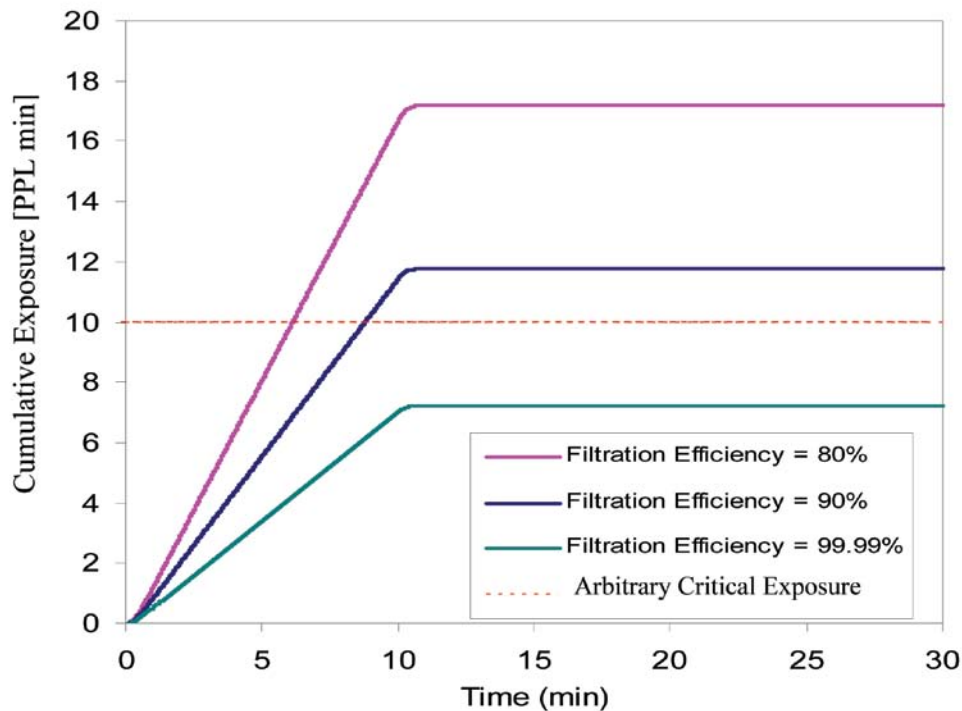
Figure 35. Illustration of Exposure-Based Metric Inadequacies for a Hypothetical Case of Various Filtration Efficiencies (80, 90, and 99.99), Equal Zone Volumes ($V_1=V_2=V_3$), Makeup Air (1 ACH), Moderate Recirculation (5 ACH), Standard Infiltration (0.5 ACH), and High Leakage (1 ACH)

For illustration, Figure 35 contains plots of cumulative exposure for Zone 2, for a hypothetical case similar to some of the experimental conditions used during the field study except that all three-zone volumes are equal. By plotting an arbitrary critical exposure value (e.g., 10 CFU/m^3 * min), the importance of both types of metrics are graphically illustrated in Figure 35. (Note that CFU stands for colony-forming unit.) The arbitrary critical exposure value is reached at 6.1 and 8.8 minutes for filtration efficiencies of 80% and 90%, respectively, while the cumulative exposure for a filtration efficiency of 99.99% never reaches the arbitrary critical value. Thus, considering a time-based metric, one might conclude that changing the filtration efficiency from 80% to 90% has relatively little impact on the system performance. However, the total cumulative exposure for these two cases varies by 50% (17.2 CFU/m^3 *min for 80% versus 11.8 CFU/m^3 *min for 90%), which may be significant to occupant survival. For these reasons, both a time-based metric and an exposure-based metric are needed to assess performance.

The goal of this impact analysis is to determine the relative impact of the various HVAC and building parameters on the performance metrics (i.e., the parameter that has the largest impact on the protection offered by the building). To accomplish this, a series of runs was performed varying parameters one at a time over their particular ranges of variability. To graphically display the sensitivity of the performance metrics to changes in various parameters, a normalization procedure was applied to eliminate any bias towards parameters with inherently small magnitudes and/or limited ranges. For example, filter collection efficiency may realistically range over five logs (i.e., ~0 to 99.99%), but infiltration rates, only one (i.e., 0.1 to 1). To this end, both the performance metrics and the parameters were normalized by baseline values and the results plotted (for examples, see Figures 36 and 37). In Figure 36, the normalized performance metric ($E_{30}/E_{30\,base}$) is plotted versus the normalized study parameter (P/P_{base}). By comparing the gradient of the plot at the analysis baseline condition (i.e., the slope of the curves at $P/P_{base}=1$), the effects of a relative change in the model parameter on the performance metric can be compared. As one would intuitively expect, a larger gradient (i.e., a steeper slope) indicates that a small relative change in the model parameter will produce a large change in the performance metric. For example, a smaller slope for the filter efficiency curve (shown in dark blue in Figures 36 and 37) and a larger slope for the leakage rate (shown in bright red in Figures 36 and 37) indicate that the leakage rate between rooms has a larger relative impact on the exposure metric for the hypothetical building than the filter efficiency. Please note that the filtration efficiencies were subjected to a log transform according to Equation 6. This log transform frames filtration efficiencies such that they may vary from zero to infinity.

$$P_{\text{Filtration Efficiency}} = \frac{1}{100 - [\text{Filtration Efficiency}]} \qquad (6)$$
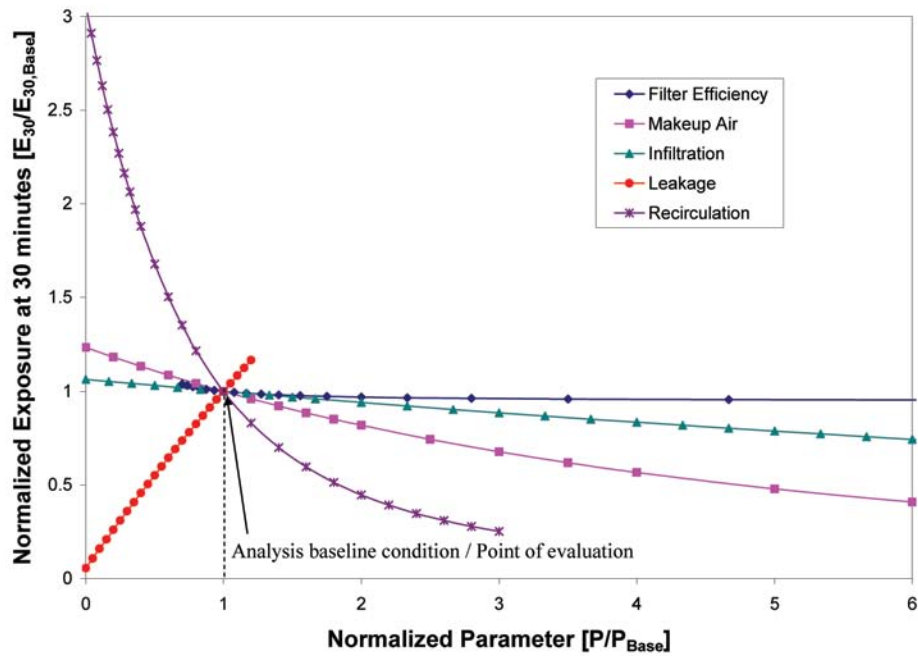
Figure 36. Normalized Exposure at 30 Minutes ($E_{30,2}$) Versus Model Input Parameters for a "Large" Notional Building
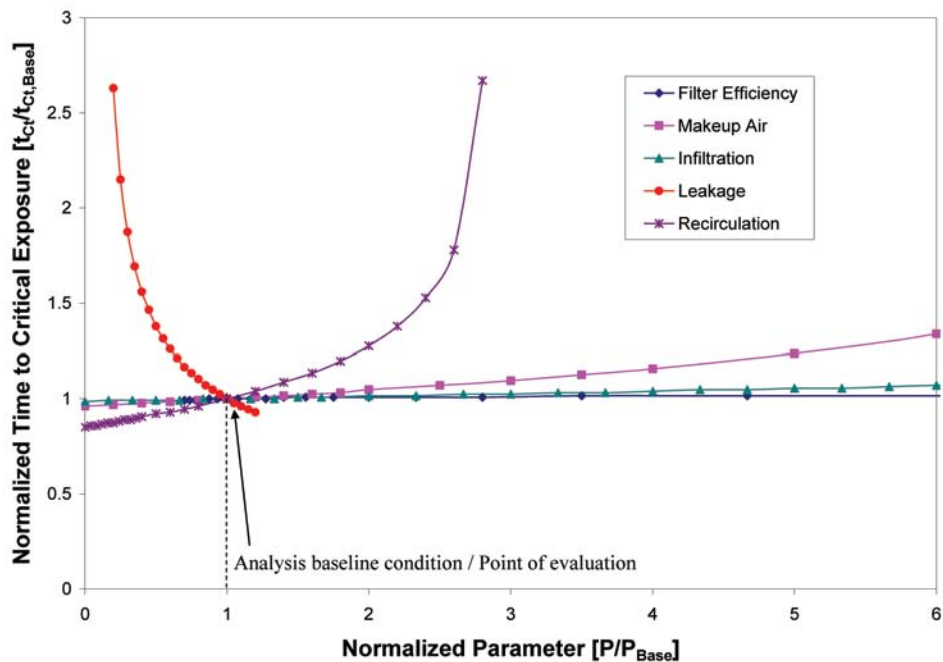
Figure 37. Normalized Time to Critical Exposure (t_{Ct}) Versus Model Input Parameters for a "Large" Notional Building

The sum of the absolute value of the gradients of the two normalized performance metric curves associated with a model parameter (i.e., the quantity $|E'_{30,P}| + |t'_{Ct,P}|$), evaluated at $P/P_{base}=1$, are an indication of how much impact a parameter has. Equation 7 describes this mathematically where $E'_{30,P}$ is the slope of the normalized exposure metric curve at $P/P_{base}=1$ for parameter P (with P denoting any of the five parameters from the legend of Figures 36 or 37), $t'_{Ct,P}$ is the slope of the normalized time to critical exposure metric curve at $P/P_{base}=1$ for parameter P (with P denoting any of the five parameters from the legend of Figures 36 or 37), P_{base} is the base case parameter value (i.e., the notional building being considered), ΔP is the change in parameter P being considered (i.e., a reasonable change in the parameter), and the quantity $(\Delta E_{30}/E_{30,base} + \Delta t_{Ct}/t_{Ct,base})$ is taken to be the cumulative change in performance metrics possible for a potential change in parameter P of ΔP.

Equation 7 provides an indication of the impact of a reasonable change in a parameter; however, it must be adjusted so that (1) any dependence on the baseline parameter is eliminated and (2) once the baseline parameter dependence has been eliminated, a factor to account for the magnitude of each parameter is included to allow for comparisons between parameters (a detail that

normalization by the baseline parameter was previously used to accomplish). To accomplish both of these items, a scale factor defined as the ratio of a set change in the parameter (e.g., changes in filter efficiencies are likely on the order of a quarter of a log while changes in leakage rates are likely on the order of 0.25 ACH) to the baseline parameter was introduced. An illustration is shown in Table 13, which lists the assumed values for typical changes in a parameter, the baseline parameter values, and the calculated scale factors.

The absolute value of the gradients of the two curves associated with a model parameter, that is the quantity $|E'_{30,P}| + |t'_{Ct,P}|$ where $E'_{30,P}$ and $t'_{Ct,P}$ denote the slopes for each of the performance metrics of the curve for a given parameter (P) evaluated at $P/P_{base}=1$, can then be multiplied by the resulting scale factors to produce an impact score for each parameter (see Equations 8 and 9). In Equations 8 and 9, I_P is the impact score, $\Delta P_{Set\ Change}$ is the set change in a parameter, and the quantity $(\Delta E_{30}/E_{30,base} + \Delta t_{CT}/t_{Ct,base})$ is taken to be the cumulative change in performance metrics possible for a potential change in parameter P of ΔP. In this way, the relative impact of each parameter on the model can be quantified.

$$\left| E'_{30,P} \right| + \left| t'_{Ct,P} \right| = \frac{\left| \dfrac{\Delta E_{30}}{E_{30,base}} \right| + \left| \dfrac{\Delta t_{Ct}}{t_{Ct,Base}} \right|}{\dfrac{\Delta P}{P_{Base}}} \qquad (7)$$

Table 13. Typical Change in Parameters for Use in Calculating Scale Factors

Model Parameter	Set Change[a]	Baseline Value[b]	Scale Factor[c]
Filter Efficiency [%]	¼ $P_{Filter\ Efficiency}$ [d]	30 %	0.25
Makeup Air Rate [ACH]	0.25 ACH	1 ACH	0.25
Recirculation Rate [ACH]	0.5 ACH	5 ACH	0.10
Infiltration Rate [ACH]	0.1 ACH	0.3 ACH	0.33
Room Leakage [ACH]	0.25 ACH	1 ACH	0.25

(a) denoted $\Delta P_{Set\ Change}$ in Equations 8 and 9

(b) denoted P_{base} in Equations 8 and 9

(c) denoted as the quantity ($\Delta P_{Set\ Change}/P_{base}$) in Equations 8 and 9

(d) ¼ $P_{Filter\ Efficiency}$ for a filter change depends on the filter efficiency. For a 10% efficient filter, ¼ of $P_{Filter\ Efficiency}$ is equal to 18.0%, while for a 99% efficient filter, ¼ of $P_{Filter\ Efficiency}$ is equal to 0.2%.

$$I_P = \frac{\left(\left|\frac{\Delta E_{30}}{E_{30,base}}\right| + \left|\frac{\Delta t_{Ct}}{t_{Ct,Base}}\right|\right)}{\frac{\Delta P}{P_{Base}}} * \frac{\Delta P_{SetChange}}{P_{Base}} = \frac{\left(\left|\frac{\Delta E_{30}}{E_{30,base}}\right| + \left|\frac{\Delta t_{Ct}}{t_{Ct,Base}}\right|\right)}{\frac{\Delta P}{\Delta P_{SetChange}}} \qquad (8)$$

$$I_P = \left(\left|E'_{30,P}\right| + \left|t'_{Ct,P}\right|\right) * \frac{\Delta P_{SetChange}}{P_{Base}} \qquad (9)$$

For the sake of simplicity, the impact scores are then renormalized by the maximum value. This sets the range of possible impact scores to between zero and unity, which provides a set scale of relative impact (i.e., an impact score of unity indicates the most important model parameter). In this way, the resulting normalized impact score indicates the relative impact of simulation parameters on model performance (i.e., the higher the normalized impact score, the stronger the effect on model performance).

Table 14 illustrates the results from this analysis. The normalized impact scores indicate that leakage is the dominant factor in determining model performance with recirculation, filtration, makeup air, and infiltration all playing lesser roles. By noting the sign (i.e., positive or negative) of the slope (see Figures 36 and 37

for the illustrative case), the nature of the dominant mechanism associated with the parameter (i.e., delivery or removal mechanism) can be ascertained. Thus, for the illustrative case, it can be concluded that the delivery of contaminant is limited by the leakage rate while removal of contaminant is limited by the combination of the recirculation, filtration, and makeup air that dilute and filter the air in the simplified HVAC system. Using this approach, it is possible to conclude that reducing the interzonal leakage is easily identifiable as the key parameter in improving the protection offered by this building. This is not to say that other parameters do not affect the exposure metrics, but rather that the interzonal leakage has the largest impact for parameters scrutinized for the set change used in the analysis. The impact analysis does not identify the magnitude of the impact; it only identifies the relative impact of each parameter.

Table 14. Normalized Impact Scores for the Base Case for a "Large" Notional Building ($V_3 = 100V_1$) Under 1 ACH Makeup Air, 5 ACH Recirculation, 0.3 ACH Infiltration, 30% Filtration, and 1 ACH Interzonal Leakage

Zone 2 Parameter	Sum of Normalized Gradients[a]	Scale Factor[b]	Impact Score[c]	Renormalized Impact Score
Filter Efficiency	0.075	0.25	0.019	0.057
Makeup Air Rate	0.245	0.25	0.061	0.18
Interzonal Leakage	1.32	0.25	0.33	1.00
Infiltration Rate	0.060	0.33	0.020	0.061
Recirculation Rate	1.16	0.10	0.116	0.35

(a) denoted $\left|E'_{30,P}\right| + \left|t'_{Ct,P}\right|$ in Equations 8 and 9
(b) denoted as the quantity ($\Delta P_{Set\ Change}/P_{base}$) in Equations 8 and 9
(c) denoted I_P in Equations 8 and 9

9.2 Impact Analysis Limitations

As with any analysis, it is important to understand the limitations of the method outlined above as well as to understand the applicability of the results. To illustrate these two concepts, an alternative set of baseline parameters with a greatly reduced leakage (i.e., all parameters are the same as the previously detailed baseline case except for an interzonal leakage of 0.01 ACH) was used for comparison with the illustrative results of the previous two sections. Comparisons between the alternative baseline results and the illustrative results from Sections 9.1 are intended to demonstrate that: (1) the results and discussion stated in this work are applicable only to cases described by the parameter set used in the analysis; (2) inferences made based on the gradients of the normalized plots (e.g., Figures 36 and 37) are valid only in the parameter space represented by the baseline case (i.e., at or near $P/P_{Base}=1$); and that (3) while this analysis was designed for typical buildings under standard daytime operation (e.g., the baseline parameters outlined in Table 13), it is valid for atypical buildings under nonstandard operating conditions (e.g., an alternative baseline with a greatly reduced leakage rate of 0.01 ACH). Thus, while the specific analysis results presented in this document may be valid only for notional buildings under standard daytime operation, the analysis approach used here is valid for virtually all buildings under any operating conditions.

Figure 38 is the analog to Figure 36 for the alternative baseline case (i.e., original baseline case with a greatly reduced leakage rate of 0.01 ACH). Note that in Figure 38, the gradient of the infiltration rate curve (shown in green) seems small in comparison to that of the filter efficiency curve (shown in blue), while in Figure 36, the two curves are very similar (i.e., they exhibit approximately the same slope at $P/P_{Base}=1$ in Figure 36).

This difference indicates that the relative importance of both the filtration efficiency and the infiltration rate depend on other parameters. This illustrates that the results of an analysis are valid only when the parameters used in the analysis describe the situation of interest. No set of parameters is universally applicable. Some situations are not represented by the parameter set used in this illustration (e.g., a building equipped with a HEPA filter).

It is also essential to note that comparing the slopes of the curves at $P/P_{Base} \neq 1$ is not valid since those parameter spaces represent the simultaneous variation of multiple parameters. For example, comparing the slopes of the curves from Figure 38 for filter efficiency and leakage rate at $P/P_{Base} = 2$ is comparing the impact of a relative change in room leakage for a leakage of 2 ACH and 30% filter efficiency to the impact of a relative change in filter efficiency for a leakage of 1 ACH and 65% filter efficiency. While this information is interesting, no conclusions can be drawn without further exploring and defining the parameter space surrounding those points (i.e., repeat the analysis of the previous two sections for an alternative set of baseline conditions corresponding to the parameter space represented by each of those points).

It is also important to note that the impact analysis outlined here is focused on zones directly linked via leakage to the zone of release. An analogous approach could be used to determine the impact of various parameters on the rest of the building (i.e., zones not directly linked to the zone of release via leakage). This could be done by treating the exposure and time to peak within the third, lumped zone in an identical manner as the exposure and time to peak for the zone of interest were treated in the impact analysis (See Section 9.1)

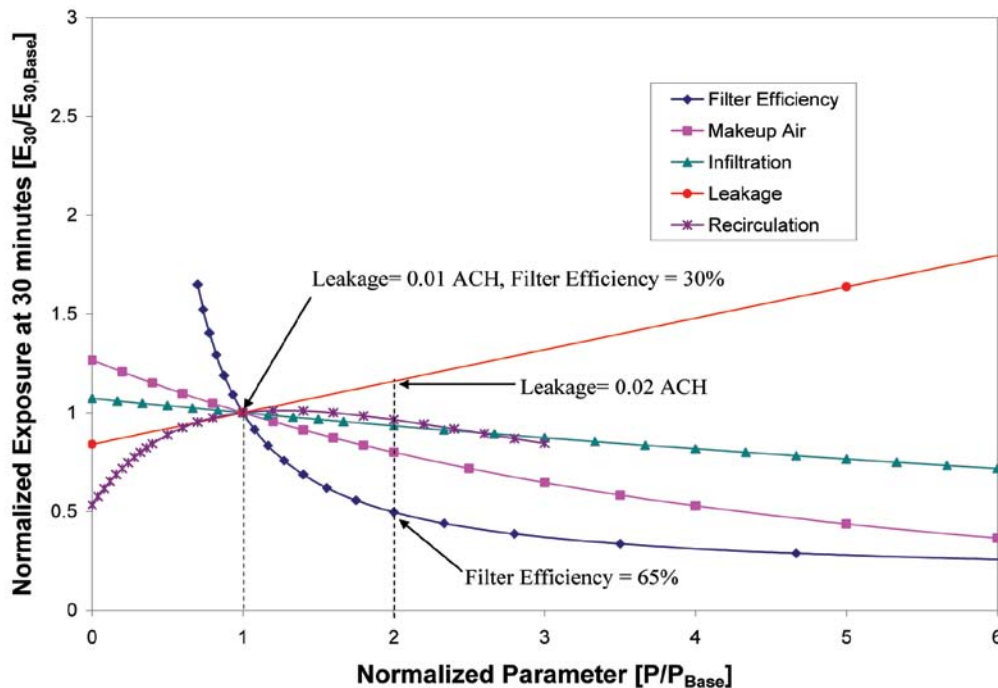**Figure 38.** Normalized Exposure at 30 Minutes ($E_{30,2}$) Versus Model Input Parameters for a "Large" Notional Building ($V_3=100V_1$) Under 1 ACH Makeup Air, 5 ACH Recirculation, 0.3 ACH Infiltration, 30% Filtration, and 0.01 ACH Interzonal Leakage. Note that $P/P_{base}=1$ signifies condition is identical to the previously described base case with the exception of a greatly reduced leakage rate (0.01 ACH).

9.3 Preliminary Impact Analysis Results

In order to identify the key parameters of interest, a preliminary set of model simulations were performed. These simulations examined the impact of the makeup air, recirculation, infiltration, leakage, and filtration efficiency for notional buildings of varying sizes for a typical set of building parameters (i.e., 1 ACH Makeup Air, 5 ACH Recirculation, 0.3 ACH Infiltration, 1 ACH Leakage, and 30% Filtration).

To examine the effects of building size, the volume of Zone 3 was set to 1, 5, 10, 25, 50, and 100 times the volume of a standard 142-m3 room, yielding Zone 3 volumes of 142; 710; 1,420; 3,550; 7,100; and 14,200 m3, respectively. Next, each of the HVAC parameters was individually varied from the typical set of building parameters. Table 15 contains the impact analysis results for the typical set of building parameters for a Zone 1 release for various Zone 3 volumes. These results can also be viewed graphically as displayed in Figure 39. Note that the curves connecting the data points are merely to help illustrate the dependency. For reference, Table 16 contains the typical set of building parameters used and the ranges used in the analysis.

The detailed results, in the form of graphs of normalized performance metrics versus normalized parameters, can be found in Appendix B.

The low normalized impact scores for the makeup air and infiltration indicate that over the range of building volumes modeled, for the typical building parameters and a release scenario within a zone (Zone 1), the makeup air and infiltration have little effect on the performance metrics. Thus, the makeup air and infiltration rates would not be parameters of interest in attempting to improve the performance of a building described by the typical building parameters against a similar release scenario. From a theoretical standpoint, it is interesting to note the shape of the system makeup air impact curve, which exhibits a maximum near a building volume of ~1,000 m^3 (which corresponds to a Zone 3 volume of five times that of Zone 2). This region indicates that for low volumes (i.e., $V_3 < 5V_2$), described by the base case conditions, the dilution provided by the system makeup airflow rate of 1 ACH is of slightly greater importance than the system recirculation rate of 5 ACH. As building volume (i.e., the Zone 3 volume) is increased beyond ~1,000 m^3, the dilution effects of the system recirculation surpass those of the system makeup air.

Table 15. Impact Analysis Results for Various Zone 3 Volumes Under 1 ACH Makeup Air, 5 ACH Recirculation, 0.3 ACH Infiltration, 30% Filtration, and 1 ACH Interzonal Leakage

	Zone 2 Parameter	Normalized Impact Score
$V_3 = 1V_2$	Filtration Efficiency	1.00
	Leakage	0.21
	System Makeup Air	0.16
	System Infiltration	0.06
	System Recirculation	0.07
$V_3 = 5V_2$	Filtration Efficiency	1.00
	Leakage	0.87
	System Makeup Air	0.26
	System Infiltration	0.10
	System Recirculation	0.20
$V_3 = 10V_2$	Filtration Efficiency	0.76
	Leakage	1.00
	System Makeup Air	0.33
	System Infiltration	0.10
	System Recirculation	0.32

	Zone 2 Parameter	Normalized Impact Score
$V_3 = 25V_2$	Filtration Efficiency	0.42
	Leakage	1.00
	System Makeup Air	0.28
	System Infiltration	0.17
	System Recirculation	0.41
$V_3 = 50V_2$	Filtration Efficiency	0.12
	Leakage	1.00
	System Makeup Air	0.21
	System Infiltration	0.07
	System Recirculation	0.37
$V_3 = 100V_2$	Filtration Efficiency	0.06
	Leakage	1.00
	System Makeup Air	0.21
	System Infiltration	0.07
	System Recirculation	0.38

Table 16. Typical Parameter Values and Model Parameter Ranges

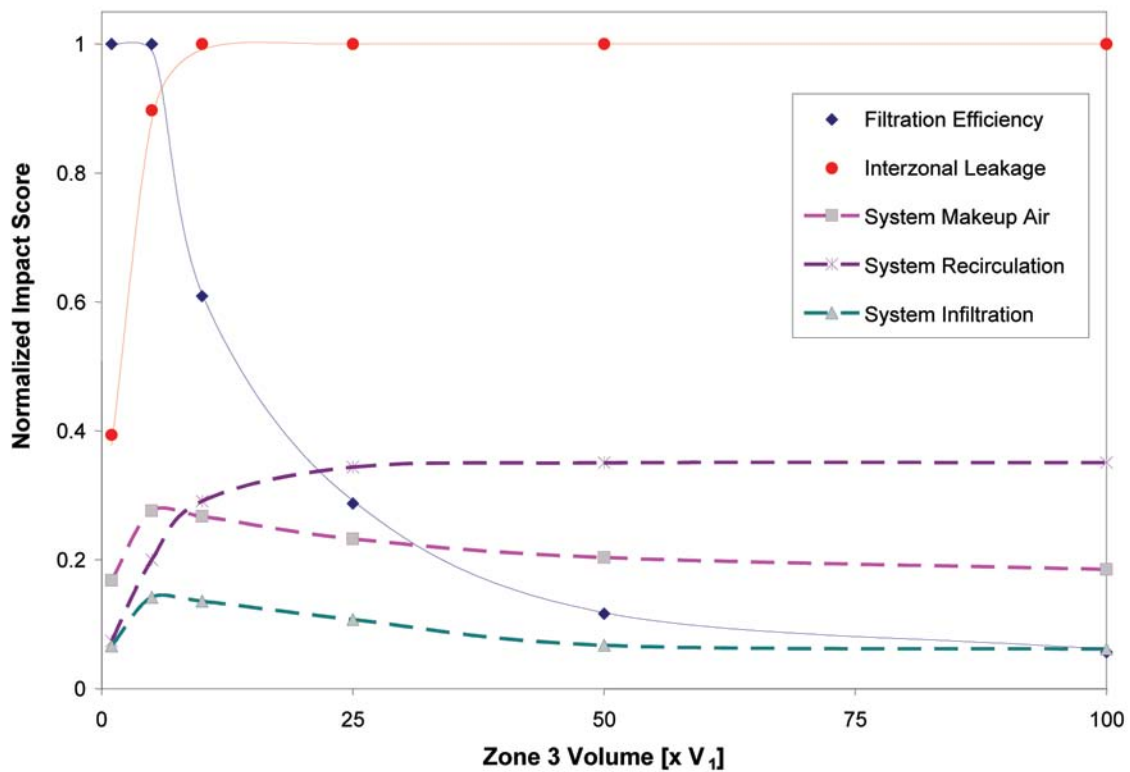| Variable	Min	Base case	Max
Filter Efficiency [%]	0	30	99.9999
Makeup Air Rate [ACH]	0	1	15
Recirculation Rate [ACH]	0	5	15
Infiltration Rate [ACH]	0	0.3	2
Room Leakage [ACH]	0	1	2
Zone 1 Volume [m³]	N/A	143	N/A
Zone 2 Volume [m³]	N/A	143	N/A
Zone 3 Volume [m³]	143	14,300	14,300

N/A is defined as not applicable.

Figure 39. Impact Analysis Results for Various Zone 3 Volumes Under 1 ACH Makeup Air, 5 ACH Recirculation, 0.3 ACH Infiltration, 30% Filtration, and 1 ACH Interzonal Leakage

The results of the filtration efficiency, recirculation rate, and leakage rate are more interesting. The analysis shows that the most important parameter affecting building performance (with respect to changing the exposure or time for a critical exposure to occur) changes as the building size —Zone 3— changes. For building volumes less than ~3,800 m^3 (which corresponds to a Zone 3 volume of 25 times that of Zone 2), the dominant factor is clearly the removal of agent from the combined recirculation stream via filtration. Figure 39 indicates that as the building volume increases beyond ~1,000 m^3 (i.e., $V_3=5V_2$), the dominant factors are the leakage rate, the recirculation rate, and, to a lesser extent, the filtration efficiency. This trend suggests that as the building size increases, or more specifically as the volume of recirculated air increases, the main mitigation mechanism becomes dilution, while the filter efficiency becomes of lesser importance. As this occurs, the interzonal leakage, which acts as a delivery mechanism, becomes of increased importance and assumes the role of the dominant factor determining performance.

The above discussion regarding the use of impact scores to assess which parameters are most important and how well the parameters need to be known illustrates that a single, global generalization cannot necessarily be made. That is, the effect of parameters on the spread of contaminant depends on numerous other parameters and on the system HVAC configuration/operation. Consequently, in assessing factors that affect building performance, a good understanding of the building operation is needed. It would then be best to assess the building of interest using the simplified model approach presented here. The usefulness of the simplified model approach is that detailed modeling and input data sets would not be required for an initial assessment.

9.4   Parameter Space Map Impact Analysis
Based on preliminary modeling results, a map of the parameter space defined by varying interzonal leakage rates, system recirculation rates, and general filtration efficiencies was constructed. For "large" and "small" notional building volumes, simulations exploring these three key variables were performed. Interzonal leakage rates of 1.0, 0.7, 0.4, and 0.1 ACH were used to examine the effects of various leakage rates. These values were chosen to approximate the range over which the interzonal leakage can realistically be controlled. General filtration efficiencies of 10, 30, 60, 90, and 99% were used to further map out the parameter space of interest. Again, these values were chosen to approximate the range over which the filter efficiency could realistically vary.

For each combination of filtration efficiencies and leakage rates, further simulations were performed at system recirculation rates of 3, 5, and 7 ACH. These values were chosen based on rough estimates of the maximum system recirculation rates achievable by conventional HVAC systems. Generally speaking, there are two main types of air handling systems used in typical commercial office buildings: (1) fixed volume systems and (2) variable air volume systems (Bell, 2000). Fixed volume systems typically operate at full capacity (100%), and thus no further increase in the system recirculation rate is possible (Bell, 2000). Variable air volume systems are used in higher-end office buildings and operate at 50 to 75% of full capacity (Bell, 2000). Based on this information, a maximum system recirculation rate of 7 ACH was determined to be appropriate for this work. In order to provide insight into the impact of the system recirculation rate, a recirculation rate of 3 ACH was also added to the simulation matrix.

Also based on preliminary results, building volumes of 5 and 100 times that of the zone of interest were chosen to represent "small" and "large" notional buildings, respectively. For "large" and "small" notional building volumes, each combination of these three parameters (i.e., filtration efficiency, leakage rate, and recirculation rate) was used as an analysis baseline case. Thus, for each possible combination of the aforementioned values, the procedure described in Section 9.1 (illustrated in Figures 36 and 37, as well as Table 14) was performed.

9.4.1 "Large" Notional Building Parameter Space Map Results
A "large" notional building was defined for this effort as having a volume of 14,600 m^3. An example of the "large" building, with a nominal ceiling height of 3 m, might include a 1,200-m^3 lobby (20 m x 20 m), ten 75-m^3 reception areas (5 m x 5 m), twelve 150-m^3 conference rooms (10 m x 5 m), one hundred twenty 75-m^3 offices (5 m x 5 m), and approximately 1,850 m^3 of hallways, stairwells, elevators, and restrooms. This "large" notional building would have a standard occupancy of 134 to 148, based on estimates of one person per office, four to eight persons in the lobby, and one to two persons in the reception areas.

The impact analysis results for the parameter space of interest for a Zone 1 release in a "large" building are listed in Table 17. The parameter space map is also illustrated by a series of three-dimensional surface plots in Figures 40 through 42. Note that the three-dimensional plots use a surface spline to connect the actual data points contained in Table 17 and are intended as an illustrative tool to graphically present the results.

Table 17. Impact Analysis Results for the "Large" Building (14,600 m³) Parameter Space Map (Note that Recirculation has been abbreviated Recirc in the Table Interior.)

Recirculation [ACH] = 7

Filtration [%]	Leakage [ACH] 0.1			Leakage [ACH] 0.4			Leakage [ACH] 0.7			Leakage [ACH] 1		
	Recirc Impact	Leakage Impact	Filtration Impact	Recirc Impact	Leakage Impact	Filtration Impact	Recirc Impact	Leakage Impact	Filtration Impact	Recirc Impact	Leakage Impact	Filtration Impact
10	0.02	1.00	0.40	0.10	1.00	0.44	0.20	1.00	0.39	0.27	1.00	0.59
30	0.03	1.00	0.22	0.12	1.00	0.20	0.21	1.00	0.32	0.35	1.00	0.24
60	0.03	1.00	0.08	0.13	1.00	0.09	0.21	1.00	0.13	0.29	1.00	0.07
90	0.05	1.00	0.02	0.13	1.00	0.01	0.20	1.00	0.02	0.32	1.00	0.01
99	0.06	1.00	0.00	0.13	1.00	0.00	0.23	1.00	0.00	0.30	1.00	0.00

Recirculation [ACH] = 5

Filtration [%]	Leakage [ACH] 0.1			Leakage [ACH] 0.4			Leakage [ACH] 0.7			Leakage [ACH] 1		
	Recirc Impact	Leakage Impact	Filtration Impact	Recirc Impact	Leakage Impact	Filtration Impact	Recirc Impact	Leakage Impact	Filtration Impact	Recirc Impact	Leakage Impact	Filtration Impact
10	0.02	1.00	0.22	0.12	1.00	0.26	0.24	1.00	0.21	0.31	1.00	0.19
30	0.03	1.00	0.13	0.13	1.00	0.17	0.23	1.00	0.12	0.36	1.00	0.13
60	0.03	1.00	0.05	0.13	1.00	0.04	0.23	1.00	0.10	0.36	1.00	0.05
90	0.03	1.00	0.01	0.14	1.00	0.01	0.25	1.00	0.01	0.33	1.00	0.02
99	0.03	1.00	0.00	0.14	1.00	0.00	0.25	1.00	0.00	0.33	1.00	0.00

Recirculation [ACH] = 3

| Filtration [%]	Leakage [ACH] 0.1			Leakage [ACH] 0.4			Leakage [ACH] 0.7			Leakage [ACH] 1		
	Recirc Impact	Leakage Impact	Filtration Impact	Recirc Impact	Leakage Impact	Filtration Impact	Recirc Impact	Leakage Impact	Filtration Impact	Recirc Impact	Leakage Impact	Filtration Impact
10	0.02	1.00	0.09	0.13	1.00	0.14	0.26	1.00	0.08	0.39	1.00	0.08
30	0.03	1.00	0.06	0.15	1.00	0.05	0.27	1.00	0.06	0.40	1.00	0.06
60	0.03	1.00	0.03	0.15	1.00	0.02	0.26	1.00	0.02	0.40	1.00	0.03
90	0.04	1.00	0.00	0.16	1.00	0.01	0.28	1.00	0.00	0.41	1.00	0.00
99	0.04	1.00	0.00	0.16	1.00	0.00	0.28	1.00	0.00	0.41	1.00	0.00
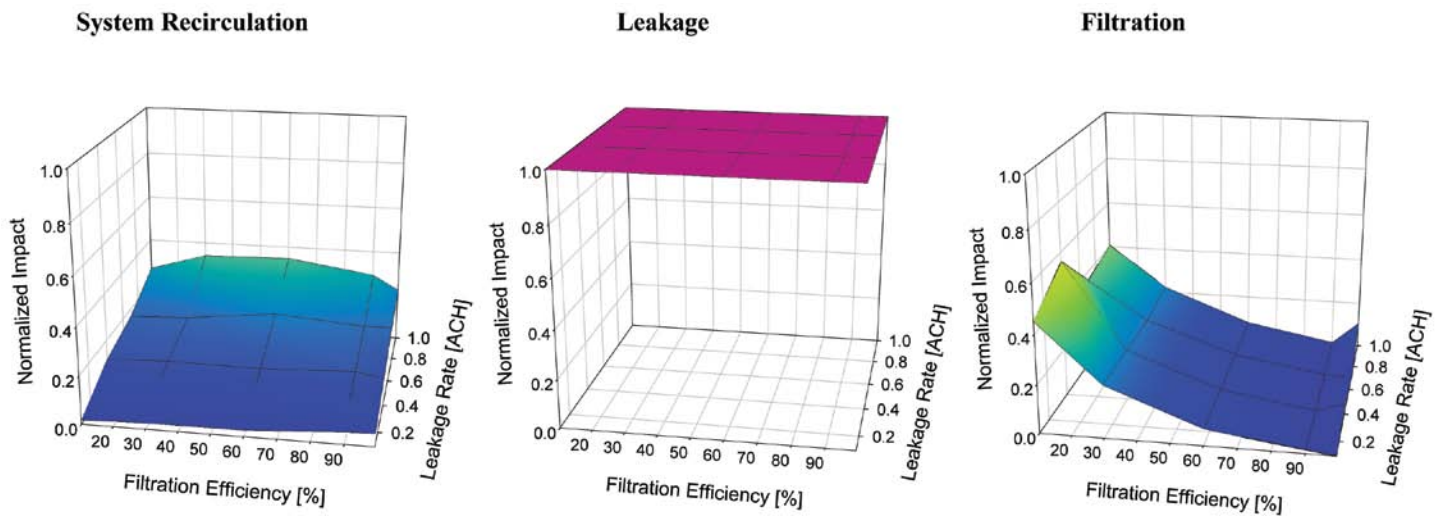
Figure 40. "Large" Building (14,600 m³) Parameter Mapping Results for a Recirculation Rate of 7 ACH
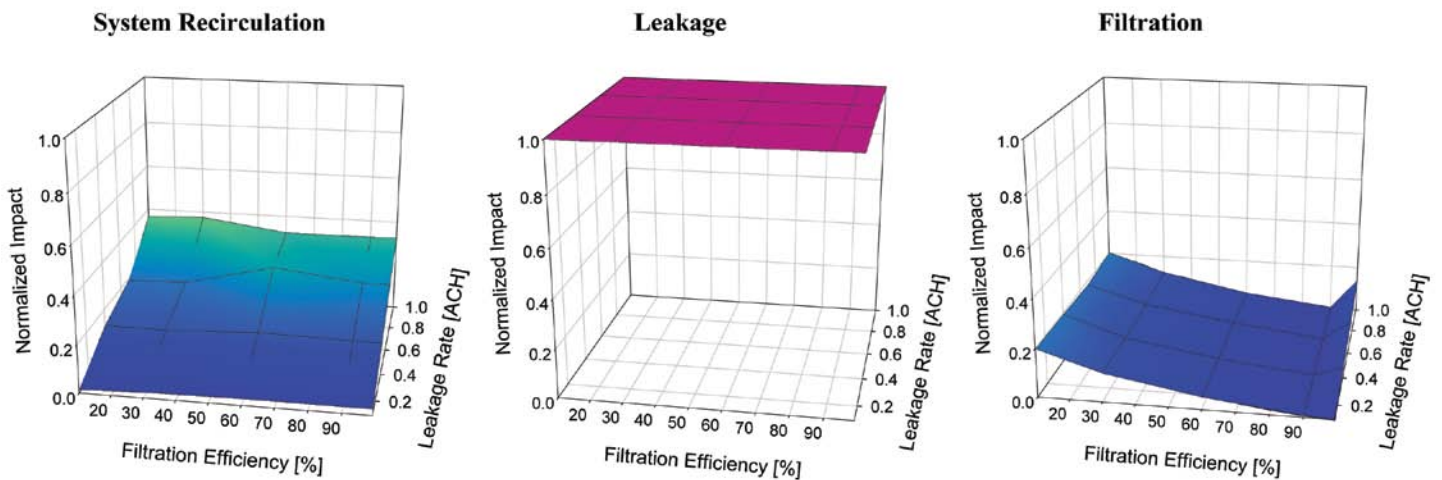

Figure 41. "Large" Building (14,600 m³) Parameter Mapping Results for a Recirculation Rate of 5 ACH
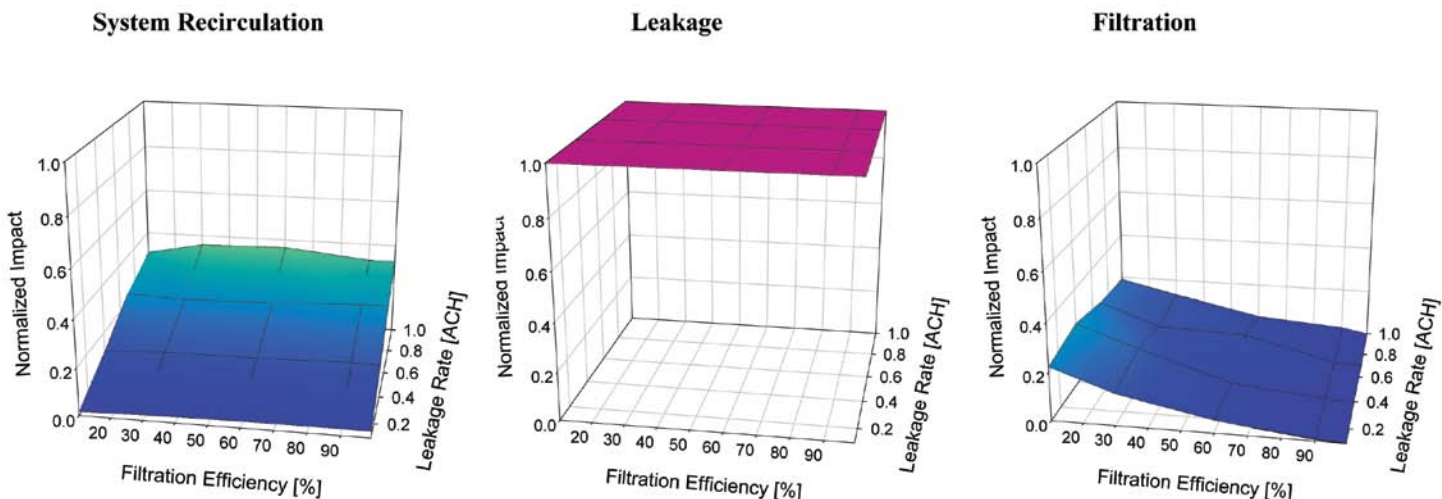

Figure 42. "Large" Building (14,600 m³) Parameter Mapping Results for a Recirculation Rate of 3 ACH

The parameter space map data for a notional "large" building indicate that under most conditions the leakage rate between zones has the largest impact on building performance for an interior release. Even for extreme conditions not sampled in this study where another parameter may have a larger impact, the leakage still would have a large impact (i.e., greater than 0.6 on a scale normalized to unity). This strongly suggests that for a "large" building, the interzonal leakage rate is the key parameter in improving the performance of the building against an internal release.

In understanding these results, it is paramount to consider that the impact analysis indicates the parameter for which a reasonable change (i.e., the Set Changes in Table 13) will produce the largest change in building performance (i.e., the sum of the performance metrics described in Section 9.1). To further elucidate this trend, let us consider our three key parameters (recirculation, leakage, and filtration) in terms of a rough mass balance around the zone of interest. Leakage from the release zone and the common HVAC recirculation represent the two potential routes by which contaminant may enter the zone of interest at any given instant in time. In the parameter space studied, leakage from the release zone to the zone of interest represents a flow path of 0.1-1 ACH with a concentration equal to that of the release zone. Similarly, in the parameter space studied, the system recirculation represents a flow path of 3–7 ACH with a concentration equal to roughly 1/100 of the concentration in the release zone, based on a building volume of 100 times that of the zone of interest. Considering these estimates, it is clear that leakage from the release zone is the dominant delivery mechanism.

Similarly, leakage from the zone of interest, system recirculation, and filtration represent the potential routes by which contamination may be removed from the zone of interest at any given instant in time. In the parameter space studied, the leakage from the zone of interest represents a removal rate of 0.1-1 ACH (for the purposes of this crude analysis, the makeup air and infiltration will be neglected). The system recirculation represents a removal rate of 3–7 ACH in the parameter space of this study. Filtration represents a reduction in the concentration delivered by the system recirculation. At first glance, filtration may appear to be the dominant removal mechanism; however, it is important to consider that the reduction in the recirculated concentration due to filtration is in addition to the reduction in the recirculated concentration due to dilution. For the "large" building, the concentration in the system recirculation has already been diluted by a factor of 100 due to the size of the building. Thus, the impact of a 90% efficient filter on the performance metrics can be approximated as the impact of changing the concentration of the recirculated flow from roughly 1/100 of the release zone concentration to roughly 1/1,000 of the release zone concentration. Clearly, the impact of this change in the recirculated concentration is much less than the impact of the leakage, which can be approximated as the impact of changing the interzonal leakage rate, which possesses a contaminant concentration equal to that in the zone of release. In this manner, the impact of filtration on the performance metrics is marginalized by dilution in the system recirculation in a "large" building under the conditions studied here.

These results imply an interesting trend in addition to the importance of the interzonal leakage. As illustrated in Figures 40 through 42, the filtration impact tends to decrease as filtration efficiency increases. The slope of this trend is increased at higher recirculation rates and minimal at lower recirculation rates, confirming the coupled nature of filtration and recirculation. Thus, although the recirculation rate has a minimal impact score in and of itself, it has a significant effect on the filtration impact.

9.4.2 "Small" Notional Building Parameter Space Map Results

A "small" notional building was defined for this effort as having a volume of 1,000 m^3. A notional example of the "small" building, with a nominal ceiling height of 3 m, might include a 300-m^3 lobby (10 m x 10 m), a 150-m^3 conference room (10 m x 5 m), six 75-m^3 offices (5 m x 5 m), and approximately 100 m^3 of hallways and restrooms. This "small" notional building would have a standard occupancy of approximately seven to eight persons based on estimates of one person per office and one to two people in the lobby.

The impact analysis results for the parameter space of interest for a Zone 1 release in a "small" building are listed in Table 18. The parameter space map is also illustrated by a series of three-dimensional surface plots in Figures 43 through 45. Note that the three-dimensional plots display use a surface spline to connect the actual data points contained in Table 18 and are intended as an illustrative tool to graphically present the results. In order to further reduce the data, a parameter space map indicating the approximate parameter with the highest impact is given in Figure 46.

The impact analysis results for the notional "small" building are more complex and "feature rich" than their "large" building counterparts. Similar to the "large" building results, the parameter space maps for the "small" building indicate that at high filtration efficiencies the interzonal leakage has the largest impact on building performance. However, at lower filtration efficiencies the filtration efficiency has the largest impact. The division between these two regimes appears to be linked to recirculation, varying from roughly 75% at a recirculation rate of 7 ACH to approximately 30% at a recirculation rate of 3 ACH. Thus, while recirculation is not a dominant parameter in terms of its direct impact, it does play a determining role in what is the dominant impact parameter. These results indicate that, generally speaking, for the notional "small" building, removal of contaminant via filtration and delivery of contaminant via interzonal leakage have the largest impacts on building performance for an interior release.

Which of these parameters dominates appears to depend mainly on the filtration efficiency with interzonal leakage dominating at high filtration efficiencies and filtration efficiency dominating at low filtration efficiencies. As described above, recirculation rate plays a secondary role by altering the division between the filtration-dominant region and the leakage-dominant region. Thus, the critical filtration efficiency value will depend on both the building size (relative to the zone of interest) and the system recirculation rate. For example, the critical filtration efficiency is approximately 50% for a building volume of 1,000 m^3 (relative

to a zone of interest volume of 143 m^3) and a recirculation rate of 5 ACH, while the critical filtration efficiency is roughly 75% for a building volume of 1,000 m^3 (relative to a zone of interest volume of 143 m^3) and a recirculation rate of 7 ACH. Again, as in previous sections, the estimated accuracy requirements follow the impact analysis results in that high impact parameters have tight estimated accuracy requirements.

The marked differences between the "small" and "large" building results imply that for a "small" building the delivery of contaminant via interzonal leakage and the removal of contaminant via filtration of the recirculated air are of comparable magnitudes. The reason for this is the large reduction in the dilution of contaminant in the recirculated stream (a factor of ~5 versus a factor of ~100). With the reduction in dilution, contaminant removal via filtration of the recirculated air becomes the dominant mechanism for the removal of contaminant from the zone of interest. Thus, the reduction in dilution has greatly increased the importance (i.e., the impact) of filtration and created regions in the parameter space where a change in the filtration efficiency will produce the largest change in building performance (i.e., the performance metrics).

Table 18. Impact Analysis Results for the "Small" Building (1,000 m³) Parameter Space Map (Note that Recirculation has been abbreviated Recirc in the Table Interior.)

| Recirculation [ACH] | Filtration [%] | Interzonal Leakage [ACH] | | | | | | | | | | | |
| | | 0.1 | | | 0.4 | | | 0.7 | | | 1 | | |
		Recirc Impact	Leakage Impact	Filtration Impact	Recirc Impact	Leakage Impact	Filtration Impact	Recirc Impact	Leakage Impact	Filtration Impact	Recirc Impact	Leakage Impact	Filtration Impact
7	10	0.03	0.17	1.00	0.02	0.19	1.00	0.02	0.16	1.00	0.03	0.16	1.00
	30	0.02	0.30	1.00	0.04	0.30	1.00	0.05	0.30	1.00	0.06	0.31	1.00
	60	0.05	0.80	1.00	0.10	0.72	1.00	0.16	0.78	1.00	0.20	0.75	1.00
	90	0.03	1.00	0.17	0.12	1.00	0.18	0.21	1.00	0.18	0.33	1.00	0.19
	99	0.04	1.00	0.01	0.13	1.00	0.01	0.20	1.00	0.01	0.35	1.00	0.01

| Recirculation [ACH] | Filtration [%] | Interzonal Leakage [ACH] | | | | | | | | | | | |
| | | 0.1 | | | 0.4 | | | 0.7 | | | 1 | | |
		Recir Impact	Leakage Impact	Filtration Impact	Recirc Impact	Leakage Impact	Filtration Impact	Recirc Impact	Leakage Impact	Filtration Impact	Recirc Impact	Leakage Impact	Filtration Impact
5	10	0.06	0.31	1.00	0.03	0.29	1.00	0.04	0.34	1.00	0.05	0.27	1.00
	30	0.05	0.48	1.00	0.05	0.52	1.00	0.09	0.46	1.00	0.13	0.42	1.00
	60	0.04	1.00	0.85	0.12	1.00	0.85	0.21	1.00	0.94	0.29	1.00	0.95
	90	0.03	1.00	0.12	0.13	1.00	0.12	0.25	1.00	0.14	0.36	1.00	0.14
	99	0.03	1.00	0.01	0.14	1.00	0.01	0.25	1.00	0.01	0.33	1.00	0.01

| Recirculation [ACH] | Filtration [%] | Interzonal Leakage [ACH] | | | | | | | | | | | |
| | | 0.1 | | | 0.4 | | | 0.7 | | | 1 | | |
		Recirc Impact	Leakage Impact	Filtration Impact	Recirc Impact	Leakage Impact	Filtration Impact	Recirc Impact	Leakage Impact	Filtration Impact	Recirc Impact	Leakage Impact	Filtration Impact
3	10	0.15	0.68	1.00	0.08	0.74	1.00	0.07	0.67	1.00	0.12	0.55	1.00
	30	0.13	1.00	0.99	0.06	0.98	1.00	0.14	1.00	0.89	0.17	0.83	1.00
	60	0.03	1.00	0.44	0.10	1.00	0.44	0.20	1.00	0.43	0.31	1.00	0.35
	90	0.03	1.00	0.07	0.14	1.00	0.07	0.27	1.00	0.07	0.39	1.00	0.08
	99	0.04	1.00	0.00	0.15	1.00	0.00	0.28	1.00	0.00	0.43	1.00	0.00
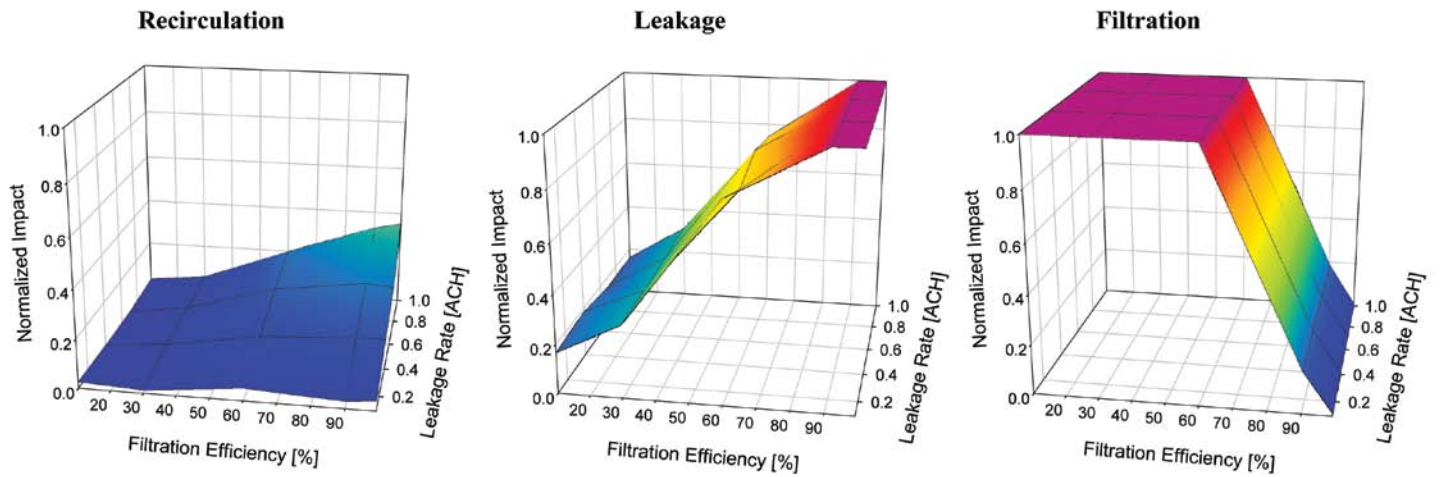
Figure 43. "Small" Building (1,000 m³) Parameter Mapping Results for a Recirculation Rate of 7 ACH
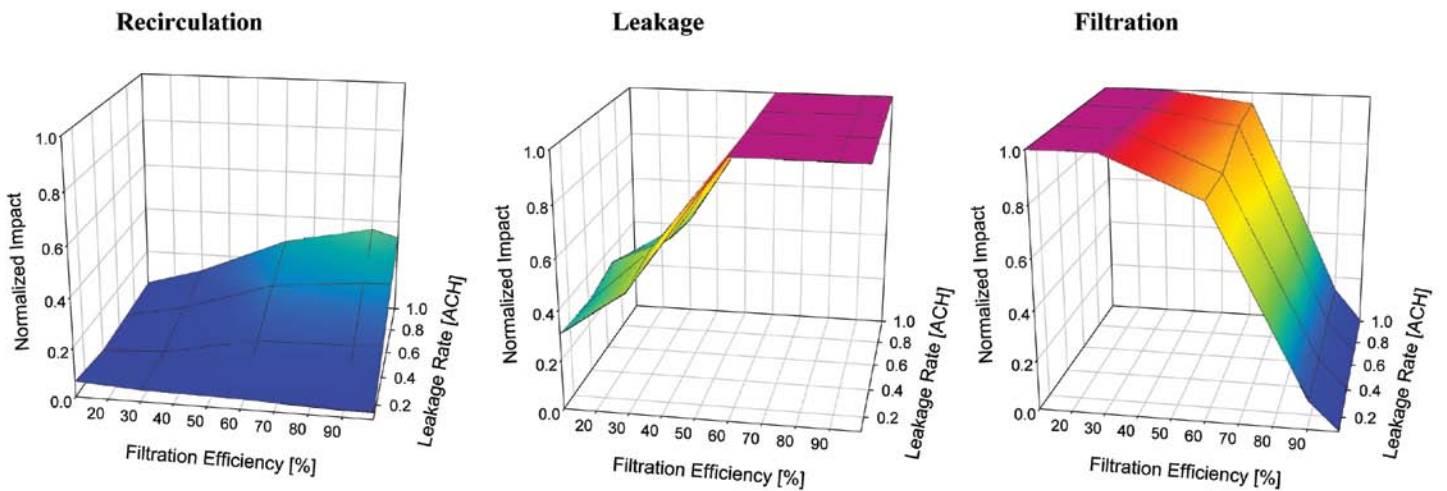

Figure 44. "Small" Building (1,000 m³) Parameter Mapping Results for a Recirculation Rate of 5 ACH
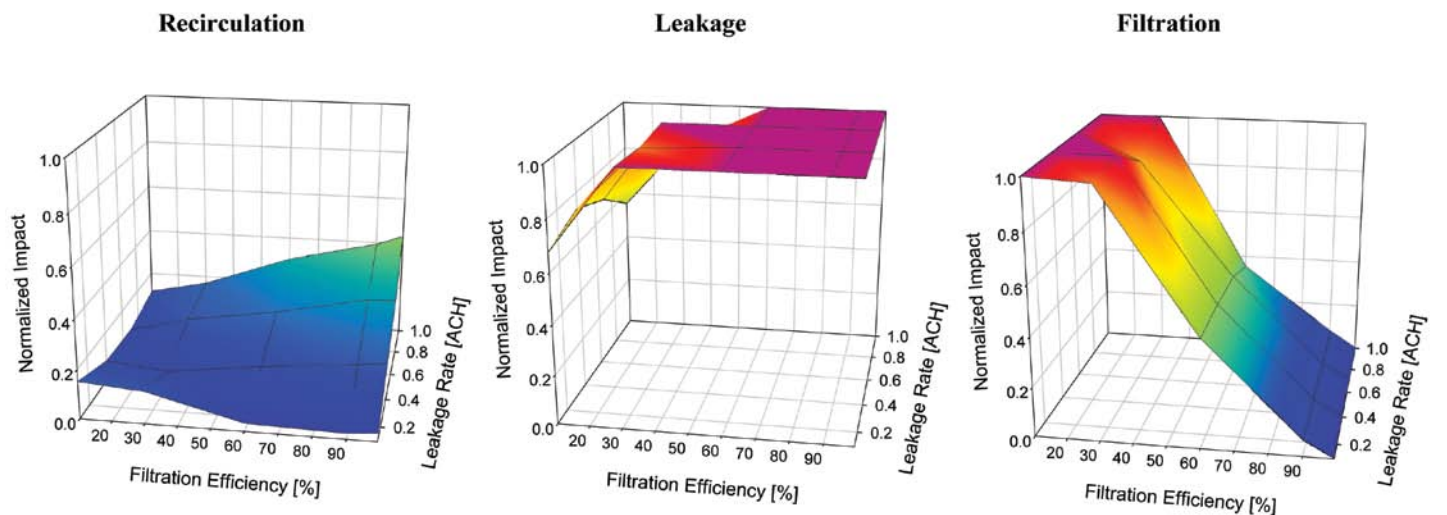

Figure 45. "Small" Building (1,000 m³) Parameter Mapping Results for a Recirculation Rate of 3 ACH
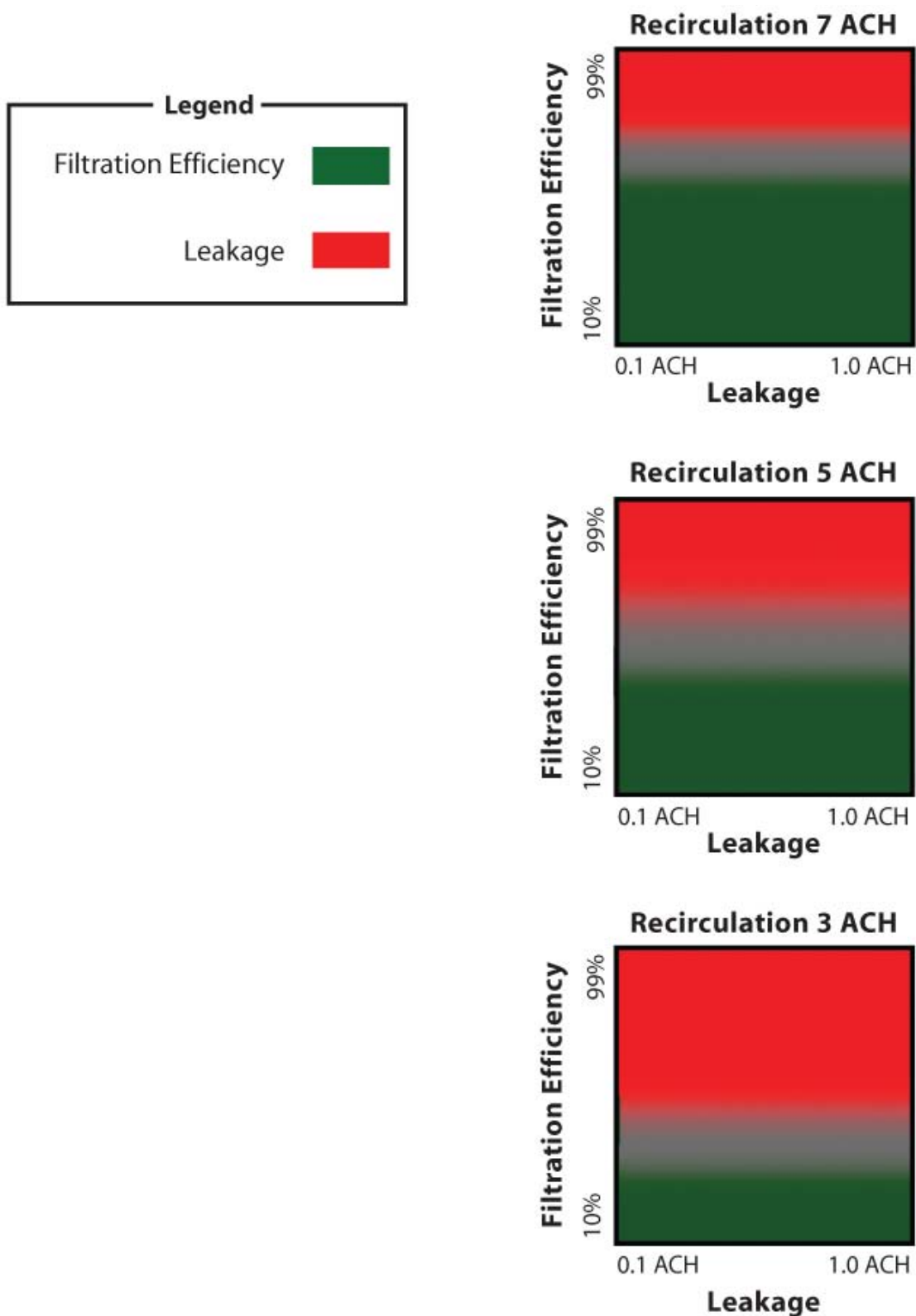
Figure 46. Parameter Space Map of the Dominant Parameter, or Parameter with the Highest Impact Score, for a "Small" Building (1,000 m³) (Note that grey regions are intended to indicate a region where two or more parameters are dominant).

9.5 Functional Analysis Guidelines

Although it is not possible to make blanket statements about dominant parameters, a simple functional analysis can be used to develop some general guidelines regarding which HVAC parameters are important for a range of situations. This simple functional analysis will generalize the key delivery and removal mechanisms for the zone of interest (i.e., Zone 2) in terms of simple functional forms.

The simplified analysis begins with combining the makeup airflow rate and the recirculation flow rate into a lumped HVAC flow rate (see Equation 10).

$$Q_{HVAC,i} \approx Q_{I,i} + Q_{R,i} \qquad (10)$$

Where $Q_{I,i}$, $Q_{R,i}$, and $Q_{HVAC,i}$ denote the makeup airflow rate, the recirculated airflow rate, and the lumped HVAC flow rate for Zone i.

Furthermore, since both the makeup air and the recirculated airflow rate are nominally functions of the zone volume, the lumped HVAC flow rate can be rewritten as an integer function of the zone volume (see Equation 11).

$$Q_{HVAC,i} \approx N * V_i \qquad (11)$$

Where V_i denotes the volume of Zone i and N is an integer frequency, nominally on the order of 3–8 hr^{-1}.

Neglecting infiltration (i.e., assuming there is no infiltration or that the magnitude of infiltration is so small that it can be ignored), there are two delivery mechanisms for the zone of interest (i.e., Zone 2). One delivery mechanism is interzonal leakage from the zone of release (i.e., Zone 1), which is functionally dependent on the product of the leakage flow rate, denoted Q_{Leak}, and the concentration within the zone of release, denoted $C_1(t)$. The other delivery mechanism is the simple HVAC system, where the delivery of contaminant is functionally dependent on the product of the lumped HVAC flow ($Q_{HVAC,2}$), the concentration in the common ductwork ($C_{HVAC}(t)$), and a filtration efficiency term (1-η). It is important to note that both the concentration within the zone of release ($C_1(t)$) and the concentration in the common HVAC ductwork ($C_{HVAC}(t)$) are functions of time under non-steady-state conditions. Despite the time dependency of the concentrations, a general functional form for the delivery term is obtained (see Equation 12).

$$[Delivery] \approx Q_{Leak} * C_1(t) + (1-\eta) * Q_{HVAC,2} * C_{HVAC}(t) \qquad (12)$$

This delivery mechanism functional form can be further reduced by approximating the concentration in the common HVAC ductwork ($C_{HVAC}(t)$) in terms of the HVAC flows and concentrations of each of the contributing zones (Equation 13). It is important to note that the resulting expression (i.e., Equation 13) is an approximation and assumes that the lumped HVAC flow rate for any given zone is much larger than the interzonal leakage entering or exiting that zone. Assuming that the concentration within the zone of release is the highest of the three zones, this approximation represents an overestimation of the contributions of the HVAC flow to contaminant delivery. While this approach is not exact, it is more than sufficient for a simple, rough analysis such as this.

$$C_{HVAC}(t) \approx \frac{Q_{HVAC,1} * C_1(t) + Q_{HVAC,2} * C_2(t) + Q_{HVAC,3} * C_3(t)}{Q_{HVAC,1} + Q_{HVAC,2} + Q_{HVAC,3}} \qquad (13)$$

Assuming that the recirculation and makeup air are system-wide variables (i.e., each zone has the same recirculation and makeup air when expressed in units of air changes per hour), this expression can be further reduced using the previously derived expression for the lumped HVAC flows as a function of zone volume (i.e., Equation 11) to a volume weighted average of the concentrations within each zone (see Equation 14). The resulting expression is quite helpful in estimating the contributions of common HVAC system to the delivery of contaminant.

$$C_{HVAC}(t) \approx \frac{V_1 * C_1(t) + V_2 * C_2(t) + V_3 * C_3(t)}{V_1 + V_2 + V_3} \qquad (14)$$

Similarly, when infiltration is neglected, there are two mechanisms for the removal of contaminant from the zone of interest (i.e., Zone 2). One removal mechanism is interzonal leakage from the zone of interest to the bulk of the building (i.e., Zone 3), which is functionally dependent on the product of the leakage flow rate, denoted Q_{Leak}, and the concentration within the zone of interest, denoted $C_2(t)$. The other removal pathway is the simple HVAC system, where the removal of contaminant is functionally dependent on the product of the lumped HVAC flow ($Q_{HVAC,2}$) and the concentration in the zone of interest ($C_2(t)$). Again, the concentration within the zone of interest ($C_2(t)$) is a function of time under non-steady state conditions. Following this approach, a general functional form for the removal of contaminant is obtained (see Equation 15).

$$[Removal] \approx Q_{Leak} * C_2(t) + Q_{HVAC,2} * C_2(t) \qquad (15)$$

Through consideration of the functional forms of the delivery mechanisms (Equation 12), removal mechanisms (Equation 15), and the contaminant concentration in the common HVAC ductwork (Equation 14) a rough, back-of-the-envelope analysis of a given situation can be performed to provide an initial indication as to which parameters are most important and which parameters, if any, can potentially be neglected or ignored.

9.5.1 Contaminant Transport Dominated by HVAC Mechanisms

One potential condition is that the delivery and removal of contaminant is dominated by the HVAC mechanisms. This would mean that the HVAC terms in the delivery and removal functional forms dominate (i.e., are much larger than their leakage counterparts). This dominance can be mathematically expressed using the individual terms from Equations 12 and 15 (see Equations 16 and 17 for the delivery and removal, respectively).

$$(1-\eta) * Q_{HVAC,2} * C_{HVAC}(t) \gg Q_{Leak} * C_1(t) \qquad (16)$$

$$Q_{HVAC,2} * C_2(t) \gg Q_{Leak} * C_2(t) \qquad (17)$$

Dividing the equation obtained from manipulating the removal functional form
(i.e., Equation 17) by the concentration within Zone 2 yields a mathematical statement which, intuitively, must be true for HVAC mechanisms to dominate (see Equation 18).

$$Q_{HVAC,2} \gg Q_{Leak} \qquad (18)$$

Assuming that the lumped HVAC flow for the zone of interest is much larger than the interzonal leakage flow rate, the derived expression for the concentration in the common HVAC ductwork as a volume weighted average of the zone concentrations can be substituted into the delivery functional form (see Equation 19).

$$(1-\eta) * Q_{HVAC,2} * \frac{V_1 * C_1(t) + V_2 * C_2(t) + V_3 * C_3(t)}{V_1 + V_2 + V_3} \gg Q_{Leak} * C_1(t) \qquad (19)$$

Assuming that the mass of contaminant in the zone of release is significantly larger than the mass of contaminant in the rest of the building (i.e., $V_1C_1(t) >> V_2C_2(t)+ V_3C_3(t)$), and dividing both sides of the equation by the concentration in the release zone and the lumped HVAC flow for Zone 2, yields a time-independent statement (see Equation 20).

$$(1-\eta)*\frac{V_1}{V_1+V_2+V_3} >> \frac{Q_{Leak}}{Q_{HVAC,2}} \qquad (20)$$

By comparing the reduced delivery and removal forms (Equations 20 and 18, respectively), it is apparent that the delivery condition is more severe (i.e., if the delivery condition stated in Equation 20 is met, the removal condition in Equation 18 will be satisfied). In this fashion, the conditions whereby the common HVAC system will dominate can be identified (i.e., Equation 20).

For example, under conditions of little or no filtration (i.e., $(1-\eta) \approx 0$), Zone 1 must represent a volume fraction of the building smaller than the ratio of the interzonal leakage flow rate to the lumped HVAC flow for Zone 2 (see Equation 21).

$$\frac{V_1}{V_1+V_2+V_3} >> \frac{Q_{Leak}}{Q_{HVAC,2}} \qquad (21)$$

Furthermore, if the interzonal leakage was equivalent to 1 ACH and the lumped HVAC flow for Zone 2 was equal to 6 ACH (e.g., 1 ACH of makeup air and 5 ACH of recirculation), Zone 1 would need to be significantly larger than 1/6 of the building volume (see Equation 22).

$$\frac{V_1}{V_1+V_2+V_3} >> \frac{1}{6} \qquad (22)$$

Thus, for the HVAC flows to dominate the delivery of contaminant, Zone 1 must represent a very large fraction of the building. Effectively, this will happen when the building, or rather volume served by the common HVAC ductwork, is small. In addition, any filtration will further increase the required size of Zone 1 in relation to the rest of the building.

9.5.2 Contaminant Transport Dominated by Interzonal Leakage

Another potential condition is that the delivery and removal of contaminant is dominated by the interzonal leakage. In this case, the leakage terms in the delivery and removal functional forms would dominate (i.e., would be much larger than their HVAC counterparts). Again, this dominance can be mathematically expressed using the individual terms from Equations 12 and 15 (see Equations 23 and 24 for the delivery and removal, respectively).

$$Q_{Leak}*C_1(t) >> (1-\eta)*Q_{HVAC,2}*C_{HVAC}(t) \qquad (23)$$

$$Q_{Leak}*C_2(t) >> Q_{HVAC,2}*C_2(t) \qquad (24)$$

Dividing the equation obtained from manipulating the removal functional form (i.e., Equation 24) by the concentration within Zone 2 yields a mathematical statement which, intuitively, must be true for leakage mechanisms to dominate (see Equation 25).

$$Q_{Leak} >> Q_{HVAC,2} \qquad (25)$$

Given that the filtration term is, by definition, less than unity (i.e., $(1-\eta) < 1$) and the concentration in the zone of release is larger than the concentration in the common HVAC ductwork under all but trivial conditions (i.e., $C_1(t) > C_{HVAC}(t)$), the removal condition is more severe than the delivery condition (i.e., if the removal condition stated in Equation 25 is met, the delivery condition in Equation 23 will be true). Thus, a very intuitive statement regarding the conditions under which the interzonal leakages dominate the removal and delivery of contaminant is derived (i.e., Equation 25).

9.5.3 Perfect Filtration

Using this approach, it is also possible to examine the effects of perfect filtration (i.e., a filtration efficiency of 100%). Under perfect filtration, the filtration term in the delivery mechanism goes to zero (i.e., $(1-\eta) \rightarrow 0$) and the leakage clearly dominates the delivery of contaminant (see Equation 26). However, the filtration has no impact on the removal functional form (see Equation 27).

$$[\text{Delivery}] \approx Q_{Leak} * C_1(t)$$

$$[\text{Removal}] \approx Q_{Leak} * C_2(t) + Q_{HVAC,2} * C_2(t)$$

Thus, while perfect filtration eliminates the delivery of contaminant via the common HVAC system, it does not affect the removal functional form. Under the nominally "common" conditions of 1 ACH of leakage and 6 ACH of lumped HVAC flow, perfect filtration would result in leakage dominating the delivery of contaminant and HVAC flows dominating the removal of contaminant.

The effects of an in-room air cleaner were also briefly investigated. During the in-room air cleaner test, a commercially available air cleaner (Whirlpool Model AP4503H0, see Figure 47) was operated in the zone of interest (B114), as well as in one of the small rooms, which were lumped together with the rest of the building (B115). Table 19 contains a comparison of the performance metrics for the zone of interest for tests performed under moderate recirculation (5 ACH) and moderate filtration (50%) with and without the in-room air cleaner operating. The results indicated that the in-room air cleaner successfully reduced the exposure at 30 minutes by roughly one order of magnitude and prevented the Ct from reaching the critical Ct value selected for this study. These results are shown graphically in Figure 48, where the impact of an in-room air cleaner on the zone of interest (B114) can be viewed as the difference between the purple and magenta data plots and the impact of an in-room air cleaner on

a small room not adjacent to the zone of release (B115) can be viewed as the difference between the neon green and turquoise data plots. In contrast to the significant reduction in exposures observed in rooms with in-room air cleaners, rooms without an in-room air cleaner displayed a negligible reduction in exposure during the in-room air cleaner tests (denoted by the difference between the neon green and dark green data plots in Figure 48).

These plots clearly illustrate that whether the in-room air cleaner is operating in a room near the release or far from the release, it can have a large impact on the concentration within that particular zone/room. This result is not surprising given the high throughput (~440 cfm) and HEPA-grade filtration efficiency of the in-room air cleaner used; however, it does serve to illustrate the potential advantages of an in-room air cleaner in a small enclosed space.

Figure 47. Photograph of In-Room Air Cleaner Used During Testing (Whirlpool Model AP4503H0)

Table 19. Comparison of Experimental Performance Metrics for the Zone of Interest for the "Moderate" Recirculation Condition with and without an In-Room Air Cleaner

Recirculation	Building Size	Leakage	Filtration	Test ID (Figure 48)	Experimentally Measured	
					Time to Ct of 50,000 ppl*min [min]	Exposure @ 30 min [ppl*min]
"Moderate" (5 ACH)	"Large"	"Low" (0.175 ACH)	"Low" (10%)	N/A	9.1	1.8×10^5
			"Moderate" (50%)	B1	11.2	1.3×10^5
			"Moderate" (50%) with IAC	**IAC1**	**N/R**	**2.9×10^4**
			"High" (90%)	N/A	15.6	8.1×10^4

N/R denotes that specified cumulative Ct was not reached.
N/A is defined as not applicable.
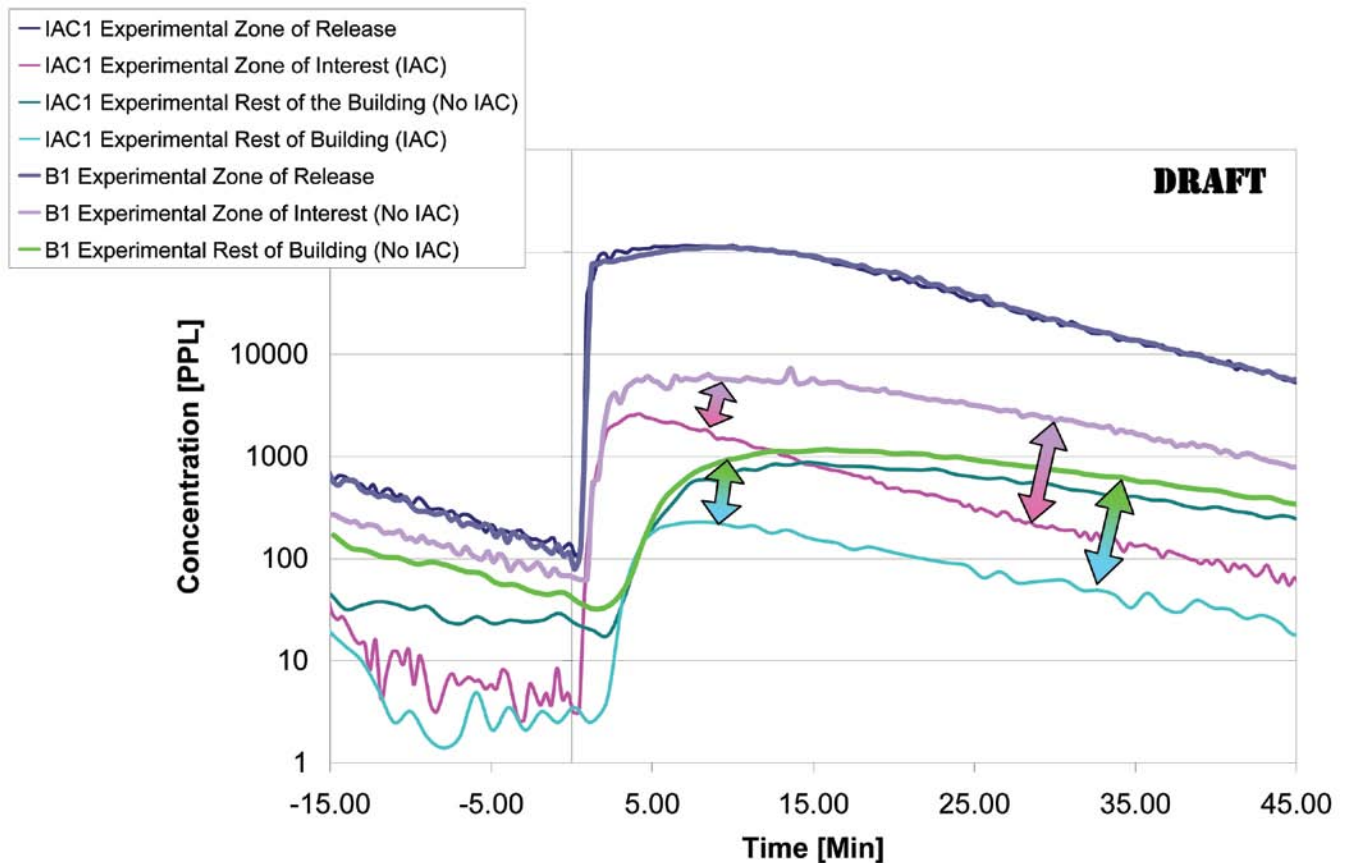
Figure 48. Comparison of Experimental Data for an In-Room Air Cleaner for a "Large" Notional Building with Moderate Recirculation (5 ACH), Low Leakage (0.175 ACH), Moderate Filtration (50% MERV 8 Filter), Standard Makeup Air (1 ACH), and Standard Infiltration (0.5 ACH)

Conclusions and Recommendations

A three-zone model of a building was developed to determine which HVAC and building operating parameters are most important, and how accurately they need to be known, to determine the impact of an indoor bio-agent attack. The three-zone model consists of a zone of release and zone of interest that are adjacent and of equal size, as well as a "lumped" zone that consists of the remainder of the building. All three zones are serviced by a single HVAC system with common recirculation.

An experimental study was then conducted to verify the effectiveness and validity of using the three-zone model to approximate contaminant spread in a building. In the experimental study in the test building, modifications were made to the building and HVAC system to assess the impact those changes had on the spread of the contaminant. The building was modified through the addition of new slab-to-slab walls, the extension of existing partial walls, and the addition of several return vents to create a test volume that resembled the model.

Two performance metrics were used to compare the model and experimental results: the cumulative exposure to the particulate agent for the first 30 minutes following a release and the time to reach a critical exposure value (referred to as Ct). On the whole, the excellent agreement observed between experimental and model-predicted data validated the use of the three-zone model to approximate contaminant spread in a representative building. Excellent agreement between the lumped third zone in the model and multiple rooms throughout the test building validated the use of a three-zone model to provide useful information on real buildings with more than three zones.

A sensitivity analysis method was then developed for the three-zone model to provide an estimate of how well a parameter must be known to assess the impact of an attack, as well as to determine which parameter has the largest impact. An initial analysis using the model simulation revealed that building makeup air and infiltration rates were noncritical parameters for an internal release scenario and that system parameters were of greater importance than single-zone parameters (i.e., the recirculation rate of the entire building was more important than the recirculation rate of the zone of interest). The initial analysis also identified the building size, interzonal leakage rate, recirculation rate, and filter efficiency as the key parameters affecting the two selected performance metrics. The simulation results also showed that the most important parameter to consider depended on building size relative to the fixed volume zone of interest (e.g., a 3,000-m³ building composed of 100 rooms that are each 30 m³ in volume is equivalent to a 50,000-m³ building composed of 100 rooms that are each 500 m³ in volume). As the building size increased, the filtration efficiency went from being a potentially dominant parameter to a lesser factor compared to the interzonal leakage. The system recirculation was found to be of secondary importance in and of itself but had a strong effect on the importance of the filtration efficiency for smaller buildings (i.e., for building volumes less than five times the zone

of interest). With all parameters studied, as the importance of the parameter increased, so did the accuracy with which it needs to be known for reliable estimates of performance metrics. The results of the experimental study corroborated the findings and trends identified by the model simulations.

The most important conclusion to be made from the model simulation results, and the supporting experimental measurements of the spread of a contaminant, is that there is not a dominant parameter, nor a single value of how accurately it needs to be known, to accurately assess the impact of an indoor release in a building. The model approach, as supported by the experimental data, provides a useful and easy tool for estimating and assessing which parameters most impact the spread of contaminant in a building. Buildings of varying size and HVAC performance can be assessed by varying the corresponding model parameters accordingly.

The analysis method provided does indicate the general trends and identifies key parameters for specific combinations of HVAC parameters and building volumes relative to the zone of interest as discussed above. The simplified modeling approach developed here could be used to assess various scenarios and buildings of specific interest, without the need for extensive knowledge of HVAC and building parameters. Using the modeling tool may have merit for rapidly identifying the value of modifying the building to enhance the protection of occupants or to mitigate the spread of contaminants.

Ancillary experiments suggest that the use of an in-room air cleaner can greatly reduce the exposure of the room's occupants. The magnitude of this reduction will vary greatly depending on the volume of the room, as well as the throughput and efficiency of the in-room air cleaner. This suggests that in-room air cleaners may represent a viable method for reducing occupant exposure in selected areas.

Recommendations for future study focus on two aspects of the well-mixed model: usability and applicability. The usability of the model could be improved by developing a user-friendly graphical user interface (GUI) that would allow casual users (e.g., building operators) to rapidly perform simple impact analyses for a building of interest given limited building information (e.g., HVAC settings, building and room volumes). The development of a GUI would increase the utility and impact of this effort by making the model available to more people. Also recommended is an enhancement to expand the applicability of the tool by developing and verifying an analogous model for a building with a more complex HVAC ductwork scheme. The present model is only applicable to a building with one common-return ductwork system. Developing an analogous model that effectively represents buildings with multiple-return ductwork systems (i.e., multiple air handling units) and performing an experimental verification, similar to this work, would aid in making a model more applicable to large buildings with more complex air handling schemes.

12.0
References

American Society of Heating, Refrigerating, and Air-Conditions Engineers (ASHRAE). *ASHRAE Terminology of Heating, Ventilation, Air Conditioning, & Refrigeration.* (2nd edition). Atlanta, Georgia: ASHRAE, 1991.

American Society for Testing and Materials (ASTM). *ASTM Standard E 779-03*: *Standard Test Method for Determining Air Leakage Rate by Fan Pressurization*. West Conshohocken, Pennsylvania: ASTM, 2003.

Bell, A.A. *HVAC Equations, Data and Rules of Thumb.* New York: McGraw Hill, 2000.

Hawkins and Hofacre, 2006.

Hecker, R.T. "Development of Performance Information for Common Ventilation Filters." Battelle Report to U.S. Environmental Protection Agency, Draft Final Report GS-10F-0275K, Task Order 1105, Task 2 (in progress).

Sparks, Leslie, Ph.D. U.S. Environmental Protection Agency, Personal Communication, 2005.

SF$_6$ Experimental Methods

Release Methods. The tracer gas used was SF$_6$. SF$_6$ is an inert, nonhazardous tracer gas and thus yields an accurate indication of the air distribution without being affected by surface interactions (e.g., reactions or adsorption). It is also safe to use in indoor applications with occupants present and can be detected at trace (tens of parts per trillion) concentrations. The amount of SF$_6$ released was calculated by considering the maximum safe concentration of SF$_6$ according to established safety limits. The maximum concentration in any zone should not exceed the time weighted average (TWA) of the permissible exposure limit (PEL) for the tracer gas used, which for SF$_6$ is equivalent to 1,000 ppm (MSDS, 2004). For the purposes of this calculation, a release zone volume of 125 m^3 was assumed (roughly 22 x 20 x 10). Since the maximum observed concentration will be in the release zone, the maximum release mass will be 0.30 kg of SF$_6$ (50 liters at STP). This amount of SF$_6$ (0.30 kg) will produce a maximum concentration of 400 ppm in a release zone with a volume of 125 m^3. If this release amount of SF$_6$ is safe for a small room, it will be safe for release in a larger, better ventilated hallway, and will certainly be safe for release into an HVAC system with even larger makeup air rates, serving an even larger area. Based on a rough calculation of the entire building as a single volume with one air change per hour, this release mass should also produce measurable levels of SF$_6$ throughout large portions of the building and, thus, will be more than adequate for this field study.

To facilitate model comparisons, the release duration of the SF$_6$ will be adjusted to correspond to release characteristics used in model simulations (i.e., a 10-minute release duration). This will be achieved through the use of an orifice (or other flow restriction) to effectively meter the flow of SF$_6$ from a cylinder.

Sampling Methods. Operation of all air samplers will be conducted per standard operating procedures (SOPs). All personnel that will operate the samplers were trained on their operation and demonstrated proficiency of use during dry runs. Operators signed the SOP acknowledgement sheet, and the test leader confirmed that the personnel were proficient with their operation.

During the testing period, an automated air sampler developed by Battelle will be used to collect air samples at selected locations within the area of interest. The functional components of the automated sampler are composed of one diaphragm pump, 12 three-way solenoid valves, 12 Tedlar® sampling bags, a flow restriction, and a custom-designed electronics control board. Up to 100 samplers will be used. A pyramidal sampling control concept will be used to centralize control of the sampling parameters. Thus, a single computer will dictate the sampling parameters for each serialized sampler in a text file. The text file containing the sampling parameters for each of the 100 serialized samplers will then be distributed via ten handheld PODs (handheld program transmitter), which also serve to retrieve the data log from the samplers and record the barcodes of sample bags (see Figure A-1). The PODs are roughly the size and shape of a standard handheld transmitter (e.g., a palm pilot). This sampling concept will allow for centralized control of the sampling parameters, while retaining the convenience of having multiple staff members distribute the sampling parameters. In addition, staff members will not be required to be present to collect samples, and thus, will not interfere with the local airflow and transport of tracer. In this approach, the test leader will direct the sample coordinator regarding the final input and verification of the sampling event to be executed.

The automated sampler will use a serial configuration of three-way valves to minimize any carryover concerns and will offer flexibility in dictating various sample parameters such as purge time, sample time, and delay time between samples. The samples collected will then be analyzed using a GC/ECD to determine the SF$_6$ concentration of each sample. A schematic diagram of the sampler's pneumatic configuration when used to collect air samples for SF$_6$ analysis is illustrated in Figure A-2. Photos depicting the internal and external view of the samplers in this configuration are provided in Figure A-3.
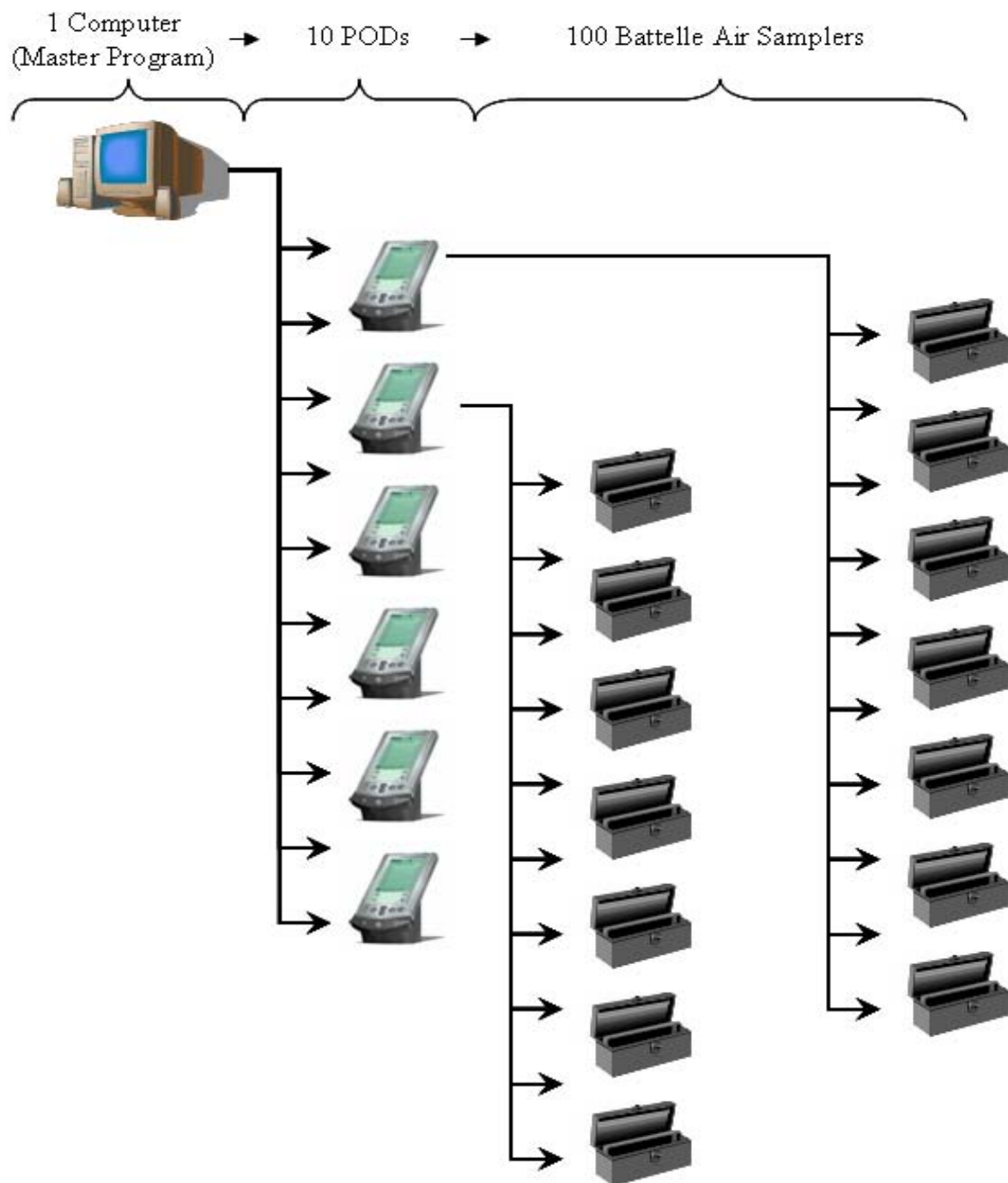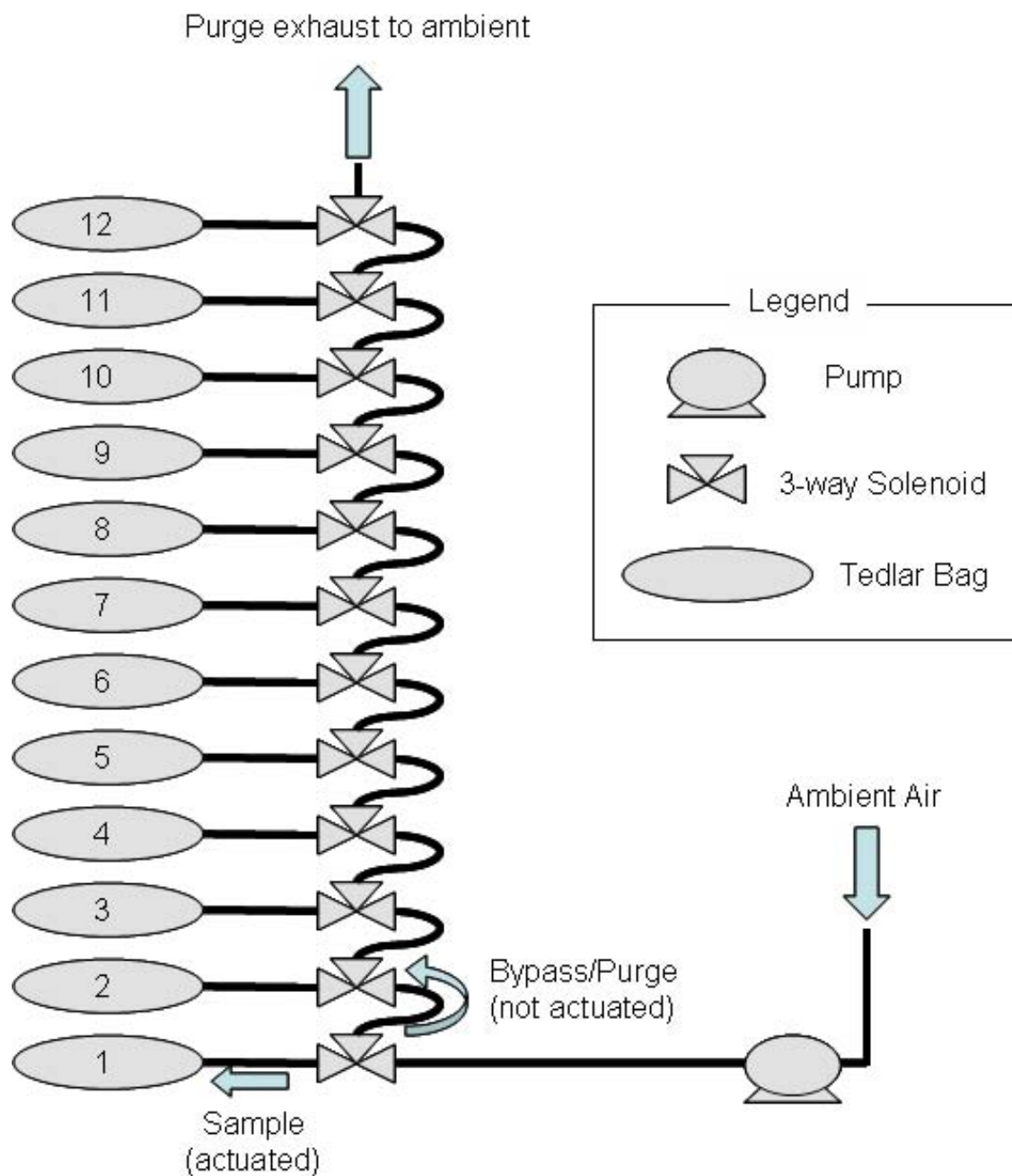
Figure A-1. Pyramidal Sampling Control Concept

Figure A-2. Automated Sampler Pneumatic Configuration
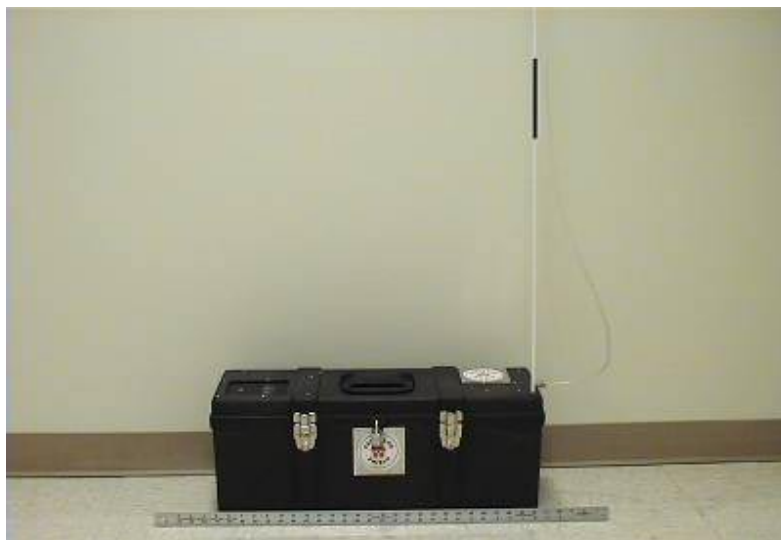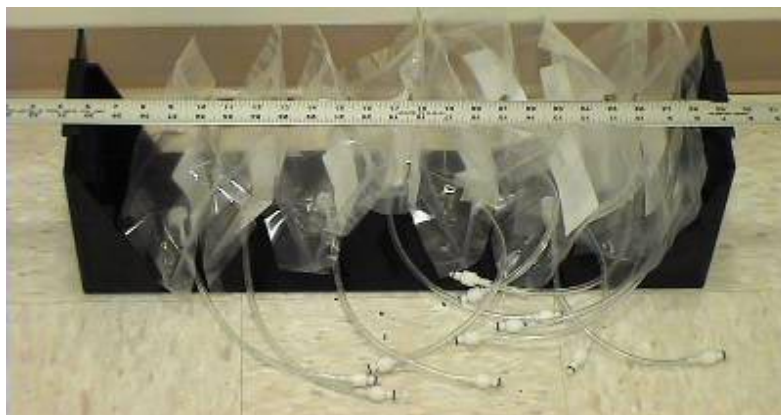
Figure A-3. Internal and External Pictures of the Automated Sample

Each of the automated samplers operate at a fixed flow, ranging from 20 to 500 cc/min. (within ± 10%), through the use of a flow restriction (e.g., a capillary tube). Exact flow rates for each test will be determined by the task leader so that the desired concentration versus time profile for the specific tests can be obtained. Operating with 500 cc Tedlar® sampling bags, sampling durations of 1 to 25 minutes are possible. The delay between samples can be controlled for each sample to allow for any desired sampling schedule. Sampling duration can be controlled in 10-second increments. The sampler is designed so that the sampling pump operates for at least 1 minute to flush the sampling lines prior to sample collection. (This occurs only when there is a delay between samples of at least 1 minute; otherwise, the sampler pump operates continuously and does not require a flush period.) This operating feature will ensure that there is no artifact associated with carryover from the previous sample, which would be most significant if the room concentration decreased rapidly. The sampler will be operated so that a minimum of 250 cc will be collected, which will allow for repeat analyses to be performed, if needed.

Sampler dimensions are 30 x 30 x 65 cm (w x h x l) and the sampler weighs 12 kg. The samplers are intended to sit on the floor or desktop. The sample inlet tube can be secured with a support rod and may be placed as high as 3 m above the sampler. Indicator lights (LEDs) are visible on the top of the control box. The LEDs indicate whether the pump is operating and which sampling bag is being filled. These provide the operator assurance of proper operation without disturbing operation.

Since the tests may rely heavily on the automated sampler, a rigorous battery of pretest checks will be performed. These pretest checks are designed to verify that everything is in working order prior to execution of the tracer gas test. Each serialized automated sampler will execute a preprogrammed sampling sequence without any sample bags attached. The

samplers will be monitored during the pretest to verify that the pump is running and the valves are operating according to the program. This monitoring will occur in the form of checking the status of the LEDs, which indicate whether the pump is running and which valves are actuated. In addition, the flow rate for all sampling lines will be verified.

After pretest checks are performed on all of the automated samplers, the samplers will be loaded with sample cartridges containing twelve 500-cc sampling bags and then deployed to the sampling locations.

SF$_6$ Leakage Test Results

The results of the initial leakage tests suggested that imperfect mixing would be one major discrepancy between the experimental results and the model-predicted concentration curves (see Figures A-4 and A-5). The results of the initial leakage tests also indicated that significant recirculation was occurring (see Figure A-4). Upon further investigation it became apparent that significant leakage was occurring across the recirculation damper and that reducing that leakage to zero was not feasible given the materials and time constraints of the project. While it was possible to estimate the actual recirculation using the theoretical model (see Figure A-5), this represented an indirect method of estimating the interzonal leakage, which depended heavily on the model-predicted value of the recirculated airflow. For example, estimating the interzonal leakage while neglecting the recirculation (as in Figure A-4) leads to an interzonal leakage estimate of 0.4 ACH, while estimating the recirculation (as in Figure A-5) leads to an interzonal leakage estimate of 0.2 ACH. Given this strong dependence of the estimated leakage rate on the estimated recirculation rate, it was clear that this did not represent a direct measure of the leakage, as planned. For this reason, a combinatorial approach to determining the leakage was adopted.
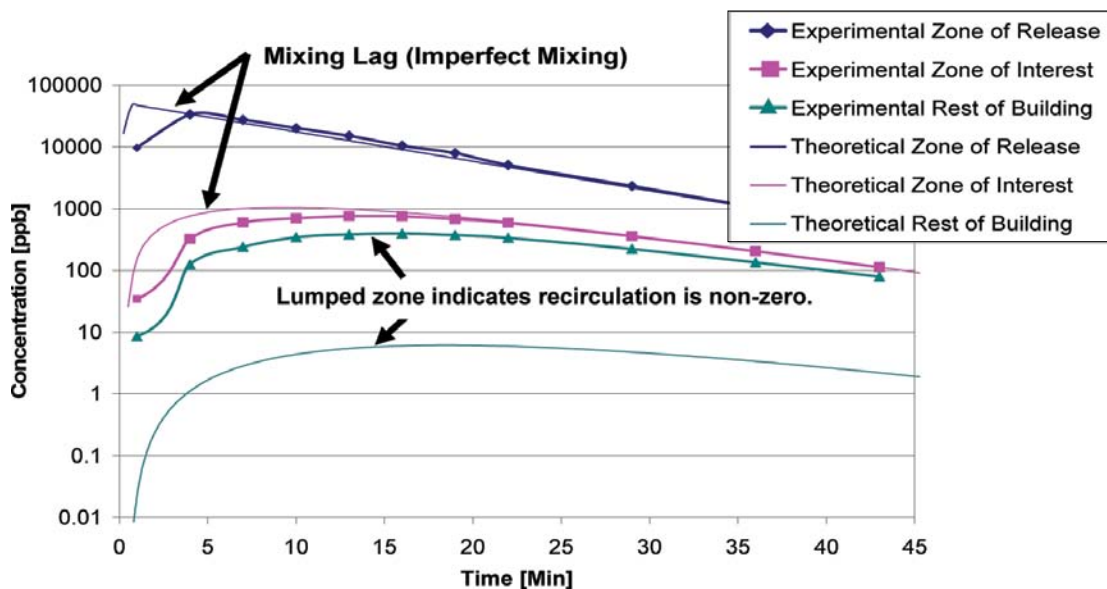

Figure A-4. Comparison of Model-Predicted and Experimental Data for an Initial Leakage Test Assuming No Recirculation. Experimental data was gathered for the "small" notional building under a 6 ACH of makeup air. Model-predicted data are for the "small" notional building under 6 ACH of makeup air with 0.4 ACH interzonal leakage.
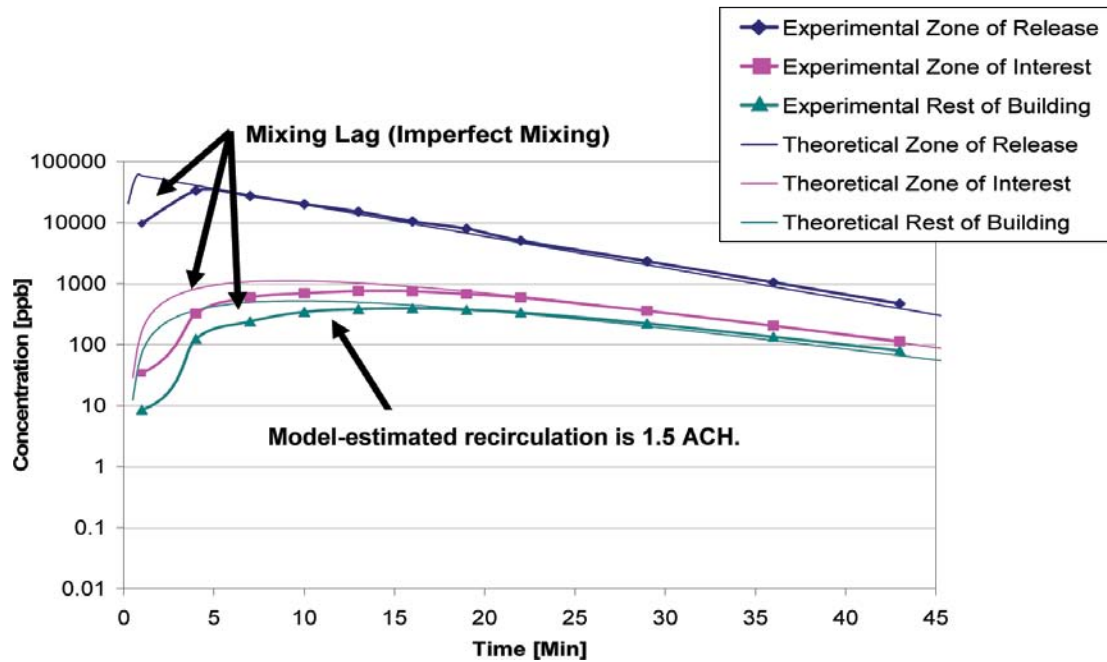
Figure A-5. Comparison of Model-Predicted and Experimental Data for an Initial Leakage Test Assuming Limited Recirculation. Experimental data was gathered for the "small" notional building under a 6 ACH of makeup air. Model-predicted data are for the "small" notional building under 5 ACH of makeup air and 1.5 ACH recirculation with 0.2 ACH interzonal leakage.
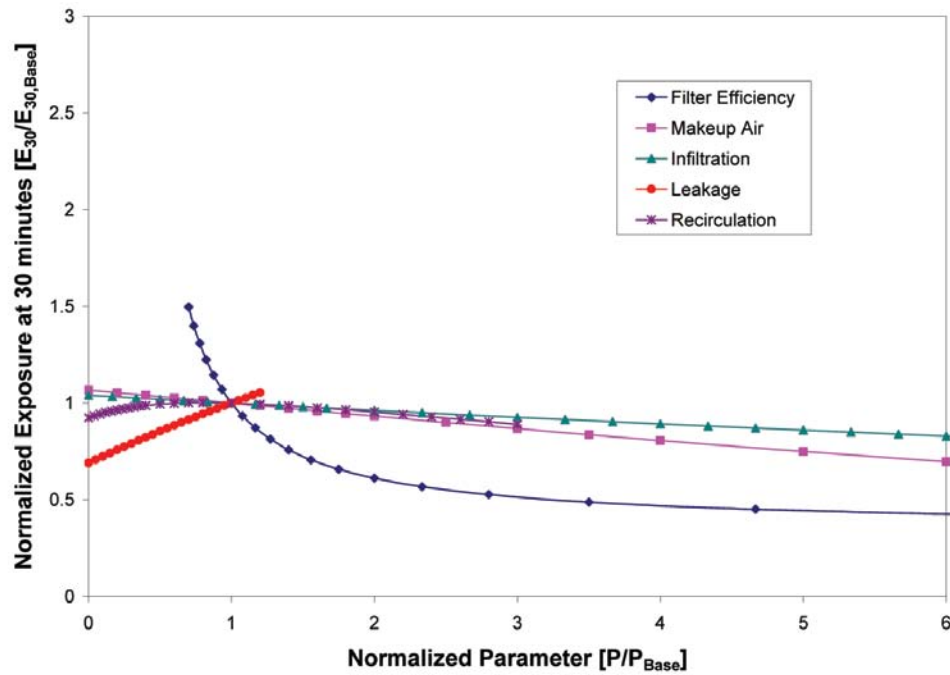
Figure B-1. Normalized Exposure at 30 Minutes ($E_{30,2}$) Versus Model Input Parameters for a Zone 1 Release with a Zone 2 Parameter Scheme for a Building ($V_3=1V_1$). Note that $P/P_{base}=1$ signifies the analysis baseline
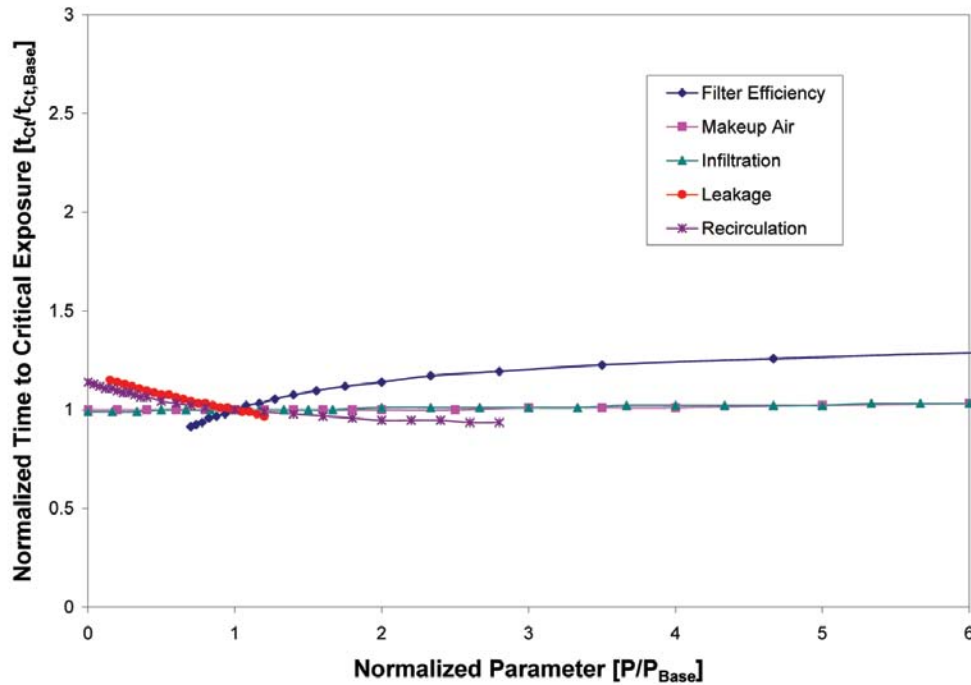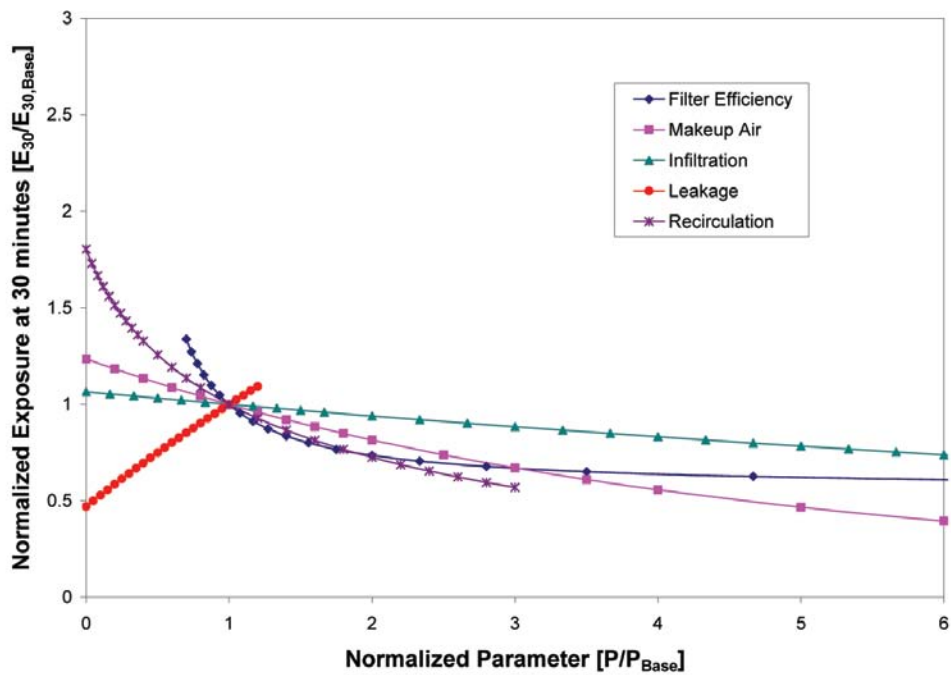

Figure B-2. Normalized Time to Critical Exposure (t_{Ct}) Versus Model Input Parameters for a Zone 1 Release with a Zone 2 Parameter Scheme for a Building ($V_3=1V_1$). Note that $P/P_{base}=1$ signifies the analysis baseline.
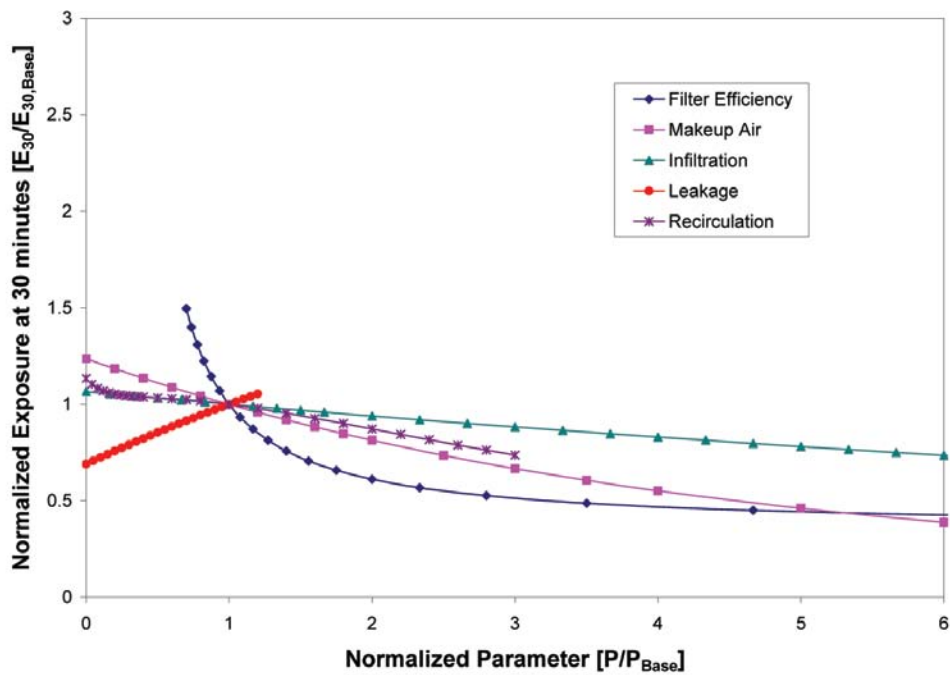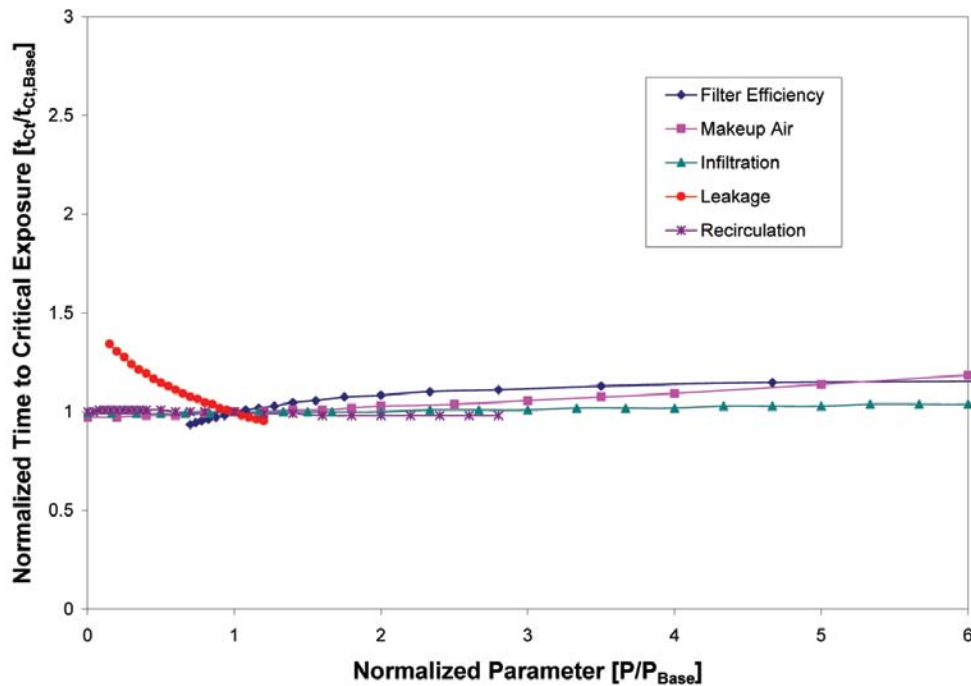
Figure B-3. Normalized Exposure at 30 Minutes ($E_{30,2}$) Versus Model Input Parameters for a Zone 1 Release with a System Parameter Scheme for a Building ($V_3=1V_1$). Note that $P/P_{base}=1$ signifies the analysis baseline.
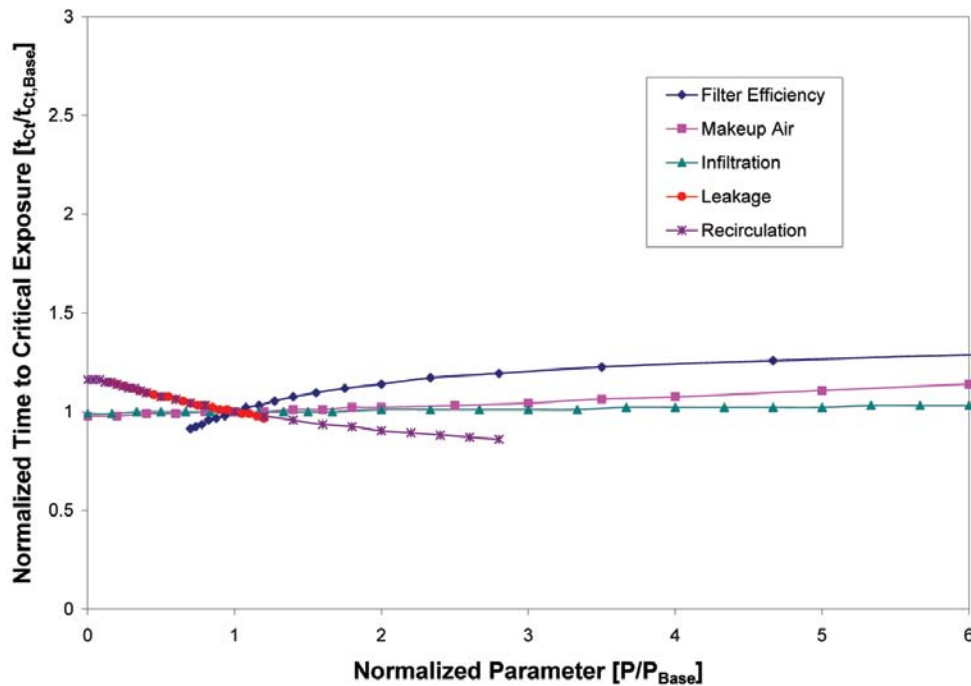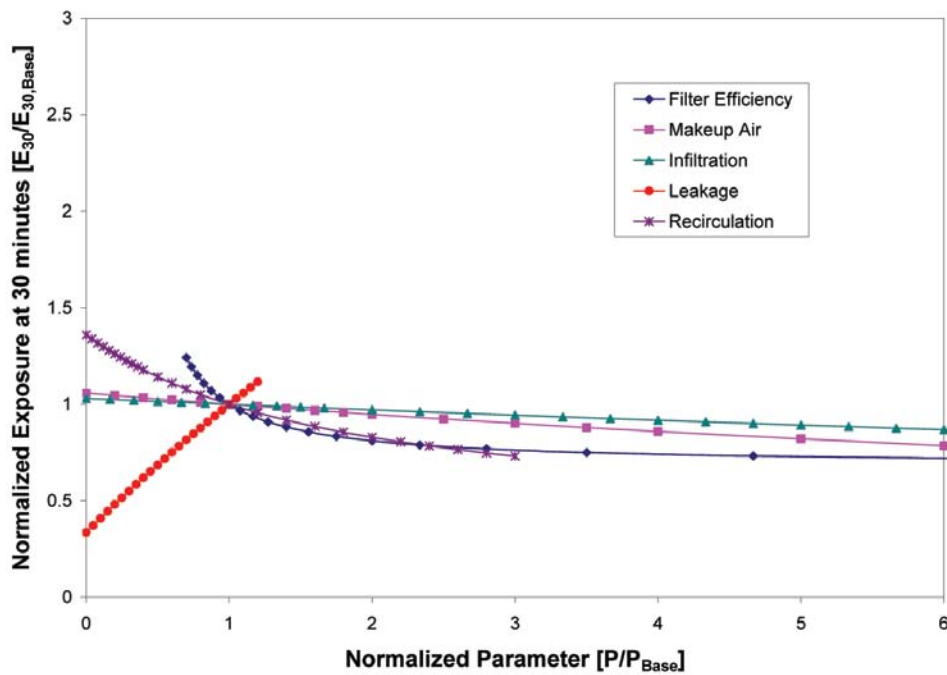

Figure B-4. Normalized Time to Critical Exposure (t_{Ct}) Versus Model Input Parameters for a Zone 1 Release with a System Parameter Scheme for a Building ($V_3=1V_1$). Note that $P/P_{base}=1$ signifies the analysis baseline.
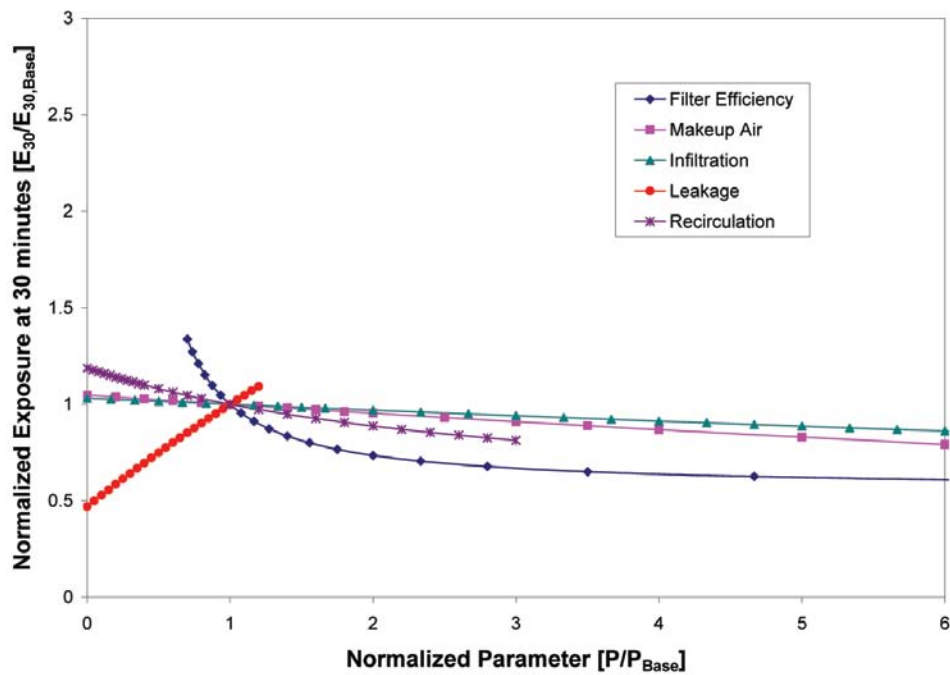
Figure B-5. Normalized Exposure at 30 Minutes ($E_{30,2}$) Versus Model Input Parameters for a Zone 1 Release with a Zone 2 Parameter Scheme for a Building ($V_3=5V_1$). Note that $P/P_{base}=1$ signifies the analysis baseline.
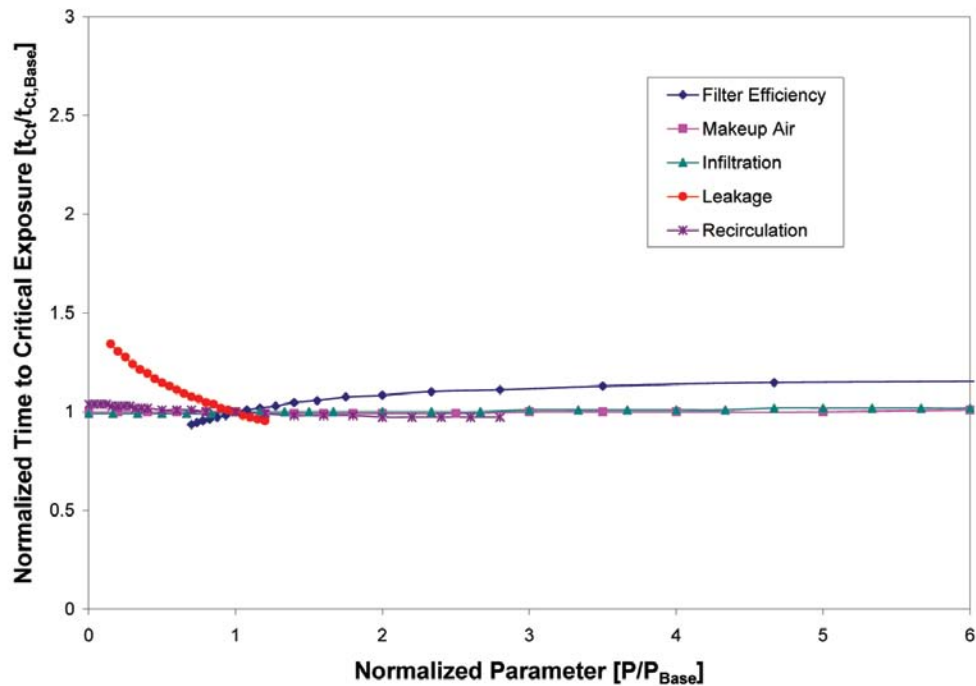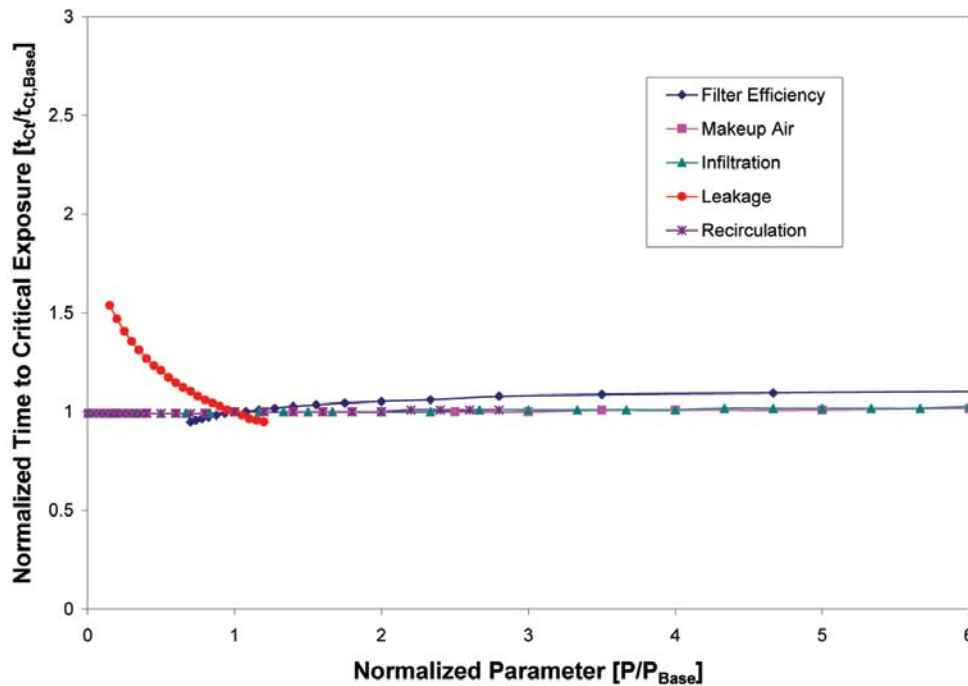

Figure B-6. Normalized Time to Critical Exposure (t_{Ct}) Versus Model Input Parameters for a Zone 1 Release with a Zone 2 Parameter Scheme for a Building ($V_3=5V_1$). Note that $P/P_{base}=1$ signifies the analysis baseline.
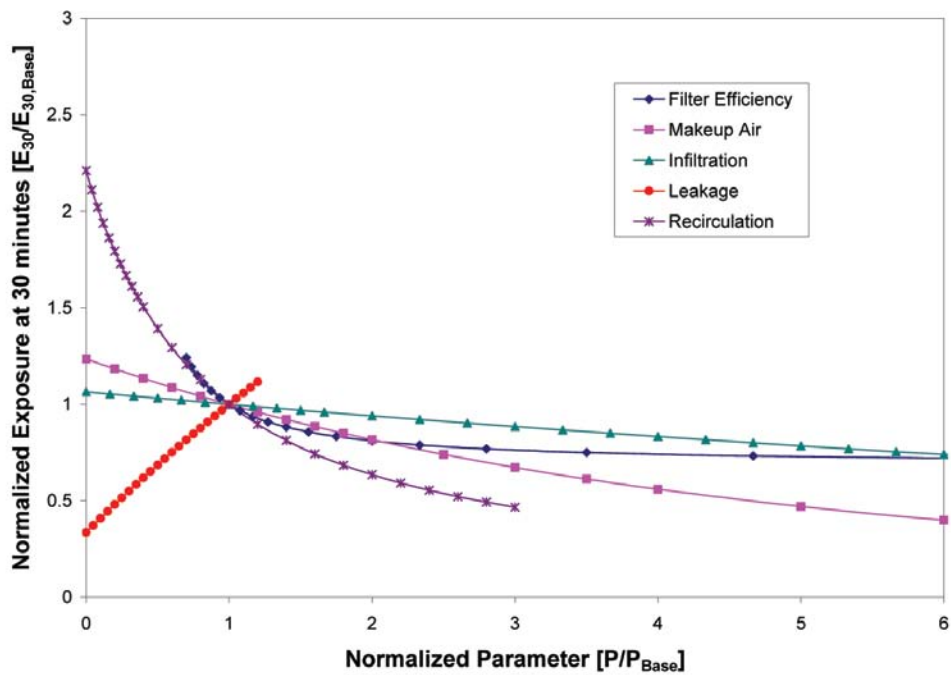
Figure B-7. Normalized Exposure at 30 Minutes ($E_{30,2}$) Versus Model Input Parameters for a Zone 1 Release with a System Parameter Scheme for a Building ($V_3=5V_1$). Note that $P/P_{base}=1$ signifies the analysis baseline.

Figure B-8. Normalized Time to Critical Exposure (t_{Ct}) Versus Model Input Parameters for a Zone 1 Release with a System Parameter Scheme for a Building ($V_3=5V_1$). Note that $P/P_{base}=1$ signifies the analysis baseline.
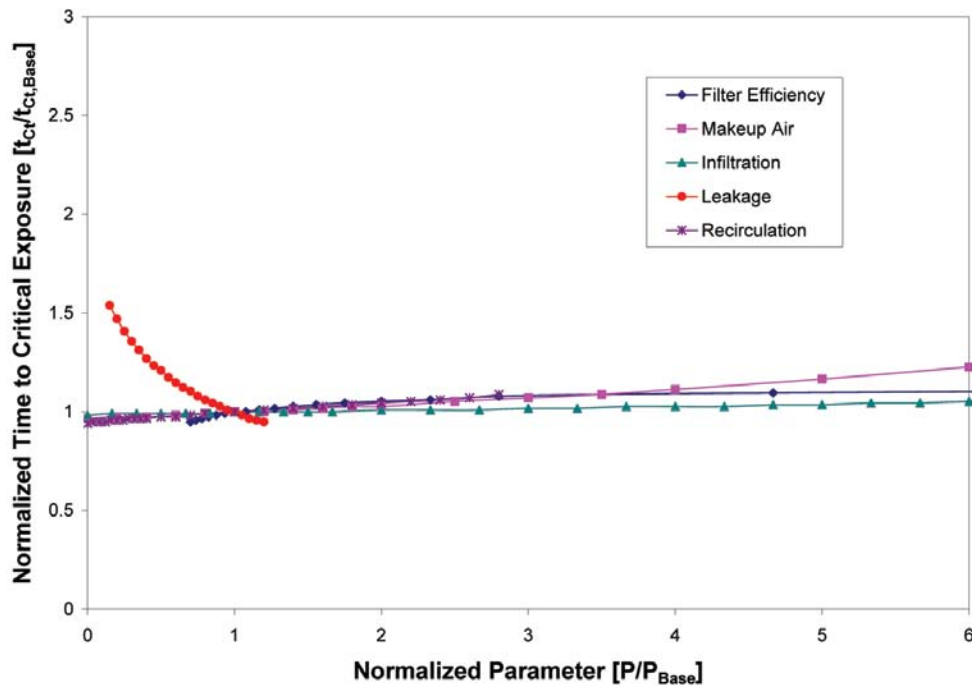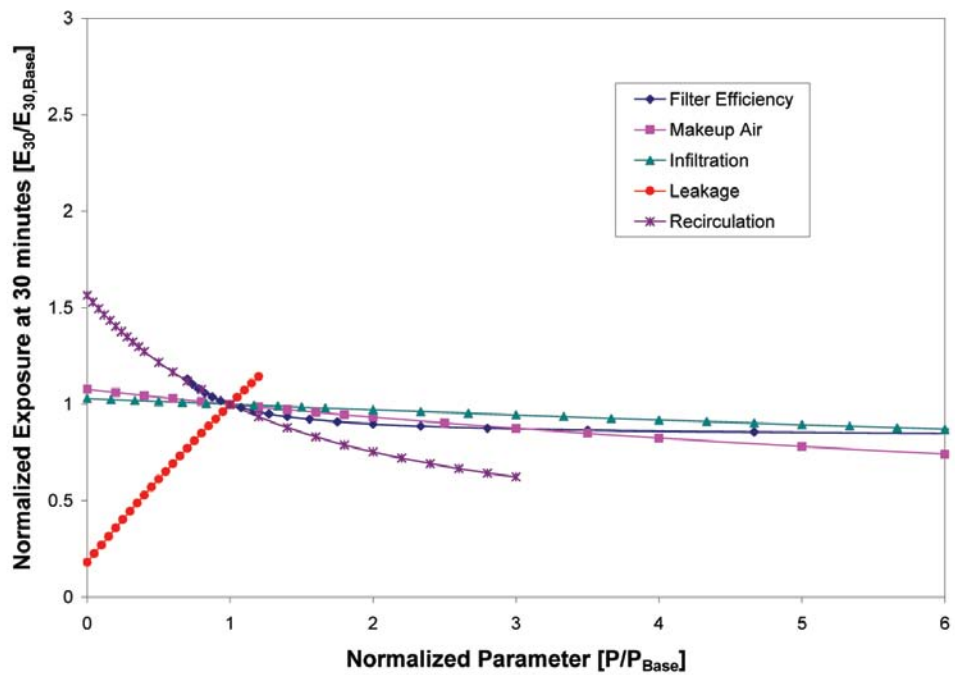
Figure B-9. Normalized Exposure at 30 Minutes ($E_{30,2}$) Versus Model Input Parameters for a Zone 1 Release with a Zone 2 Parameter Scheme for a Building ($V_3 = 10V_1$). Note that $P/P_{base} = 1$ signifies the analysis baseline.
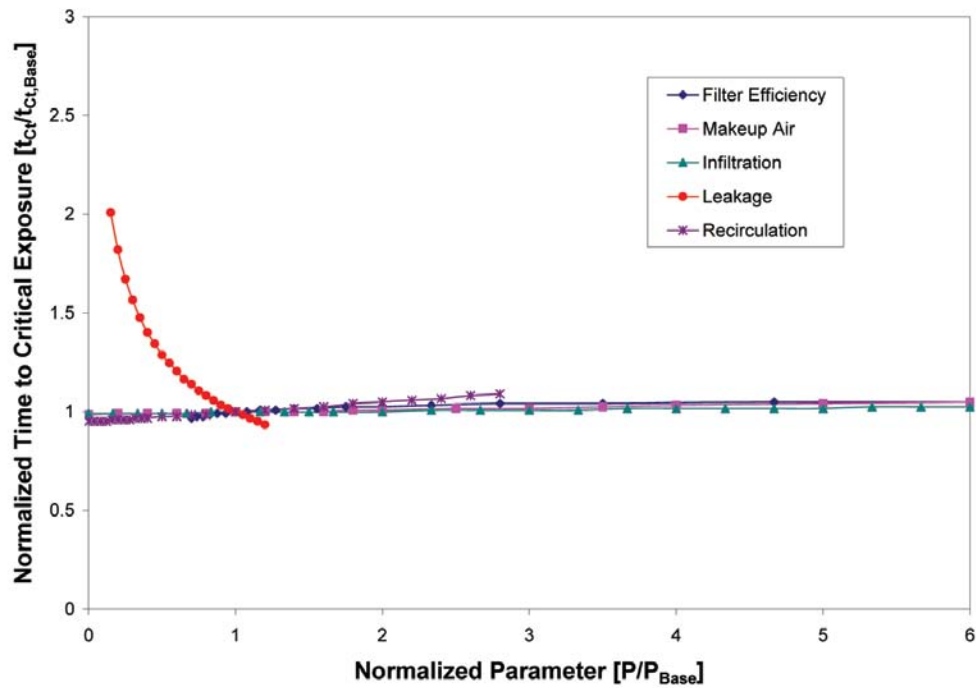

Figure B-10. Normalized Time to Critical Exposure (t_{Ct}) Versus Model Input Parameters for a Zone 1 Release with a Zone 2 Parameter Scheme for a Building ($V_3 = 10V_1$). Note that $P/P_{base} = 1$ signifies the analysis baseline.

Figure B-11. Normalized Exposure at 30 Minutes ($E_{30,2}$) Versus Model Input Parameters for a Zone 1 Release with a System Parameter Scheme for a Building ($V_3=10V_1$). Note that $P/P_{base}=1$ signifies the analysis baseline.

Figure B-12. Normalized Time to Critical Exposure (t_{Ct}) Versus Model Input Parameters for a Zone 1 Release with a System Parameter Scheme for a Building ($V_3=10V_1$). Note that $P/P_{base}=1$ signifies the analysis baseline.

Figure B-13. Normalized Exposure at 30 Minutes ($E_{30,2}$) Versus Model Input Parameters for a Zone 1 Release with a Zone 2 Parameter Scheme for a Building ($V_3=25V_1$). Note that $P/P_{base}=1$ signifies the analysis baseline.
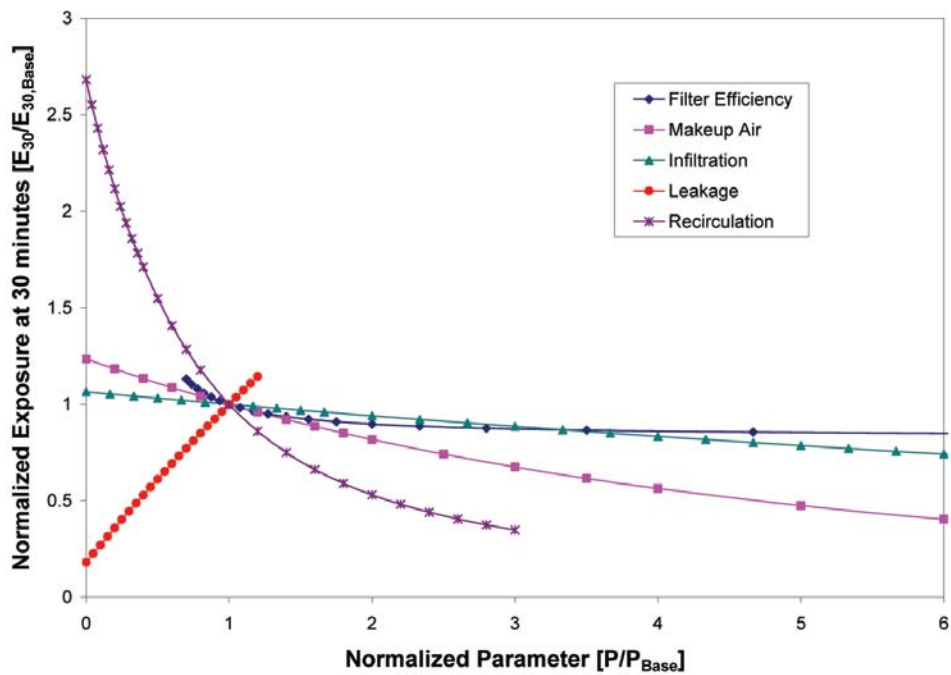

Figure B-14. Normalized Time to Critical Exposure (t_{Ct}) Versus Model Input Parameters for a Zone 1 Release with a Zone 2 Parameter Scheme for a Building ($V_3=25V_1$). Note that $P/P_{base}=1$ signifies the analysis baseline.

Figure B-15. Normalized Exposure at 30 Minutes ($E_{30,2}$) Versus Model Input Parameters for a Zone 1 Release with a System Parameter Scheme for a Building ($V_3 = 25V_1$). Note that $P/P_{base} = 1$ signifies the analysis baseline.
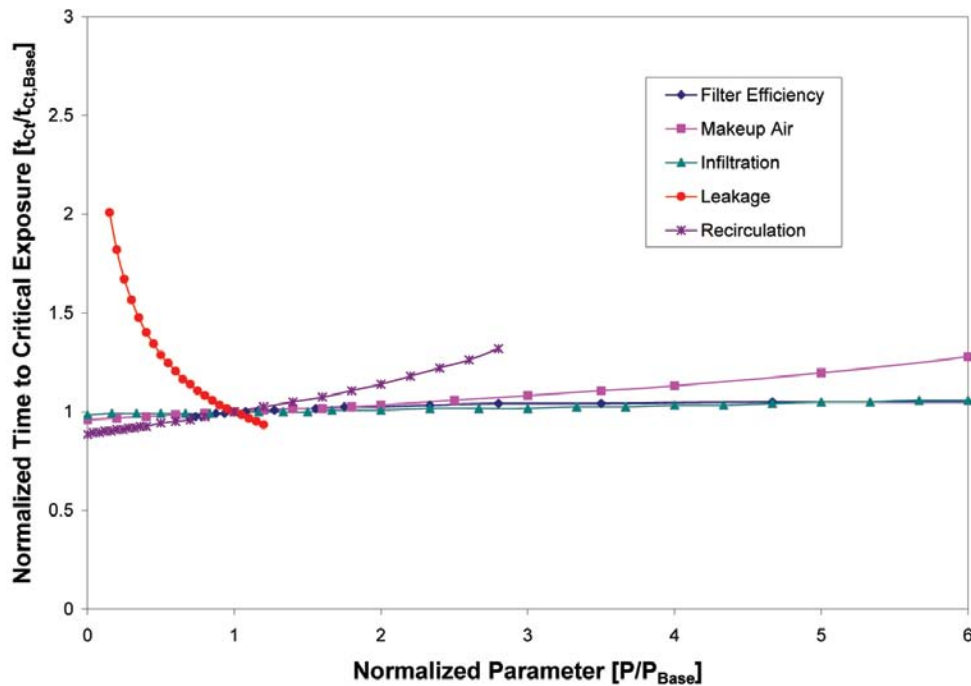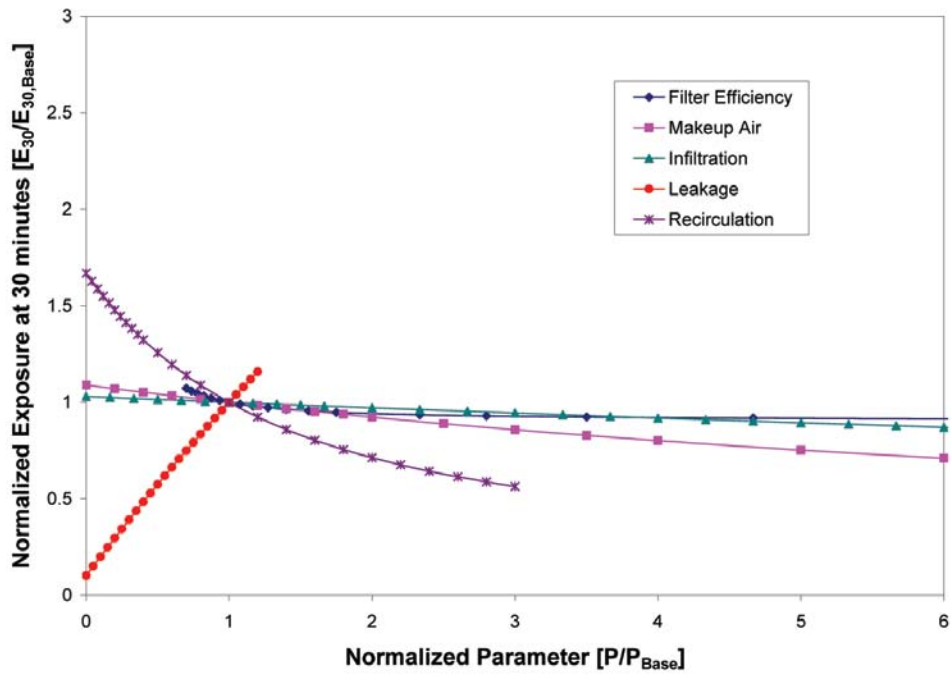

Figure B-16. Normalized Time to Critical Exposure (t_{Ct}) Versus Model Input Parameters for a Zone 1 Release with a System Parameter Scheme for a Building ($V_3 = 25V_1$). Note that $P/P_{base} = 1$ signifies the analysis baseline.

Figure B-17. Normalized Exposure at 30 Minutes ($E_{30,2}$) Versus Model Input Parameters for a Zone 1 Release with a Zone 2 Parameter Scheme for a Building ($V_3 = 50V_1$). Note that $P/P_{base} = 1$ signifies the analysis baseline.
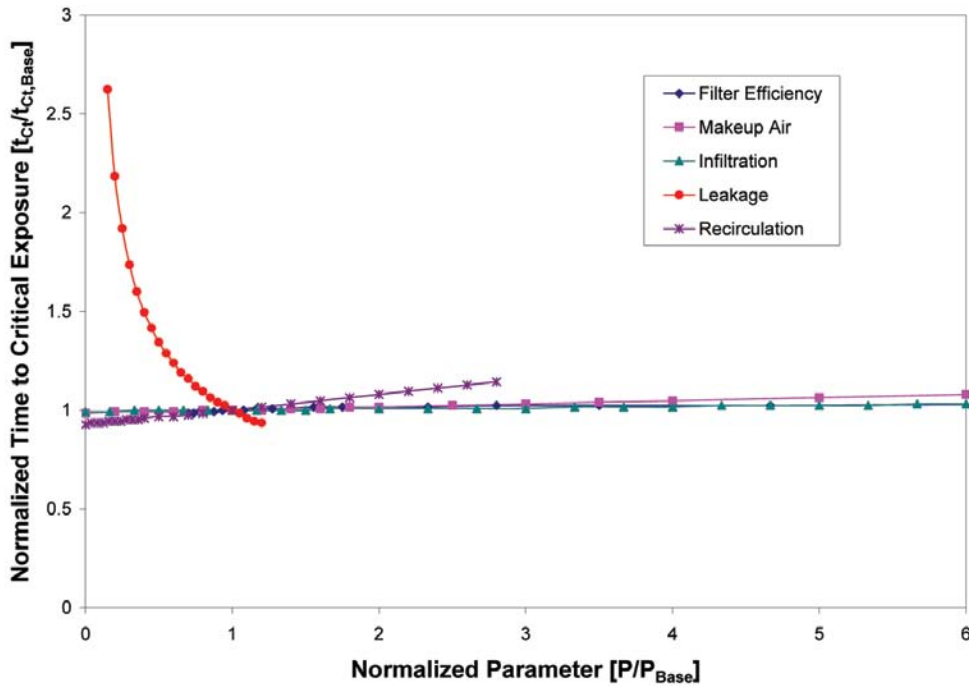

Figure B-18. Normalized Time to Critical Exposure (t_{Ct}) Versus Model Input Parameters for a Zone 1 Release with a Zone 2 Parameter Scheme for a Building ($V_3 = 50V_1$). Note that $P/P_{base} = 1$ signifies the analysis baseline.
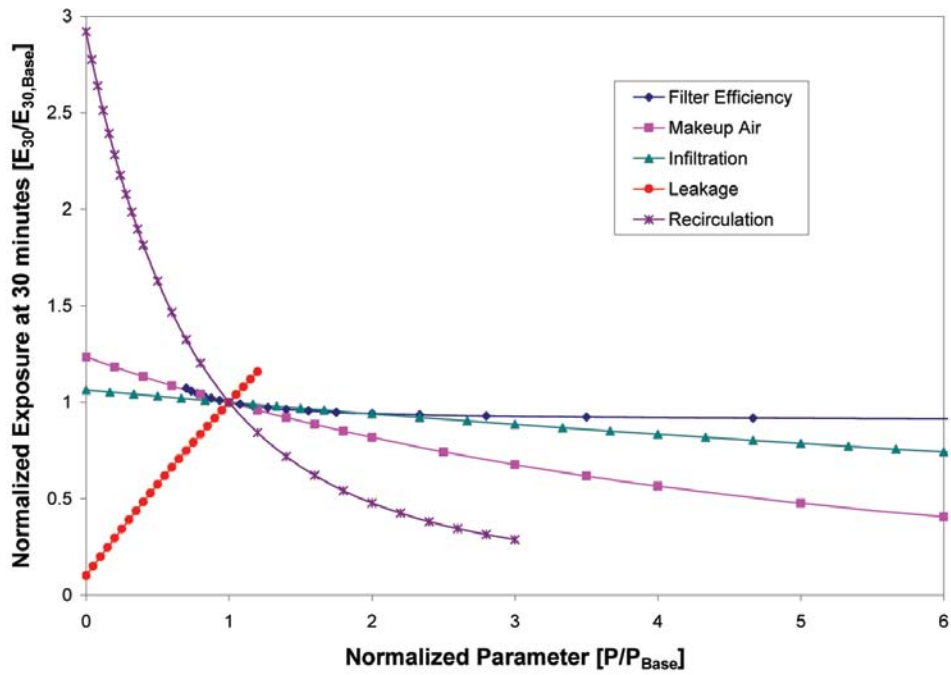
Figure B-19. Normalized Exposure at 30 Minutes ($E_{30,2}$) Versus Model Input Parameters for a Zone 1 Release with a System Parameter Scheme for a Building ($V_3=50V_1$). Note that $P/P_{base}=1$ signifies the analysis baseline.

Figure B-20. Normalized Time to Critical Exposure (t_{ct}) Versus Model Input Parameters for a Zone 1 Release with a System Parameter Scheme for a Building ($V_3=50V_1$). Note that $P/P_{base}=1$ signifies the analysis baseline.
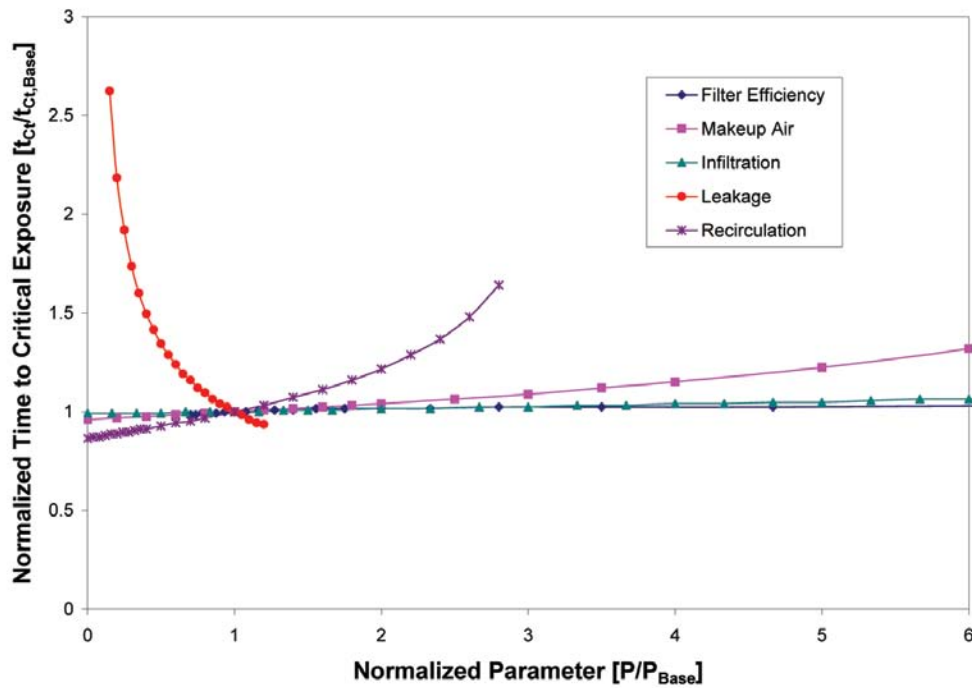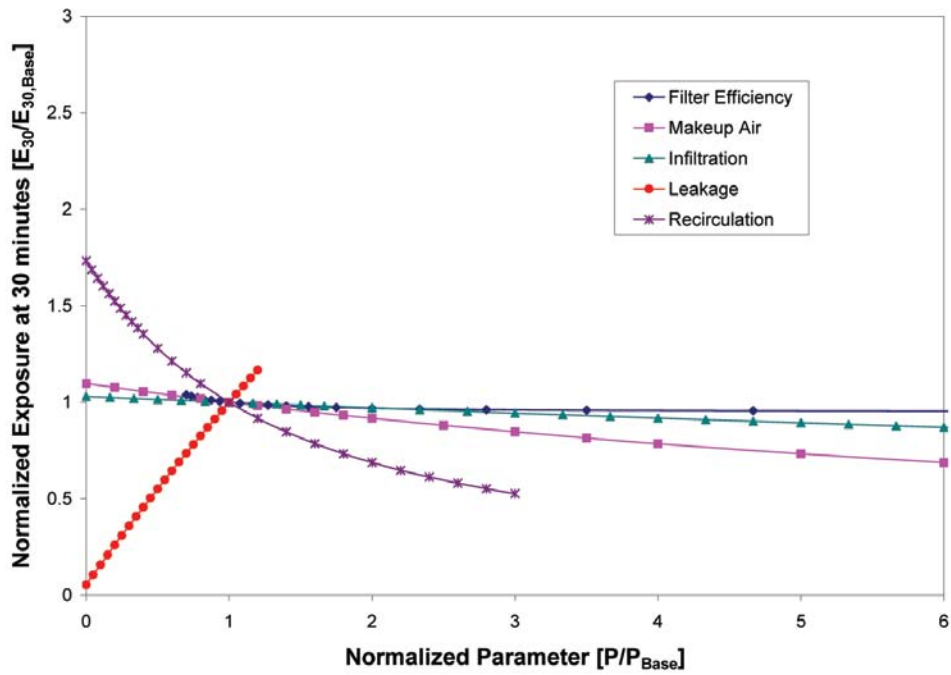
Figure B-21. Normalized Exposure at 30 Minutes ($E_{30,2}$) Versus Model Input Parameters for a Zone 1 Release with a Zone 2 Parameter Scheme for a Building ($V_3=1V_1$). Note that $P/P_{base}=1$ signifies the analysis baseline.
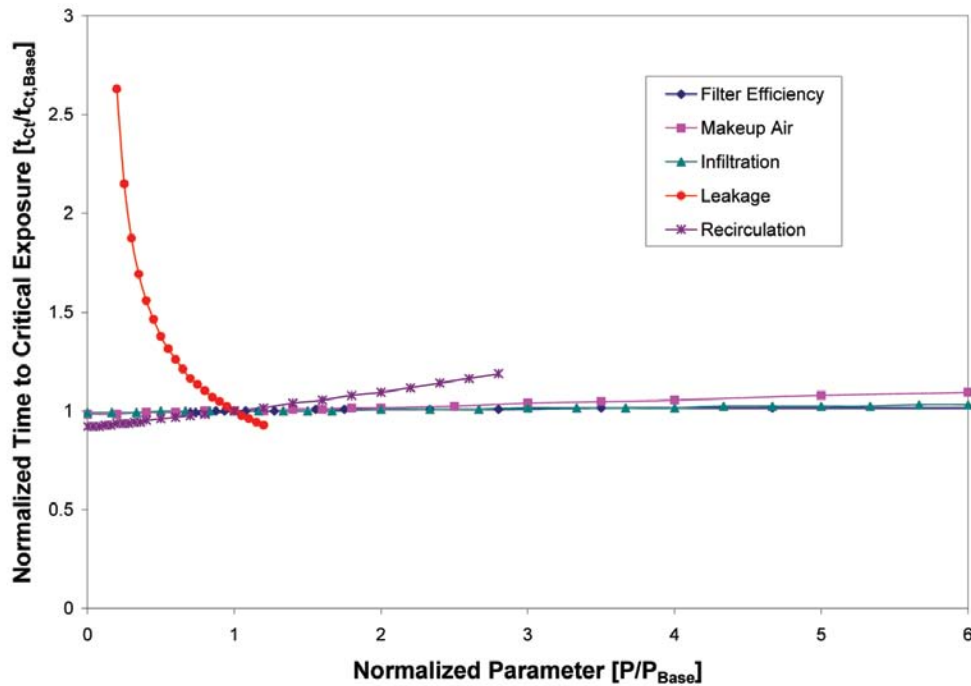

Figure B-22. Normalized Time to Critical Exposure (t_{Ct}) Versus Model Input Parameters for a Zone 1 Release with a Zone 2 Parameter Scheme for a Building ($V_3=1V_1$). Note that $P/P_{base}=1$ signifies the analysis baseline.
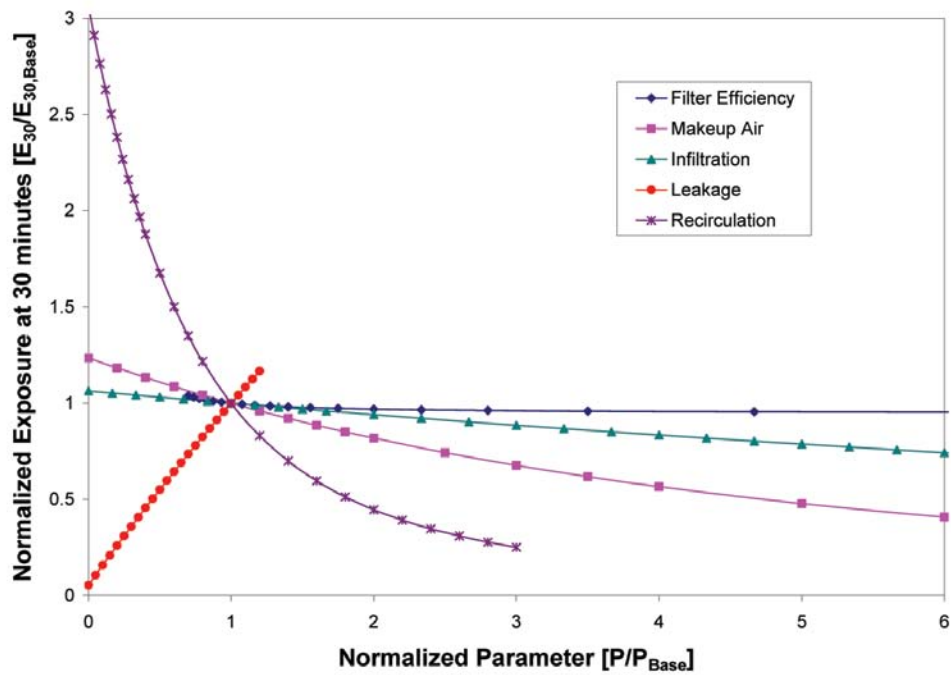
Figure B-23. Normalized Exposure at 30 Minutes ($E_{30,2}$) Versus Model Input Parameters for a Zone 1 Release with a System Parameter Scheme for a Building ($V_3=1V_1$). Note that $P/P_{base}=1$ signifies the analysis baseline.

Figure B-24. Normalized Time to Critical Exposure (t_{Ct}) Versus Model Input Parameters for a Zone 1 Release with a System Parameter Scheme for a Building ($V_3=1V_1$). Note that $P/P_{base}=1$ signifies the analysis baseline.
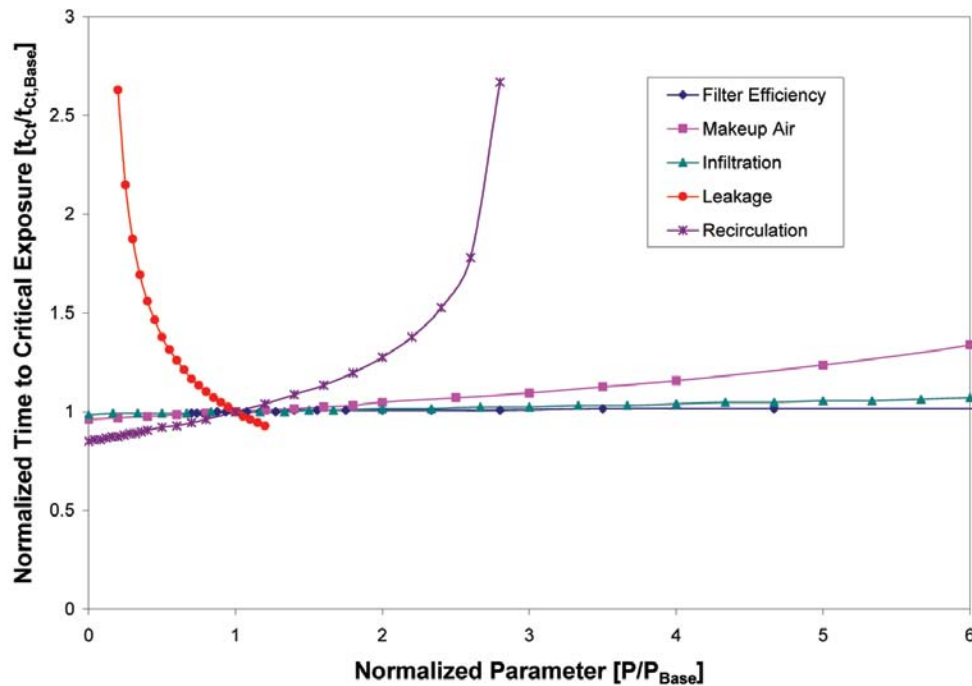
Data Quality

Data Quality Objectives (DQOs) are qualitative and quantitative statements designed to ensure that the type, quality, and quantity of data used are appropriate for the intended application. As discussed in the body of the report (Sections 1, 2, 3, and 5), the experiments performed had two purposes. One purpose of the experiments was to evaluate the effect of HVAC, architectural, and operating procedure modifications on the spread of gases and aerosols through a building. The other purpose was to experimentally demonstrate the validity of the three-zone, well-mixed model developed in Task 7. In an effort to collect a wide range of data, replicate testing was not performed under this project; therefore, it was not possible to quantitatively state the required agreement between replicates.

The type of data being collected during these tests, particulate concentrations, are appropriate since they can be compared to one another to determine the effect of the modification on the spread of gases and aerosols. A qualitative analysis of the collected data was performed by comparing these data to those collected on similar projects and to the results of the Task 7 theoretical analyses to confirm the trends noted in the Task 7 results. For example, a short-term or instantaneous release in a well-mixed volume zone serviced by a typical HVAC system would be expected to produce a rapid increase in contaminant concentration, followed by a logarithmic decay in the concentration. The height of the peak is indicative of the ratio of the mass released to the zone volume, while the decay is indicative of the removal constant. The removal constant is an aggregation of many potential factors, including contaminant decay (if applicable), particle deposition (if applicable), filtration (if applicable), and exhaust (if applicable).

Engineering logic was also used to compare the data sets to each other to determine whether or not they made qualitative sense. (For example, one would expect a lower particulate concentration when a higher efficiency filter was used in the HVAC system.) Although some variation is expected, gross deviations from past

data and logically expected results were immediately investigated as they were indicative of problems that arose. An excellent example of this was observed in the SF_6 leakage test results discussed in Appendix A. The results of the SF_6 leakage tests showed that the building HVAC system was unable to operate with 100% makeup air (i.e., no recirculated air). This prompted a physical inspection of air handling dampers in which a test technician climbed inside of the air handling unit, revealing that significant leakage was occurring across the recirculation damper. Another example of the use of engineering logic in achieving data quality objectives is apparent in the discussions of MetOne particle counter saturation in Section 7.0. In this example, experimental measurements indicated that the release mass used was sufficiently large to cause saturation of the MetOne optical particle counter in the zone of release. In this case, an engineering judgment was made not to reduce the release mass in order to maintain a sufficient particle concentration in zones far from the release. This judgment was deemed appropriate for two reasons. The first reason was that the concentration within the release zone exhibited the expected logarithmic decay from the saturation concentration within the test timeframe, indicating a high likelihood that the particle concentration within the release zone was behaving as expected. The second reason was that the concentration in zones far from the release was sufficiently above baseline noise to prove useful to model comparisons. Furthermore, given that subsequent planned tests would use higher efficiency filtration, it was the judgment of the test leader that reducing the release mass would result in concentrations below background in zones far from the release. In this manner, engineering logic was used in conjunction with qualitative analyses to scrutinize the quality of data sets, make data-based test decisions, and achieve the data quality objectives of this task.

Sample calculations are detailed throughout the body of the report, particular in Sections 7, 8, and 9. The raw data gathered during testing is included on a CD in the form of Excel files as Appendix D.

Electronic Data Archive

The electronic data archive includes an Excel file (Test_List.xls) containing a table of the test details (e.g., Test ID, Test Date, HVAC Conditions), as well as Excel files for each test, labeled by Test ID (e.g., A1.xls). The Excel file for each test contains a graph and table of the MetOne data for each zone used in the analysis (i.e., the 2.0 to 5.0 µm size channel), as well as the raw data file for each MetOne, which contains all six size channels.

SCIENCE

EPA
United States
Environmental Protection
Agency

Office of Research and Development
National Homeland Security Research Center
Cincinnati, OH 45268

Official Business
Penalty for Private Use
$300

Recycled/Recyclable
Printed with vegetable-based ink on
paper that contains a minimum of
50% post-consumer fiber content
processed chlorine free